Composite

Structural Program

Rensselaer Polytechnic Institute
Troy, N.Y. 12181

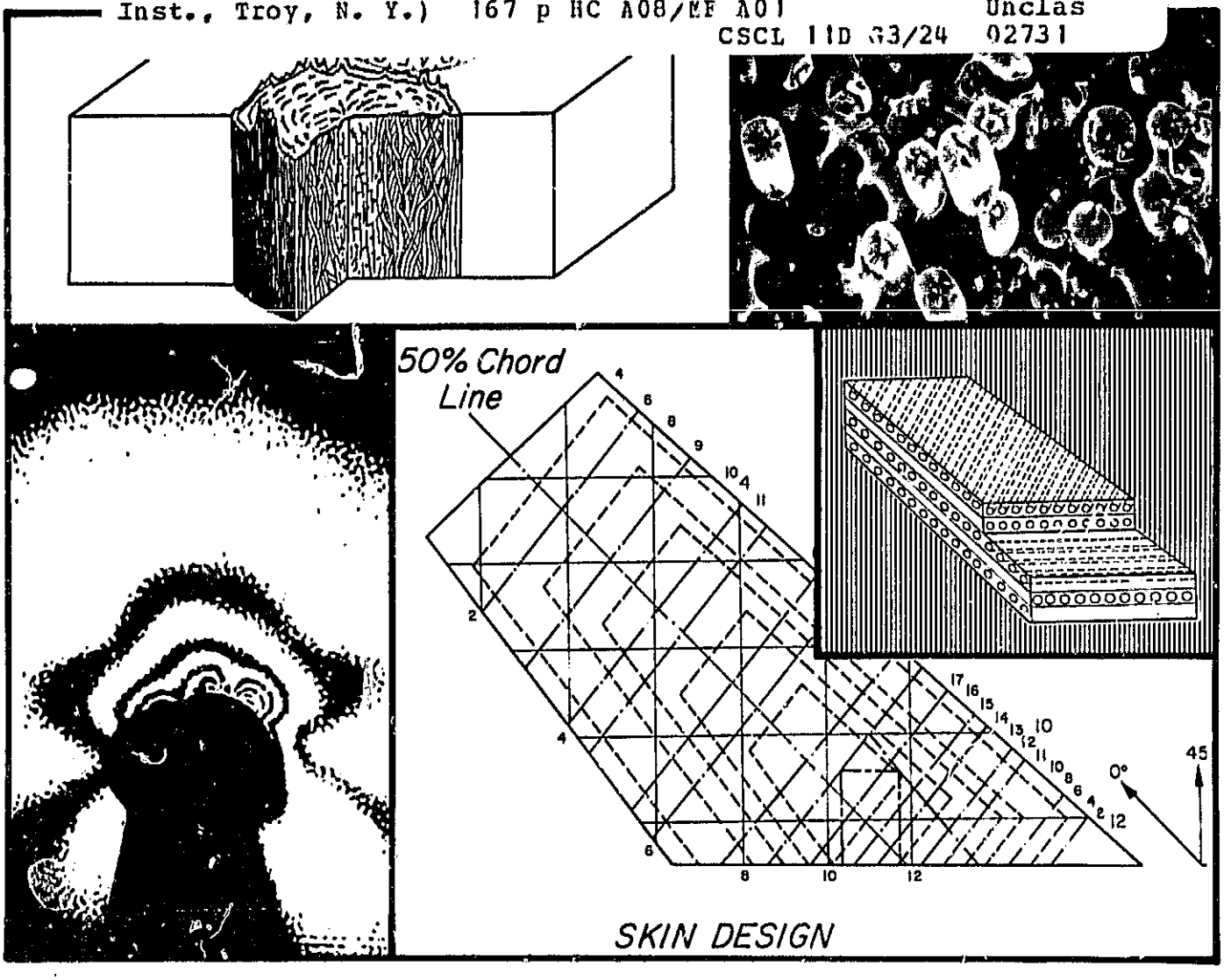

Sponsored by
NASA/AFOSR

Semi-Annual Progress Report

April 30, 1982 through September 30, 1982

COMPOSITE STRUCTURAL MATERIALS

Air Force Office of Scientific Research
and
National Aeronautics and Space Administration
Grant No. NGL 33-018-003

Co-Principal Investigators:

George S. Ansell
Dean, School of Engineering

Robert G. Loewy
Institute Professor

and

Stephen E. Wiberley
Professor of Chemistry

Rensselaer Polytechnic Institute
Troy, New York 12181

NASA Technical Officer

Michael A. Greenfield
Materials and Structures Division

NASA Headquarters

CONTENTS

LIST OF TABLES

LIST OF FIGURES

PART I
INTRODUCTION

INTRODUCTION

The promise of filamentary composite materials, whose development may be considered as entering its second generation, continues to generate intense interest and applications activity. Such interest and activity are well-founded, since they are based on the possibility of using relatively brittle materials with high modulus, high strength, but low density in composites with good durability and high tolerance to damage and which, when they do fail, do so in a non-catastrophic manner. Fiber reinforced composite materials of this kind offer substantially improved performance and potentially lower costs for aerospace hardware.

Much progress has been achieved since the initial developments in the mid 1960's. Rather limited applications to primary aircraft structure have been made, however, mainly in a material-substitution mode on military aircraft, except for a few experiments currently underway on large passenger airplanes in commercial operation and a few military developments which have not seen service use.

To fulfill the promise of composite materials completely requires a strong technology base. NASA and AFOSR recognize the present state of the art to be such that to fully exploit composites in sophisticated aerospace structures, the technology base must be improved. This, in turn, calls for expanding fundamental knowledge and the means by which it can be successfully applied in design and manufacture.

As technology of composite materials and structures moves toward fuller adoption into aerospace structures, some of the problems of an earlier era are being solved, others which seemed important are being put into perspective as relatively minor, and still others unanticipated or put aside are emerging as of high priority. The purpose of the RPI program as funded by NASA and AFOSR has been to develop critical advanced technology in the areas of physical properties, structural concepts and analysis, manufacturing, reliability and life prediction.

Our approach to accomplishing these goals is through an interdisciplinary program, unusual in at least two important aspects for a university. First, the nature of the research is comprehensive - from fiber and matrix constituent properties research, through the integration of constituents into composite materials and their characterization, the behavior of composites as they are used in generic structural components, their non-destructive and proof testing, to the logical conclusion of such activities; namely research into the composite structure's long term integrity under conditions pertinent to service use. Inherent in the RPI program is the motivation which basic research into the structural aspects provides for research at the materials level, and vice versa.

Second, interactions among faculty contributing to program objectives - which is a group wider than that supported under the project - is on a day to day basis, regardless of

organizational lines. Program management is largely at the working level, and administrative, scientific and technical decisions are made, for the most part, independent of considerations normally associated with academic departments. Involvement of this kind includes - depending on the flow of the research - faculty, staff and students from chemistry, chemical engineering, civil engineering, materials engineering, and the department of mechanical engineering, aeronautical engineering and mechanics.

Both of these characteristics of the NASA/AFOSR program of research in composite materials and structures foster the kinds of fundamental advances which are triggered by insights into aspects beyond the narrow confines of an individual discipline. This is a program characteristic often sought in many fields at a university, but seldom achieved.

Overall program emphasis, is on basic, long-term research in the following categories: (a) constituent materials, (b) composite materials, (c) generic structural elements, (d) processing science technology and (e) maintaining long-term structural integrity. Progress in the program will be reported in the following pages under these headings. Those computer software developments are also undertaken which both support Rensselaer projects in composite materials and structures research in the areas listed above and which also represent research with the potential of widely useful results in their own right.

In short, the NASA/AFOSR Composites Aircraft Program is a multi-faceted program planned and managed so that scientists and engineers in a number of pertinent disciplines will interact to achieve its goals. Research in the basic composition, characteristics and processing science of composite materials and their constituents is balanced against the mechanics, conceptual design, fabrication and testing of generic structural elements typical of aerospace vehicles so as to encourage the discovery of unusual solutions to present and future problems. In the following sections, more detailed descriptions of the progress achieved in the various component parts of this comprehensive program are presented.

PART II
CONSTITUENT MATERIALS

II-A THE SURFACE ENERGY OF ANHYDRIDE-CURED EPOXY RESINS

II-A THE SURFACE ENERGY OF ANHYDRIDE-CURED EPOXY RESINS

Senior Investigator: R. J. Diefendorf

1. Introduction

The comparatively low interlaminar shear strength of high modulus graphite composites compared to that of glass and boron fibers has resulted in an extensive and intensive search for techniques to modify the fiber-matrix interface to optimize the interlaminar shear strength of these composites.

Several ingenious routes have been taken to modify the fiber surfaces and to improve the bond between the fibers and epoxy matrices. Some of these approaches include oxidative treatments (Drzal[1,2]*, Donnet and Ehrburger[3]) which increase the shear strength of the composite but, generally, at the expense of composite tensile strength. Interfacial condensation methods and electrolytic deposition processes which lead to the polymerization of monomers on the fiber surfaces have been developed to form a flexible interlink or tie coat.

These various techniques have met with differing degrees of success. However, an effective and predictable method of modifying or designing the interlaminar shear strength of these composites is yet to be developed. The aims of this study are to describe the surface energy components of fibers

*Numbers in brackets in this section refer to the references which are listed on page 16.

and resins and to further develop models which can predict these components from the architecture of the polymeric matrices.

This research, conducted by graduate student C. E. Uzoh, is part of an effort to understand and catagorize the fundamental principles which govern the design of an effective and predictable interfacial bond between fiber and matrix. In this report, the semiempirical geometric mean model of Girifalco-Good-Fowkes-Kaeble-Young and Zisman was used to describe the role of anhydride curing agents in determining the surface energies of cured epoxy resins.

2. Status

During the last period, the surface energy components of various epoxy resins, curing agents and several non-epoxide polymers were characterized.

3. Progress During Report Period

a. Surface Energy Components

Wetting studies of various liquids on the surfaces of resins indicate that the curing agent is the critical factor that dictates the dispersive and polar fractions of the surface energies of these epoxies. Epoxies studied include nadic methyl anhydride (NMA) and dodecenyl succinic anhydride (DDSA)-cured bisphenol A, novolac, cycloaliphatic and tetraglycidyl derivatives of epoxy with benzyldimethylamine (BDMA) as catalyst.

For instance, the polar components for all DDSA-cured epoxies are consistently less than 5 erg/cm^2, even though the total surface energy is about 30 erg/cm^2 (see Table II-A-1). Also, DDSA-cured Epon 828, Epon 152, Aradite CY-179 and MY-720 have about the same value of γ^p and γ^d, irrespective of the anhydride/resin (A/R) ratio. Even though the NMA cures have higher γ^p and γ^d than DDSA cures, the surface energy components have the same insensitivity to A/R ratio. This insensitivity of surface energy components to A/R ratio is due to the splitting-off of the excess epoxy components during post-curing at elevated temperature.

Comparative studies on surfaces of amine-cured epoxies and other non-epoxides indicate that the observed difference in NMA and DDSA-cured samples is due to the architecture of the curing agents. The difference is caused by the flexibility induced by the long aliphatic chain and the steric hindrance of methylene groups in DDSA, compared to the more compact structure of NMA. This explanation is supported by the microhardness of the polished surfaces of these epoxies (see Table II-A-2).

b. Critical Surface Energy

The critical surface energy γ_c of a low energy solid was operationally defined by Zisman as:

$$\text{Cos}\,\theta = 1 + b(\gamma_c - \gamma_L)$$

where θ is the contact angle, γ_L the surface energy of the contacting liquid and b is a constant. Homologous series of

TABLE II-A-1

SURFACE ENERGY COMPONENTS OF ANHYDRIDE-CURED EPOXIES

Substrates	Dispersive Component	Polar Component	Total Surface Energy*
DDSA** Cure			
CY - 179 (85-100 phr)	29.2 ± 0.6	2.9 ± 0.7	32.1 ± 1.4
MY - 720 (68-102 phr)	26.2 ± 1.2	3.5 ± 1.4	29.8 ± 2.6
Epon - 828 (130-140 phr)	30.1 ± 0.6	2.5 ± 0.7	32.6 ± 1.4
Epon - 152 (106-144 phr)	27.1 ± 1.2	2.3 ± 1.5	29.4 ± 2.7
NMA*** Cure			
CY - 179 (62-74 phr)	34.3 ± 1.2	10.2 ± 1.4	44.4 ± 2.6
MY - 720 (52-66 phr)	35.5 ± 0.7	9.2 ± 0.8	44.6 ± 1.5
Epon - 152 (77-89 phr)	34.3 ± 0.8	7.8 ± 1.0	42.1 ± 1.8
DTA/Epon - 828 (12 phr, 24°C)	36.4 ± 0.7	8.5 ± 0.8	42.9 ± 1.5

*All values in erg/cm^2

**DDSA (dodecenyl succinic anhydride)

***NMA (nadic methyl anhydride)

TABLE II-A-2

MICROHARDNESS OF ANHYDRIDE-CURED EPOXIES

Resins	Microhardness (khn) NMA* Cure	DDSA** Cure
Aradite CY-179	22.0 ± 2.7	12.6 ± 1.0
Aradite MY-720	24.7 ± 2.3	14.4 ± 1.2
Epon - 152	25.6 ± 2.9	------
Epon - 828	-------	12.4 ± 0.4

*NMA (nadic methyl anhydride)

**DDSA (dodecenyl succinic anhydride)

liquids are known to obey this approximate model, however, where non-homologous series of liquids are used, the value of γ_c for a given solid is poorly defined because of scatter.

J. L. Gordon[7] observed that γ_c of polymers tends to increase with the solubility parameter, δ, and he related γ_c to the surface energy of a solid, γ, as:

$$\gamma = \gamma_c/\phi^2$$

where ϕ refers to the interaction between the polymer and the class of liquids used in the experiment.

L. H. Lee[6,7], by taking the entropy term into consideration in the modified heat-of-mixture equation, related γ_c

to the cohesive energy density, δ^2, and the molar volume, V_m, in the form of:

$$\delta^2 = 16.81 \frac{\left(\gamma_c / V_m^{1/3}\right)^{0.06}}{\phi^2}$$

where ϕ is a correction term for the deviation from the geometric mean model. Although γ_c is still a useful parameter in characterizing the surface of a solid, its full meaning still remains a matter of conjecture.

In this work, the critical surface energies, γ_c, of all the various epoxy and non-epoxide polymers studied, were always observed to be somewhere between the dispersive component of the surface energy and the total surface energy predicted by their geometric mean model.

Statistical analysis of the results indicated that, to a first approximation, γ_c can be expressed as a linear combination of the dispersive and polar components of the surface energy (see Figure II-A-1). This relationship can be conveniently expressed as:

$$\gamma_c = \gamma^d + \tfrac{1}{4}\gamma^p \qquad R^2 = 0.9759$$

$$N = 43$$

$$\text{Lim } \gamma_c \longrightarrow \gamma^d$$

$$\gamma^d \longrightarrow 0$$

It can be argued that dispersive interactions will always be fully operable and the full contribution of the dispersive

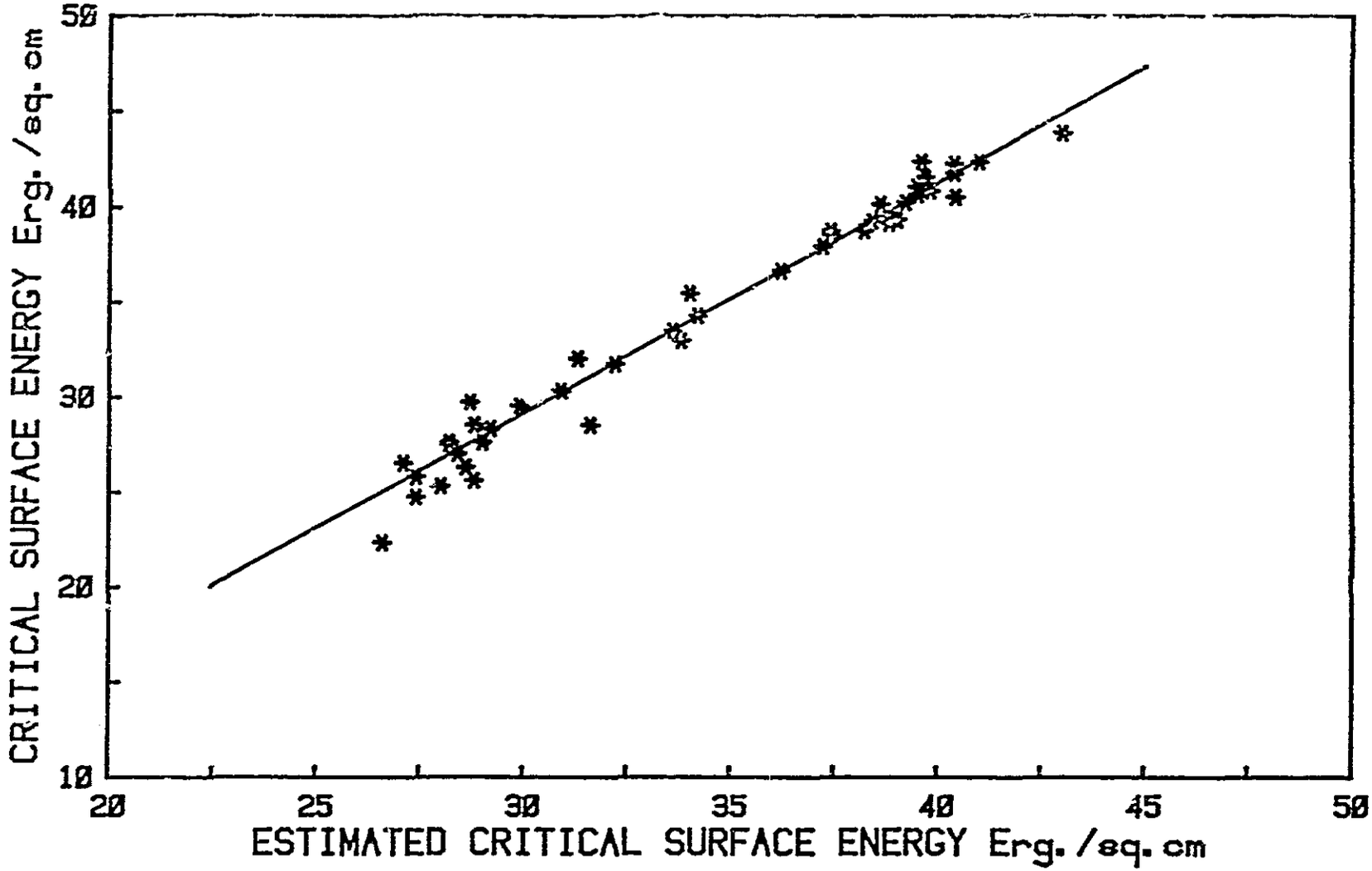

Figure II-A-1. Estimated Critical Surface Energy of Polymers

component of the surface energy is required. For a random polymer solid with a constituent polar group, free rotation is severely restricted. Hence, polar-polar interaction will be considerably less than that of less restricted dipoles, as in liquid-liquid or liquid-gel interactions. In the liquid phase of a polymer, any reorientation by one molecule will invariably involve the cooperation of neighboring molecules or chain ends. Thus, the consequent reduction in polar interaction is an entropic effect. These screening effects and the inability of the molecules at the solid surface to reorient themselves to the desired configuration in response to the contacting liquid are best represented at low temperatures, when only half the value of the nondispersive contribution is used.

The observed scatter in the experimental result is consistent with the standard deviations of the surface energy components of the liquids used in this study. From these results, a fundamental understanding of the interactions of fiber/resin interfaces is emerging. We hope to exploit this understanding during the next two report periods to determine if better interfaces can be designed.

4. Plans for Upcoming Period

Future work will be devoted to a systematic study of the interfacial bond between various low energy surfaces, to graphite fiber surface modification and to techniques to measure energy of fiber bundles.

5. References

1. Drzal, L. T., J. A. Mescher and D. L. Hall, "Carbon", Vol. 17, 1979, p. 375.

2. Hammer, G. E. and L. T. Drzal, "Applied Surface Science", Vol. 14, 1980, p. 340.

3. Ehrgurger, P. and J. B. Donnet, "Philosophical Transactions of Royal Society (London)", Series A, Vol. 294, 1980, p. 495.

4. Crammer, J. H., G. C. Tesoro and D. R. Uhlmann, "Ind. Eng. Chem. Prod. Res. Dev.", Vol. 21, 1982, pp. 185-190.

5. Diefendorf, R. J. and C. E. Uzoh, "Composite Structural Materials", 39th Semi-Annual Progress Report under NGL-33-018-003, May 1980 - September 1980, pp. 124-155.

6. Lee, L. H., "J. Applied Polymer Science", Vol. 12, 1968, p. 719.

7. Gordon, J. L. and J. P. Teas, "Solubility Parameter", Characterization of Coatings, Physical Technique II, R. R. Myers and J. S. Long, Eds., 1976.

8. Kaeble, D. H., "Physical Chemistry of Adhesion", Wiley Interscience, New York, 1971, pp. 84-188.

9. Lee, L. H. and K. Neville, "Handbook of Epoxy Resin", McGraw Hill, 1967, 5-23, 12-2.

10. Schroder, J., "Journal of Colloid and Interface Science". Vol. 72, No. 2, November 1979.

11. Good, R. J. and E. Elbing, "Ind. Eng. Chem.", Vol. 62, 1970, p. 54; Good, R. J., "J. Colloid and Interface Sci.", Vol. 59, 1977, p. 398.

12. Bruce, Davis W., "Journal of Colloid and Interface Science", Vol. 59, No. 3, May 1977.

13. "Interfacial Synthesis", Vols. I and II, F. Millich and C. E. Carraher, Jr., Marcel Dekker, Inc., New York, 1977.

6. Current Publications or Presentations by Professor Diefendorf on this Subject

"Physical, Thermal and Chemical Parameters Affecting the Development of Pitch Mesophase", with S-H. Chen, S. L. Eilenberg and D. M. Riggs.

Published in Carbon '82, Society of the Chemical Industry, London, 1982, pp. 180-184.

Presented at Carbon '82, London, UK, September 23, 1982.

"Discotic Liquid Crystals"

Presented at CFRC Meeting, Bonbanne, France, September 17, 1982.

PART III
COMPOSITE MATERIALS

III-A ADVANCED ANALYSIS METHODS

III-B FATIGUE IN COMPOSITE MATERIALS

III-C VISCOELASTIC CHARACTERIZATION OF IN SITU RESINS AND NEAT RESINS

III-D NUMERICAL INVESTIGATION OF MOISTURE EFFECTS

III-E NUMERICAL INVESTIGATION OF THE MICROMECHANICS OF COMPOSITE FRACTURE

III-A ADVANCED ANALYSIS METHODS

Senior Investigator: E. J. Brunelle

1. Introduction

The quest continues to find solutions for composite plates in terms of a minimum number of generalized variables. This approach continues to promise that a general parametric understanding of composite plates can be promulgated.

2. Status

The principal results of the last period are summarized as follows: (a) The relations governing the location of double frequencies were developed for a simply-supported orthotropic plate; (b) The general solution, in terms of the similarity variable $T = \frac{an}{bm}$, was presented for the static deformation, vibration and buckling of antisymmetric cross-ply plates with 52 boundary conditions and (c) The extremum solutions ($D^* = 0$) for antisymmetric cross-ply plates were outlined for arbitrary boundary conditions, and a sample solution was presented, namely, the minimum uniaxial buckling coefficient envelope versus affine aspect ratio (k_o versus a_o/b_o) for antisymmetric cross-ply plates with all four edges clamped.

3. Progress During Report Period

Progress in the last reporting period has been made principally in the following two areas.

First, the complete Karman-Rostovstev plate equations (including the in-plane and stress-strain laws) have been correctly restretched and several approximate solutions (as suggested by Donnell for the corresponding isotropic Karman equations) have been carried out as shown in Figures III-A-1 through 4.

Second, new material parameters R and X, defined as

$$R = (G_{12}/E_2)/\nu_{12}$$

$$X^2 = (E_1/E_2)/(\nu_{12})^2$$

have been used to express the fundamental plate parameters D*, ε and H*. These results are given by

$$D^* = \frac{1}{X}\left[1 + 2(1 - X^{-2})R\right]$$

$$\varepsilon = \left[1 + 2(1 - X^{-2})R\right]^{-1}$$

$$H^* = \frac{X}{2R} - \frac{1}{X} \qquad \text{Note: } X > (2R)^{\frac{1}{2}}$$

and using the values for fourteen materials collected from three sources (Tsai, Jones and Pipes) are plotted in Figure III-A-5 as three mini-figures. The range of the linear horizontal X scale is $0 \leq X \leq 30$ for all three mini-figures; the vertical one-cycle log scales for D*, ε and 1/H* go from .1 to 1.0 and the R parameter has values shown from .1 to 10.

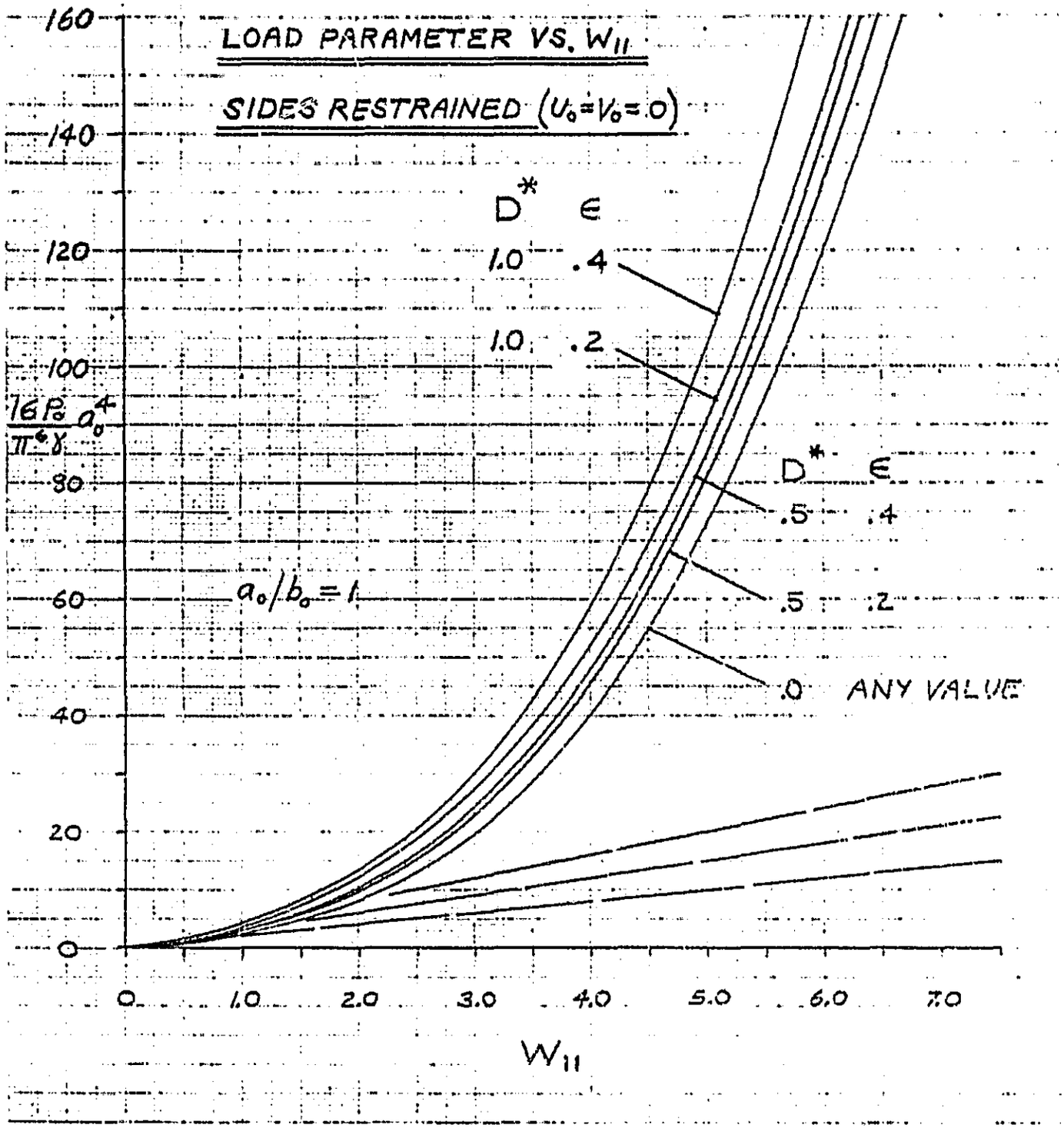

Figure III-A-1.

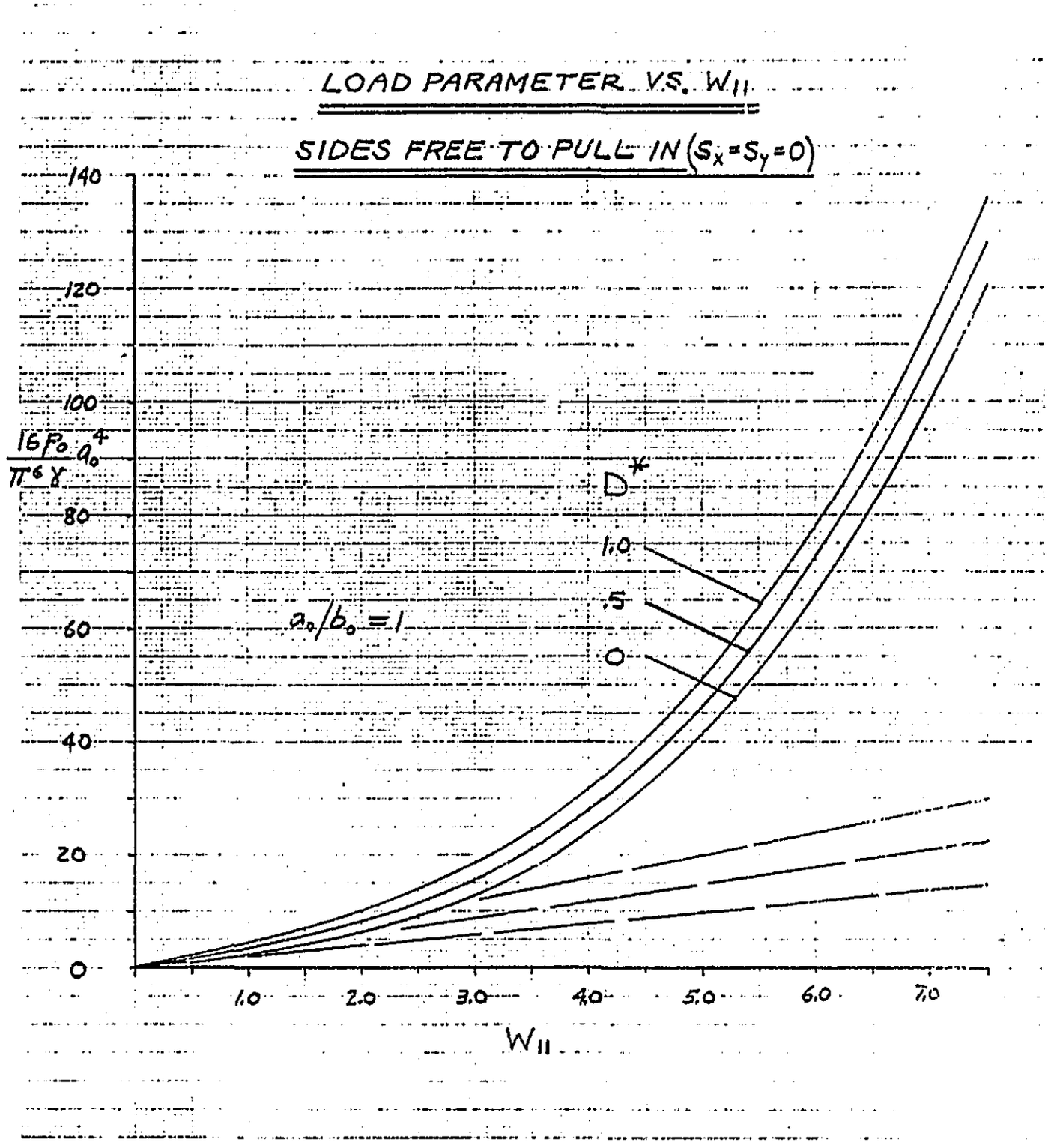

Figure III-A-2.

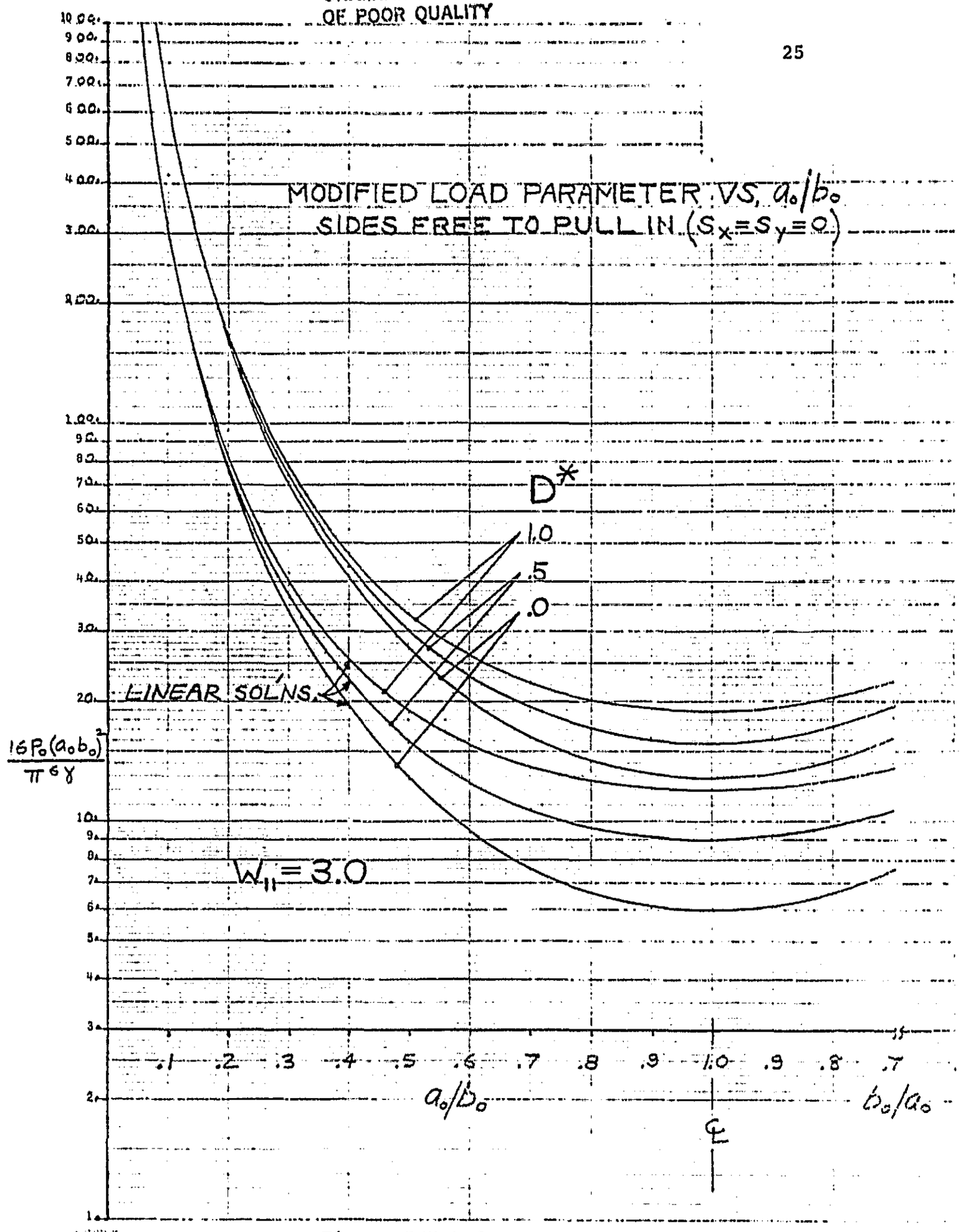

Figure III-A-3.

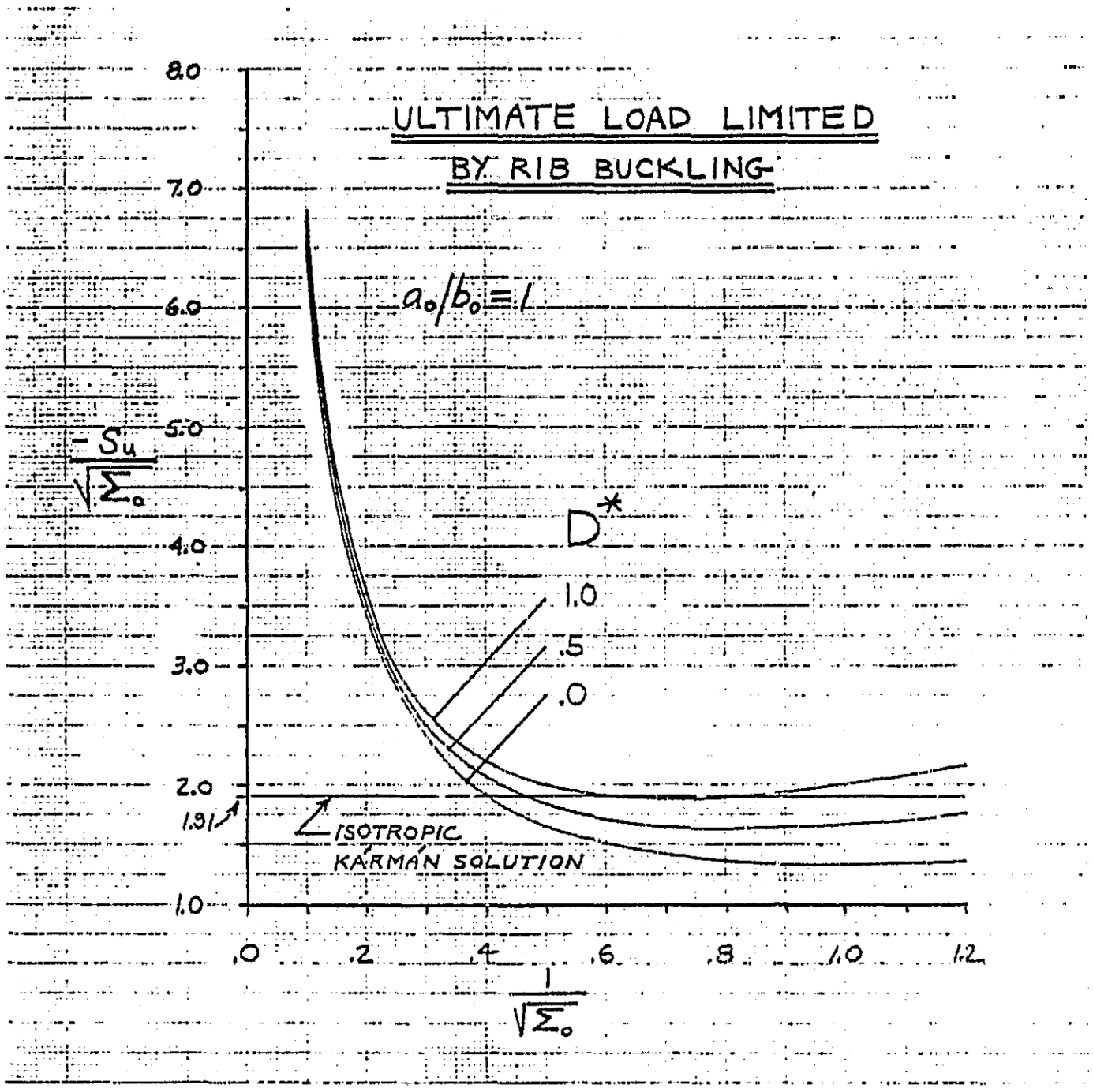

Figure III-A-4.

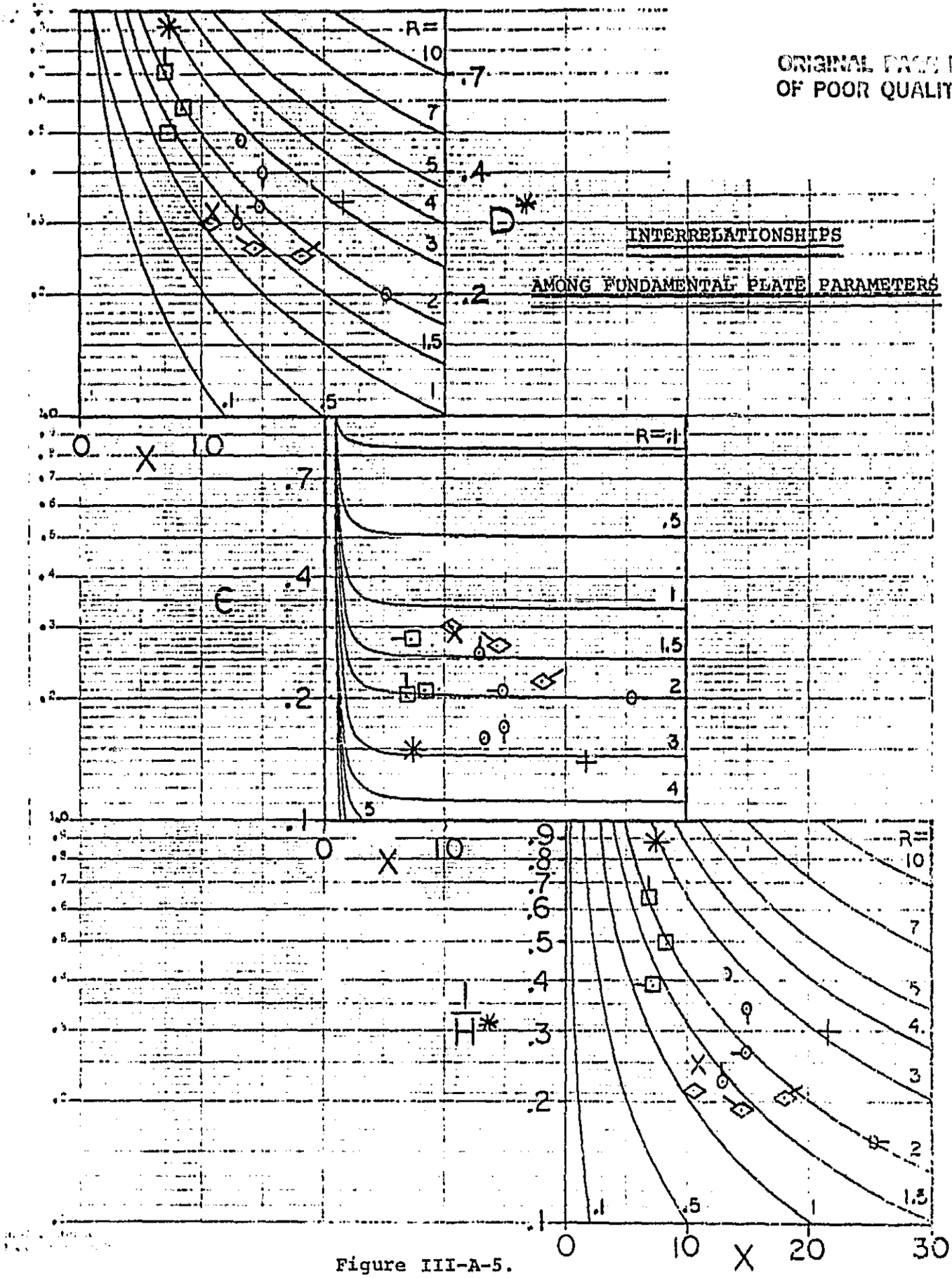

Figure III-A-5.

4. Plans for Upcoming Period

A general solution scheme will be attempted for cross-ply symmetric laminated plates, and an attempt will be made to extend the Karman-Rostovstev stretched equations for orthotropic plates to include cross-ply symmetric laminated plates. Also, extremum solution details will be scrutinized carefully in an effort to find similarity solutions for the orthotropic Mindlin plates (i.e., shear deformable plates).

5. Current Publications or Presentations by Professor Brunelle on this Subject

"Eigenvalue Similarity Rules for a Class of Rectangular Specially Orthotropic Laminated Plates"

Presented at the Ninth U. S. National Congress of Applied Mechanics, Ithaca, NY, June 21-25, 1982.

"A Similarity Variable for Generating the Frequency of Initially Stressed Specially Orthotropic Laminates"

To be presented at the AHS Composite Structures Specialist's Meeting, Philadelphia, PA, March 23-25, 1983.

"The Affine Equivalence of Local Stress Distributions in Damaged Composites and Batdorf's Electric Analogue"

To be submitted to the AIAA Journal, December 1982.

III-B FATIGUE IN COMPOSITE MATERIALS

Senior Investigator: E. Krempl

1. Introduction

The deformation and failure behavior of graphite-epoxy tubes under biaxial (tension, torsion) loading is being investigated with the assistance of Ph.D. candidate T.-M. Niu. The aim of this research is to provide basic understanding and design information on the biaxial response of graphite-epoxy composites.

2. Status

Using graphite-epoxy $[\pm 45]_s$ thin-walled tubes, the static axial and torsional strength were determined together with the elastic moduli. Fatigue tests under completely reversed, load-controlled axial loading showed comparatively poor axial fatigue strength; furthermore, fatigue life was affected by frequency. A paper on this subject has appeared in the Journal of Composite Materials[1]*.

3. Progress During Report Period

During the report period, the previously generated data were analyzed and interpreted. The analyses are contained in the forthcoming Doctor of Engineering thesis of Mr. Niu's.

Of particular interest was the observation of time-dependent effects in axial and combined axial-torsion cyclic loading.

---

*Numbers in brackets in this section refer to the references which are listed on page 35.

a. Time-Dependence of Deformation

The deformation behavior of the $[\pm 45]_s$ thin-walled graphite-epoxy tubes was found to be characterized by a fiber-controlled torsional and a matrix-controlled axial behavior. It was shown[1] that significant time-dependent deformation ensued at stress levels exceeding twenty-five percent of the axial ultimate strength while, in torsion, time dependent effects were negligible.

The studies of time-dependent deformation during biaxial loading can be obtained from in-phase multistep creep and relaxation tests. These tests were performed in an MTS servo-controlled testing machine controlled by an MTS 463 Data/ Control Processor.

After stabilizing the properties of the specimen by applying two completely reversed triangular loading cycles, multistep creep or relaxation loadings were then performed in the next two cycles under load or strain control in in-phase loading; i.e., with maximum torsion applied at the same instant as maximum axial load. The amplitude of the oscillatory load or displacement was held constant at 0, 50 and 100 percent of the maximum value to be used in the tests. The frequency was chosen to be 0.05 Hz. The hold time for each step was 9 cycles or 180 seconds.

In the case of in-phase loading, the stress component angle, θ, in the σ-τ plane was chosen to be 131°. The negative twist then coincides with the tensile stretch, thus eliminating

the torsional buckling. The test results show that local buckling, in fact, did not occur (see the τ-γ diagram in Figure III-B-1). In both hysteresis loops, the most pronounced creep strains were observed at the stress level extremes of cycles 3 and 4. It was observed that the creep strains at zero stress level are not the smallest encountered. Due to fiber dominance of deformation, the torsional creep strain at each step is much less than the corresponding axial strain.

By switching the control mode from stress to strain in the same running program, multistep in-phase relaxation can be studied. The strain component angle, θ', in ε-γ plane was chosen to be 162°. The hysteresis loops at a frequency of 0.05 Hz for torsion and axial deformation are shown in Figure III-B-2. The maximum relaxed stresses, $\Delta\tau$ and $\Delta\sigma$, were found at the extrema of the strain levels. Again, the relaxed shear stress at each step is less than the corresponding relaxed axial stress.

In-phase, load-controlled loading applied along θ = 49° constitutes the most severe loading for the occurrence of local buckling. In this case the negative twist and the compression occur simultaneously. The hysteresis loops for such a loading are shown in Figure III-B-3. The creep effects in the tensile part developed similarly to those shown in Figure III-B-1, and the torsional creep strains for positive torque are generally small. When, at cycle 3, creep hold times were introduced, local torsional buckling was observed at the

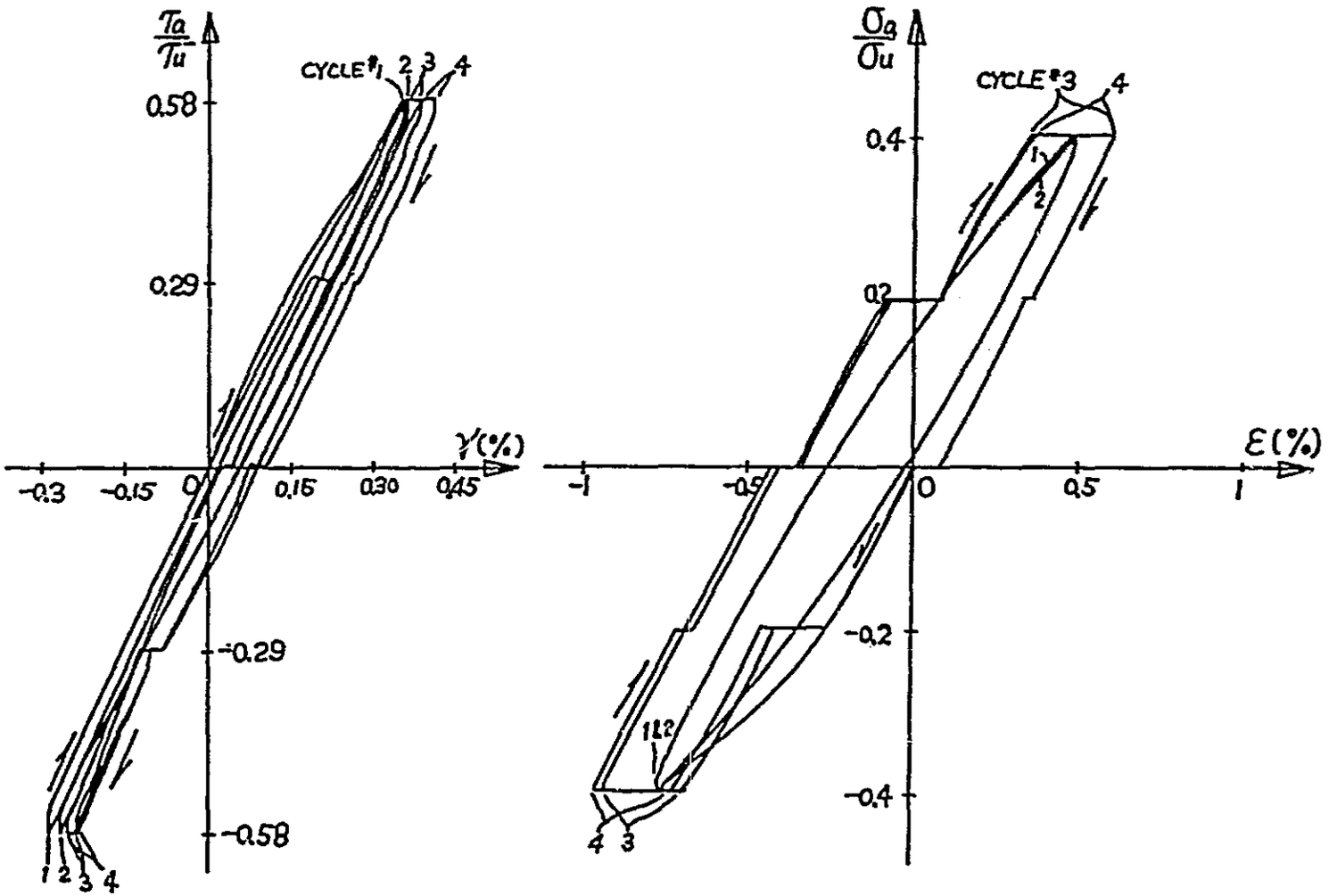

Figure III-B-1. Hysteresis Loops during In-phase Multistep Creep, Three-Minute Periods of Creep, Freq. = 0.05 Hz, $\theta = 131°$ in the σ-τ Plane (Tube 88).

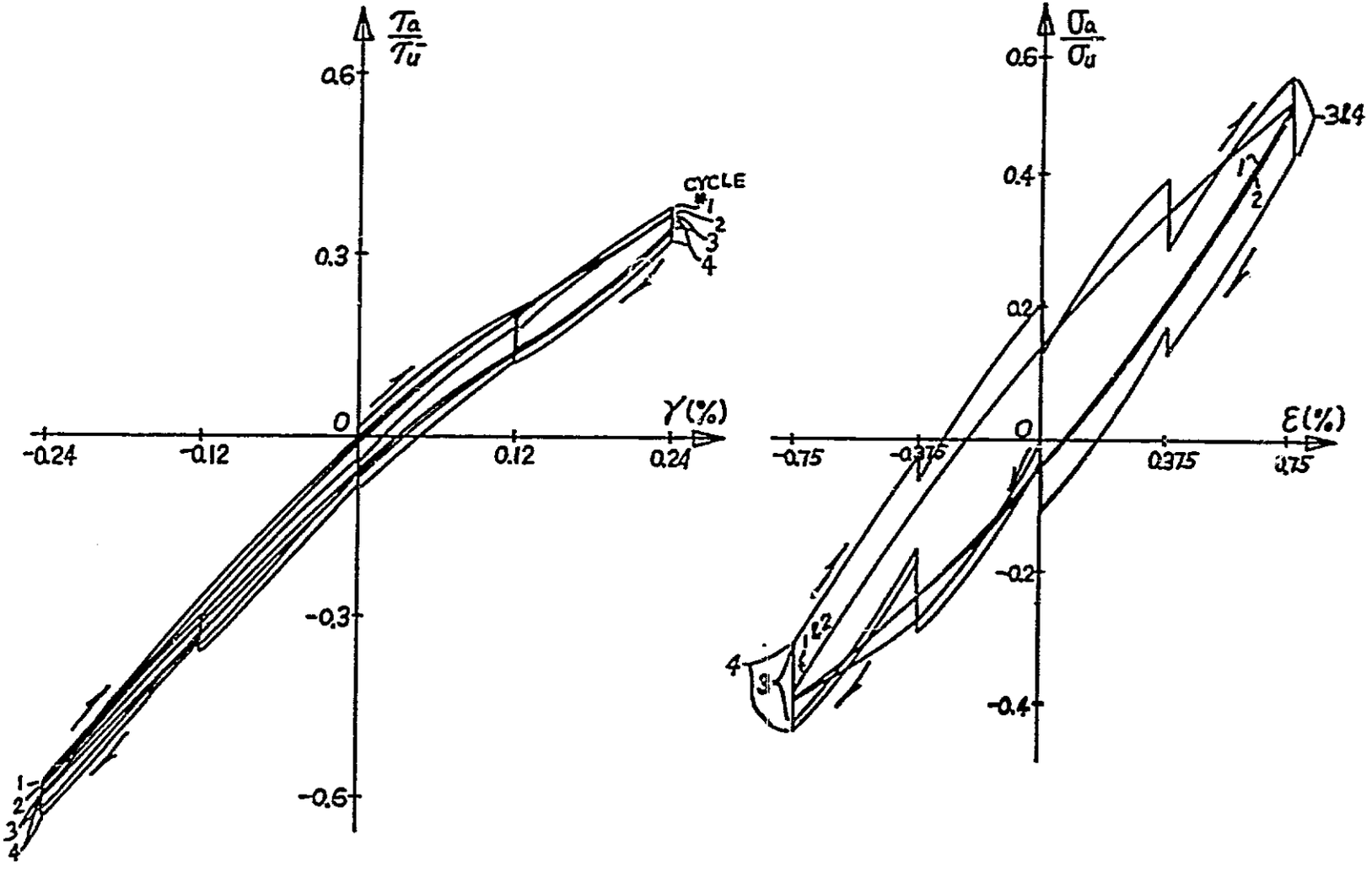

Figure III-B-2. Hysteresis Loops during In-phase Multistep Relaxation, Three-Minute Periods of Relaxation, Freq. = 0.05 Hz, $\theta' = 162°$ in the ε-γ plane (Tube 88).

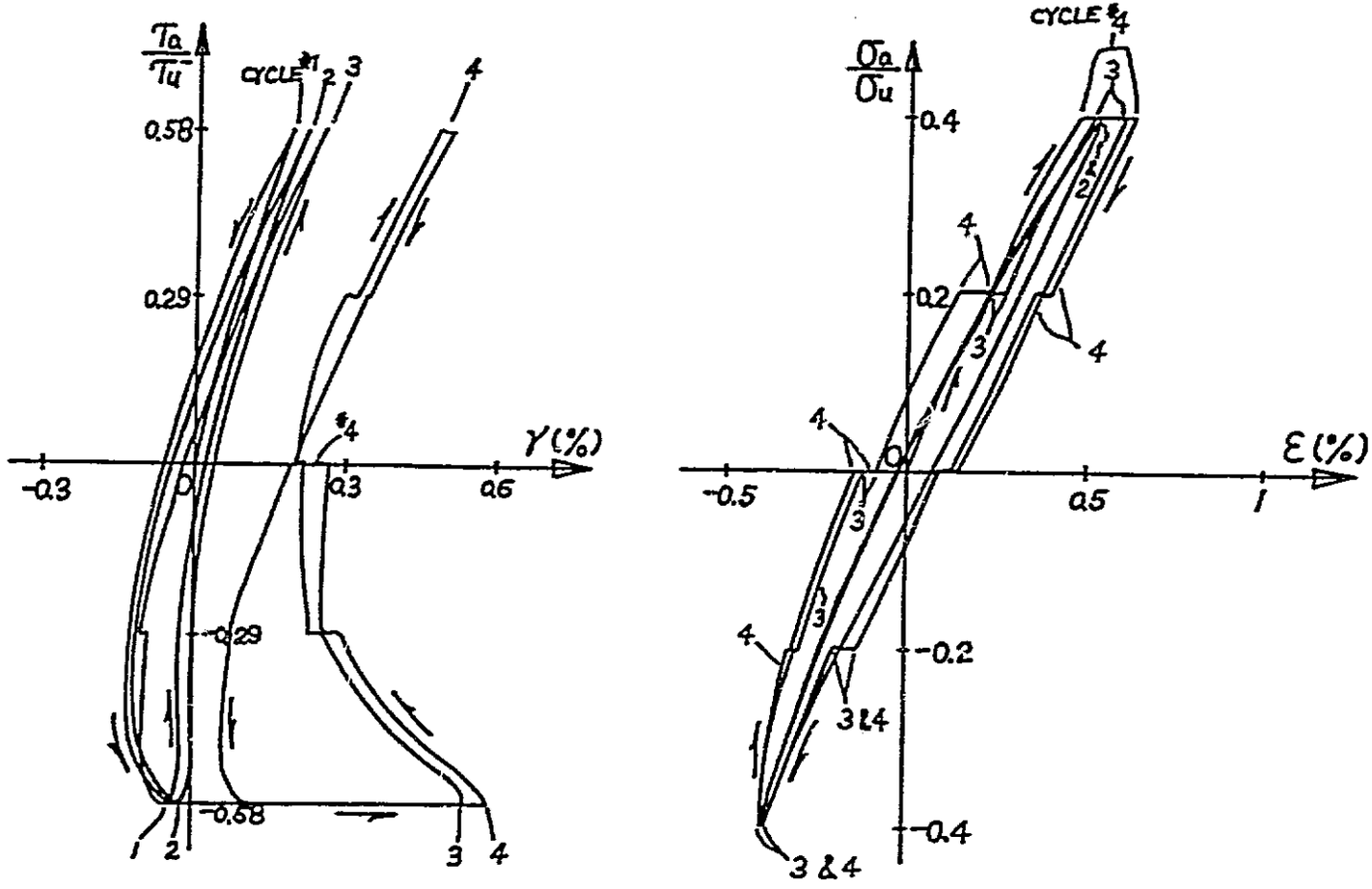

Figure III-B-3. Hysteresis Loops during In-phase Multistep Creep, Three-Minute Periods of Creep, Freq. = 0.05 Hz, $\theta = 49°$ in the σ-τ plane (Tube 88).

minimum load level - as evidenced by the increase of shear strain (see points 2 and 3 in Figure III-B-3). On subsequent cycles the torsional creep strain repeated itself. This example shows that time-dependent effects can be found even under fiber controlled deformation, when combined loading is imposed.

4. Plans for Upcoming Period

The properties of tubes with a new lay-up $[0/\pm45]_s$ of graphite-epoxy material will be determined. In this case, axial and torsional deformation are fiber dominated. The fabrication of several batches of this new specimen is in progress. Subsequently, the static and fatigue properties of this tube will be explored.

5. References

1. Krempl, E. and T.-M. Niu, Journal of Composite Materials, Vol 16, 1982, pp. 172-187.

6. Current Publications or Presentations by Professor Krempl on this Subject

"Biaxial In-Phase and Out-of-Phase Behavior of Graphite-Epoxy Tubes"

To be presented at the ASTM Conference on Biaxial/Multiaxial Fatigue, San Francisco, California, December 15-17, 1982.

III-C VISCOELASTIC CHARACTERIZATION OF IN SITU RESINS AND NEAT RESINS

Senior Investigator: S. S. Sternstein

1. Introduction

This project is concerned with those properties of high performance composites which are strongly dependent on the physical properties of the matrix resin. To date, the research has involved the precise viscoelastic characterization of epoxy neat resins, interlaminar failure of composites and the inhomogeneous swelling of and the effects of moisture on composites.

2. Status

The effects of moisture uptake in neat resins and composites on the viscoelastic characteristics (loss factor, dispersion anomolies and location of the glass transition of the matrix) of various samples has been investigated. The composite samples have been tested using the centro-symmetric deformation (CSD) geometry described previously. Samples were cut from laminates having a $(0/90)_{3s}$ stacking sequence and prepared from prepreg material s plied by the Fiberite Corporation (HYE1048A1E). Neat resin samples were tested in uniaxial tension using thin rectangular strips.

3. Progress During Report Period

A set of composite samples exposed for various periods of time to a boiling water environment were tested (prior to

any drying history) and the in-phase (storage) stiffness (M') results are shown in Figure III-C-1 versus weight gain moisture). The values of M' are normalized by the value of M' for the dry sample and also normalized by the cube of the thickness for the wet sample (as tested). It is clear that at about 2.5% moisture pickup, the slope of the curve markedly increases, suggesting a change in the structure-moisture interaction mechanism.

The results of a similar set of experiments on neat resins is shown in Figure III-C-2, where the slope change is also obvious, but occurs at about 7% moisture. Since the composite samples are about 35% resin, this suggests that the slope change in the composite is due to the excessive softening of the matrix and is, therefore, matrix controlled. The variation of loss factor (M''/M' or the so-called tan δ) with weight gain for the neat resin samples is given in Figure III-C-3. The ordinate represents the increase (or increment) in loss factor which is obtained in a wet sample relative to a dry sample.

During the previous report period, we reported that large permanent increases in loss factor and decreases in stiffness occur when a wet composite sample is dried and then tested. This effect (hysteresis) does not occur, or is minimal, in the neat resin samples. Thus, in Figure III-C-3 a dried sample would lie on the curve shown and not exhibit a large residual loss factor. For the reader's convenience,

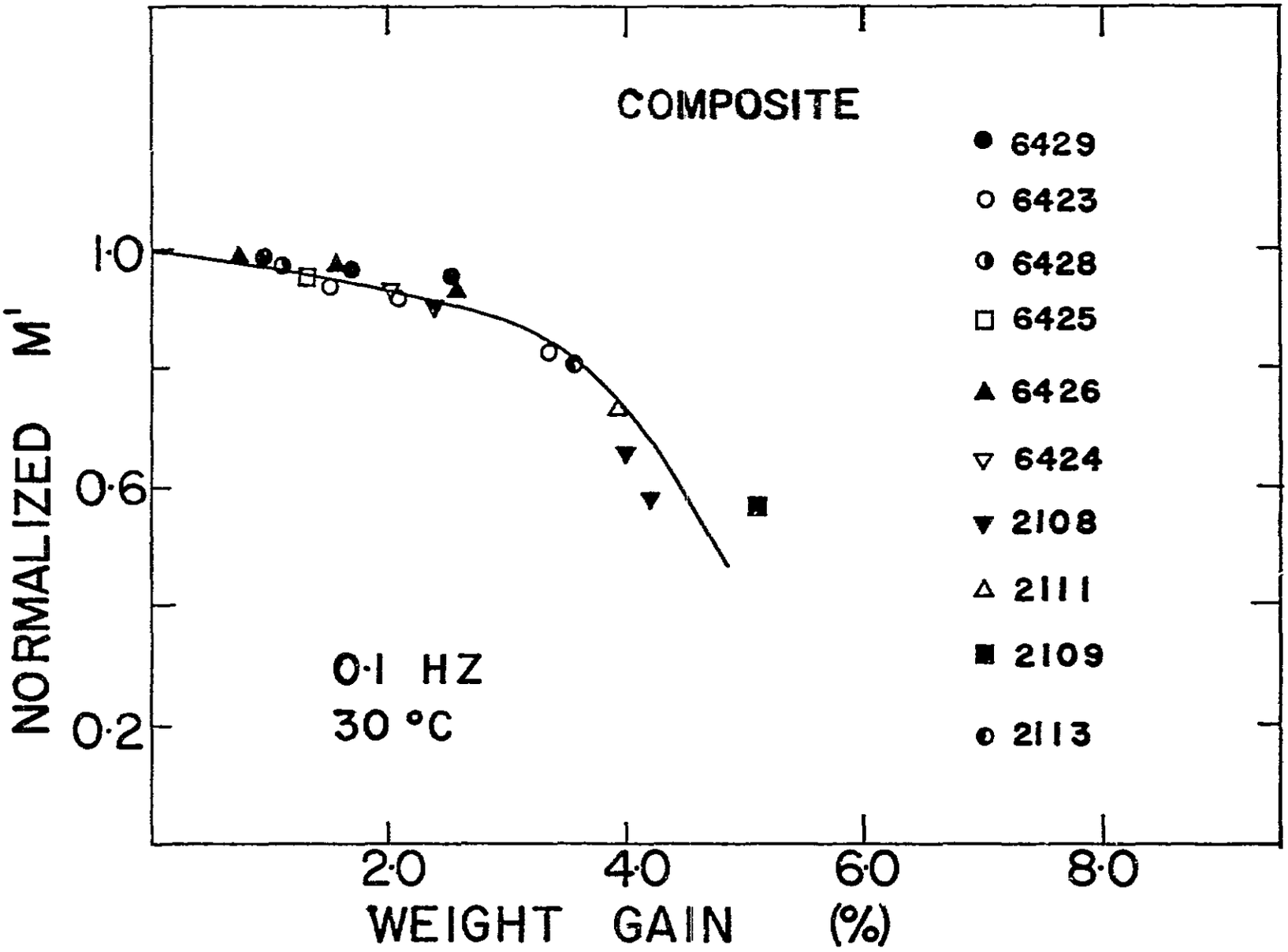

Figure III-C-1.

Normalized Storage Modulus Vs. Moisture Weight Gain for Composite Laminates

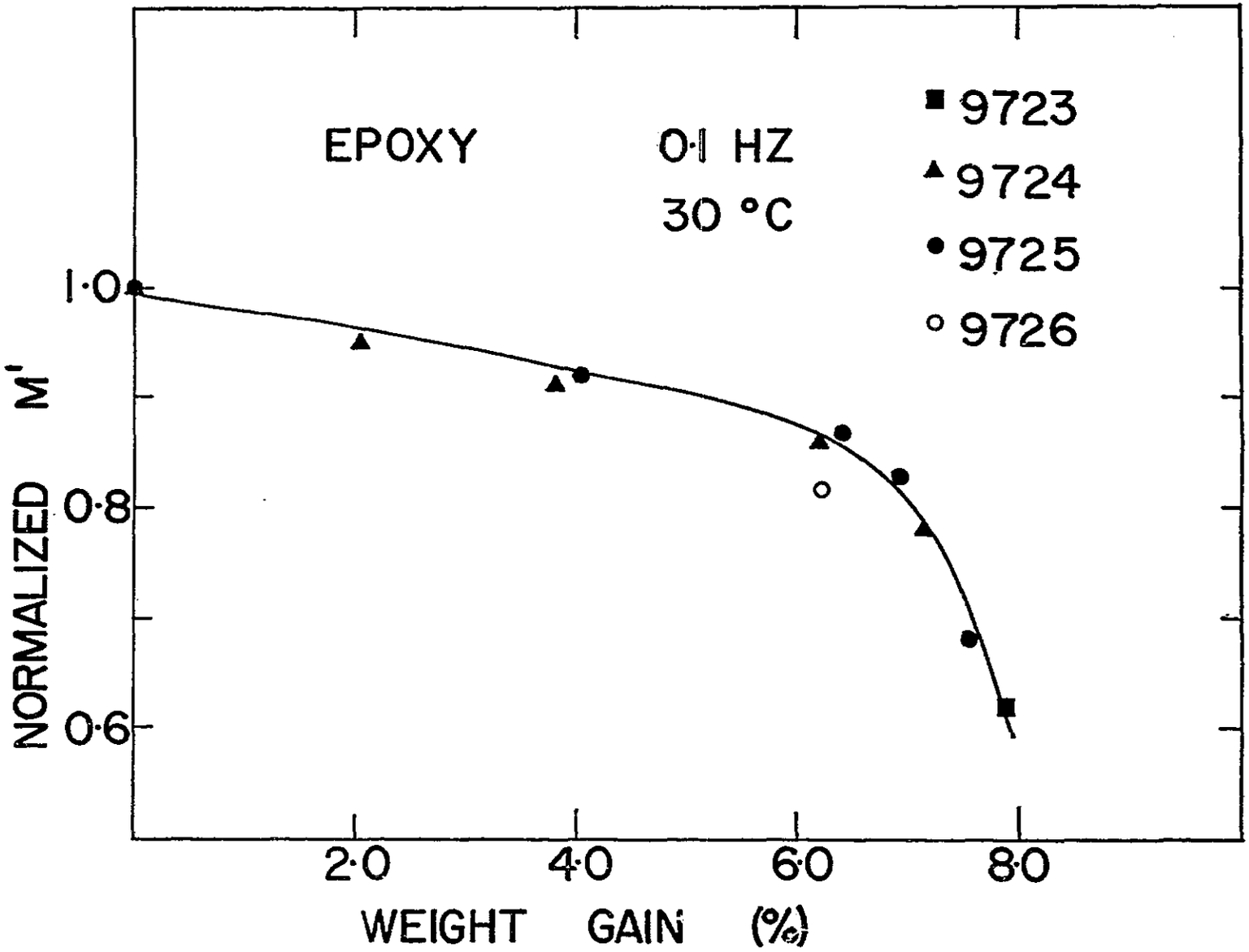

Figure III-C-2.
Normalized Storage Modulus Vs. Moisture Weight Gain for Neat Resins

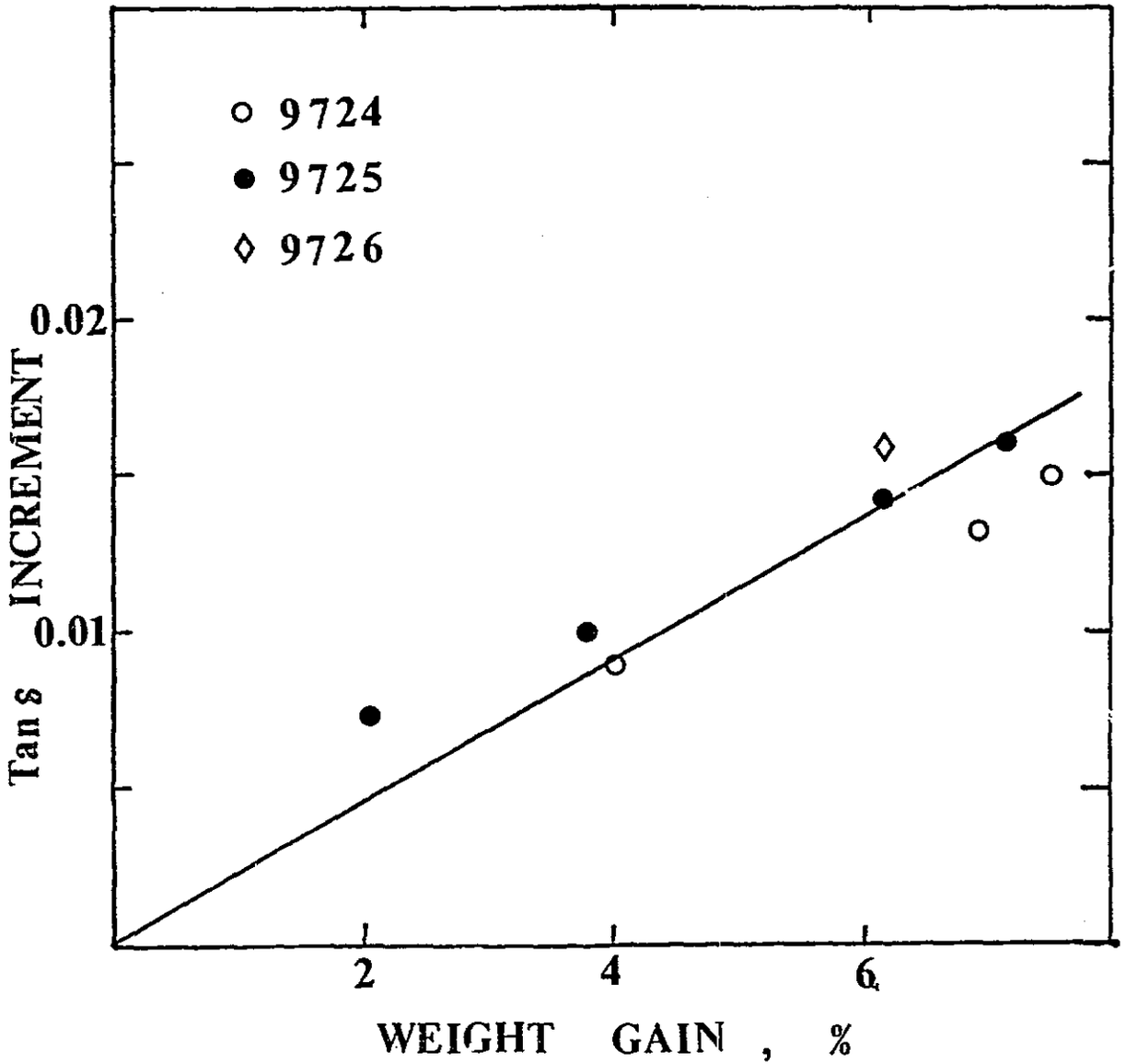

Figure III-C-3.
Variation of Loss Factor (m"/m') with Moisture Weight Gain for Neat Resins

Figure III-C-4 is a repeat of our previous result on loss factor hysteresis for composites.

The stoichiometric relationship between the stiffness-moisture relationship of the composite (Figure III-C-1) and the neat resin (Figure III-C-2), the absence of drying hysteresis on the loss factor of the neat resin (Figure III-C-3) and the presence of hysteresis in the composite (Figure III-C-4) suggest that (a) the matrix stiffness is a significant factor in the out-of-plane stiffness of the composite; (b) matrix stiffness is very nonlinear with respect to moisture content and a significant mechanism change occurs at about 7% moisture content (resin basis - 948) and (c) drying hysteresis in the composite represents a failure mechanism either between the fibers and matrix and/or delamination.

4. Plans for Upcoming Period

It is planned to conclude this study of moisture uptake and drying effects on neat resins and composites and to supplement the mechanical data with suitable microscopic evidence of the failure patterns.

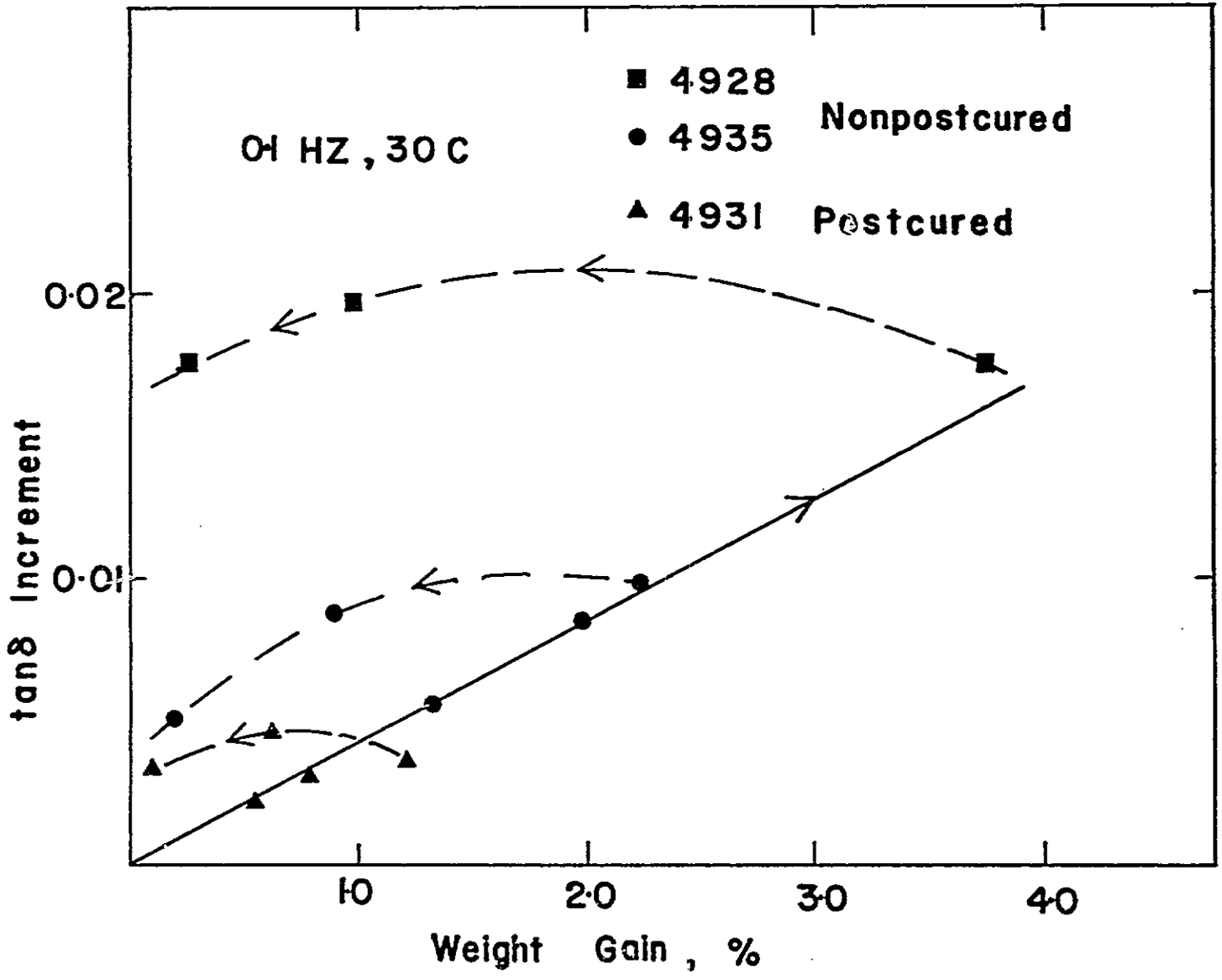

Figure III-C-4. Summary Comparison of Carbon/Epoxy Specimen Loss Moduli (with moisture level and history as a parameter)

III-D NUMERICAL INVESTIGATION OF MOISTURE EFFECTS

Senior Investigator: M. S. Shephard

1. Introduction

This analysis builds on the theoretical developments of Professor S. Sternstein (reported in progress reports dated December '79 and June '80) in which the fully-coupled, nonlinear thermomechanical equations of inhomogeneous swelling of composites in the presence of moisture and temperature are analyzed. Here the one-dimensional case of a single fiber in an infinite matrix has been extended to two-dimensional, multiple fiber cases with far field stresses.

2. Status

As discussed in earlier progress reports, moisture effects were introduced into the problem through a nonlinear constitutive relation, the principle of virtual displacements was employed to develop a nonlinear matrix equation using displacement-based finite elements and these nonlinear equations were solved using quasi-Newton methods. Subsequently, the constitutive equation was built into the finite element analysis. The results of a single fiber comparison analysis and two fiber analysis were also given.

3. Progress During Report Period

During the last reporting period, graduate student Frida Lumban-Tobing has continued to run addition problems and to

collect data on both the results obtained and the computer solution times required using different quasi-Newton updates. The additional cases run include a four-fiber square pack arrangement and a seven-fiber hexagonal pack arrangement. Both cases considered one radius fiber spacing under 100% humidity conditions, with and without far field stresses.

a. Example of Problems

a.1) Square Packed Four Fiber Case. Figure III-D-1 shows the basic model considered for the case of four fibers in a square pack at a one radius spacing while Figure III-D-2 shows the finite element mesh of six-noded quadratic isoparametric elements for the quarter of the plate that was considered. The cases analyzed for this configuration included zero far field stress and various combinations of uniform non-zero far field stress, all at 100% humidity.

There is a strong interaction between the fiber and matrix for the zero load case, as indicated in Figure III-D-3, which shows a set of maximum principal stress contours in the area directly around the fiber. The peak stress values in the matrix for this case are approximately 25% higher than for the unloaded single fiber case presented previously.

Three different loading cases were considered for this problem under 100% humidity. The first was a uniform load in one direction (PX), uniform loads of the same sign in both directions (PX = PY) and opposite uniform loads in both

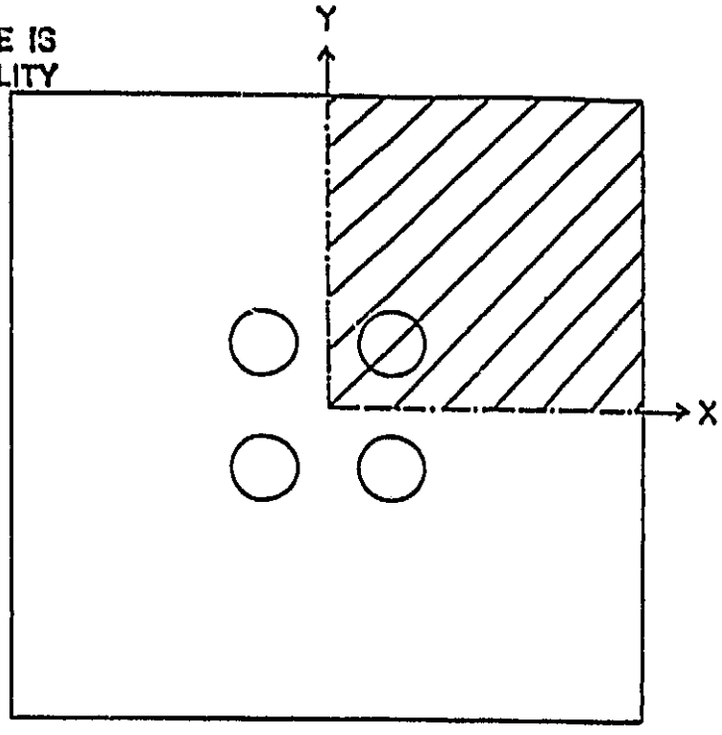

Figure III-D-1 Square Packed Geometry Configuration

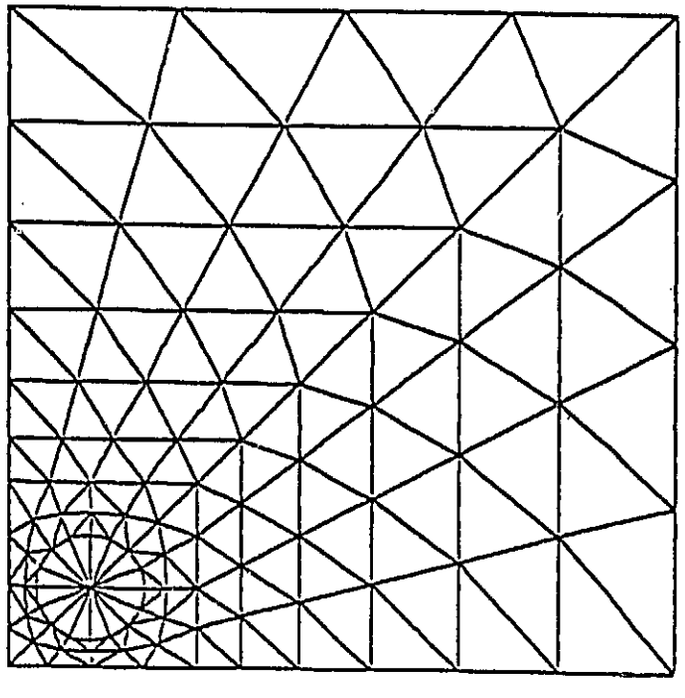

Figure III-D-2 Square Packed Finite Element Mesh

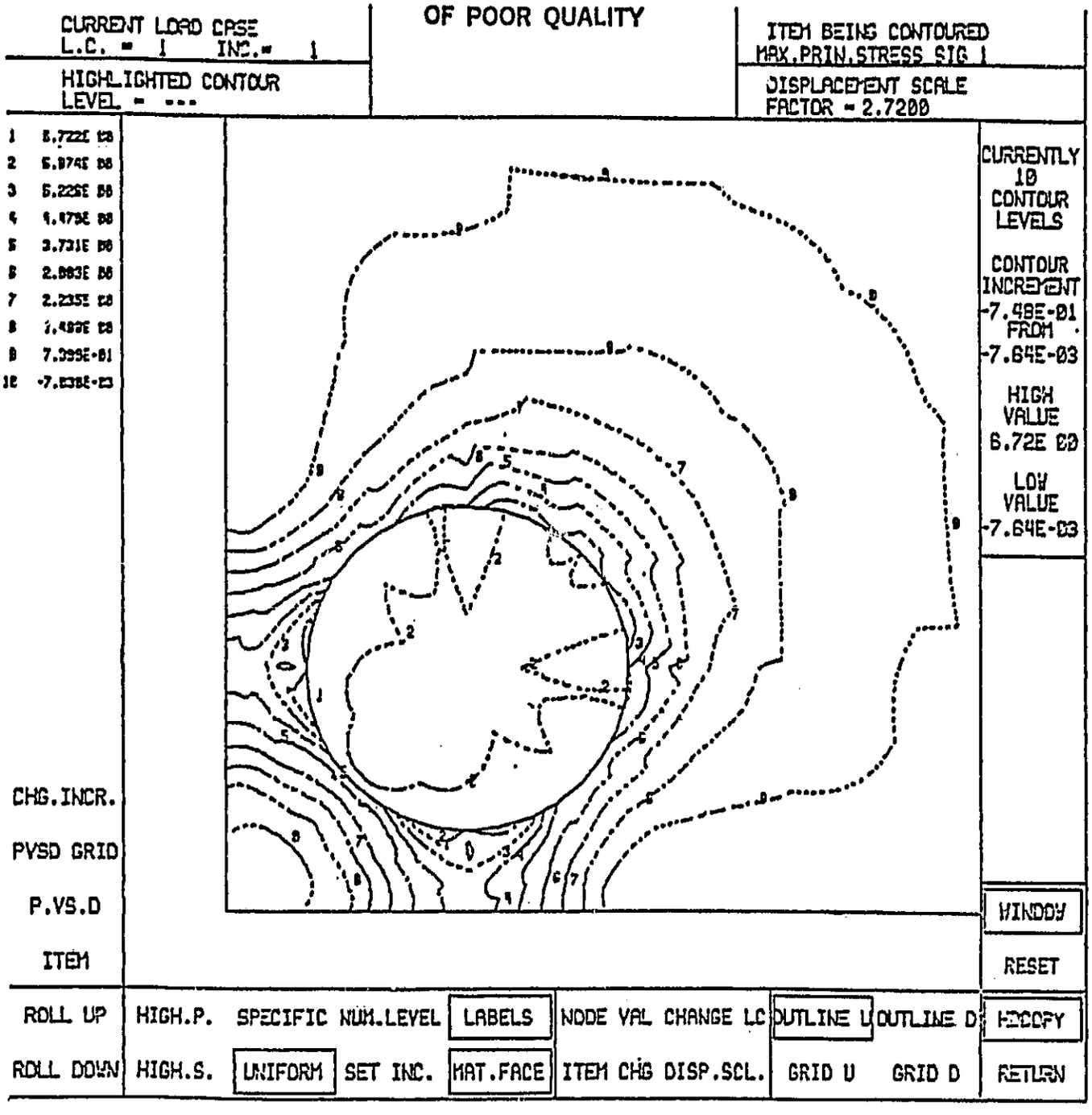

Figure III-D-3 Maximum Principal Stress Contours in Area of Fiber for Square Packed Case

directions (PX = -PY). Figure III-D-4 summarizes the results for these load cases. This figure plots the maximum value of the first principal stress obtained at any point in the matrix as a function of load for the various load cases. The trends are similar to those obtained for the two fiber case with the highest stresses occurring for the case of PX = -PY.

a.2) Hexagonal Packed Seven Fiber Case. Figure III-D-5 shows the basic model considered for this case using a minimum fiber spacing of one radius. The mesh of six-noded quadratic isoparametric triangles used to analyze this case is shown in Figure III-D-6. The cases analyzed for this configuration also include zero far field stress and various combinations of non-zero far field stress at 100% humidity.

Again there is a strong interaction between the fiber and matrix for the zero load case, as indicated in Figure III-D-7, which shows a set of maximum principal stress contours in the area around the fiber. The peak stress value in the matrix for this case is 10% higher than the one fiber case.

Four different 100% humidity loading cases were considered for this problem. They are uniform x-direction load (PX), uniform y-direction load (PY), uniform loads of the same sign in the x- and y-direction (PX = PY) and uniform loads of opposite signs in the two directions (PX = -PY).

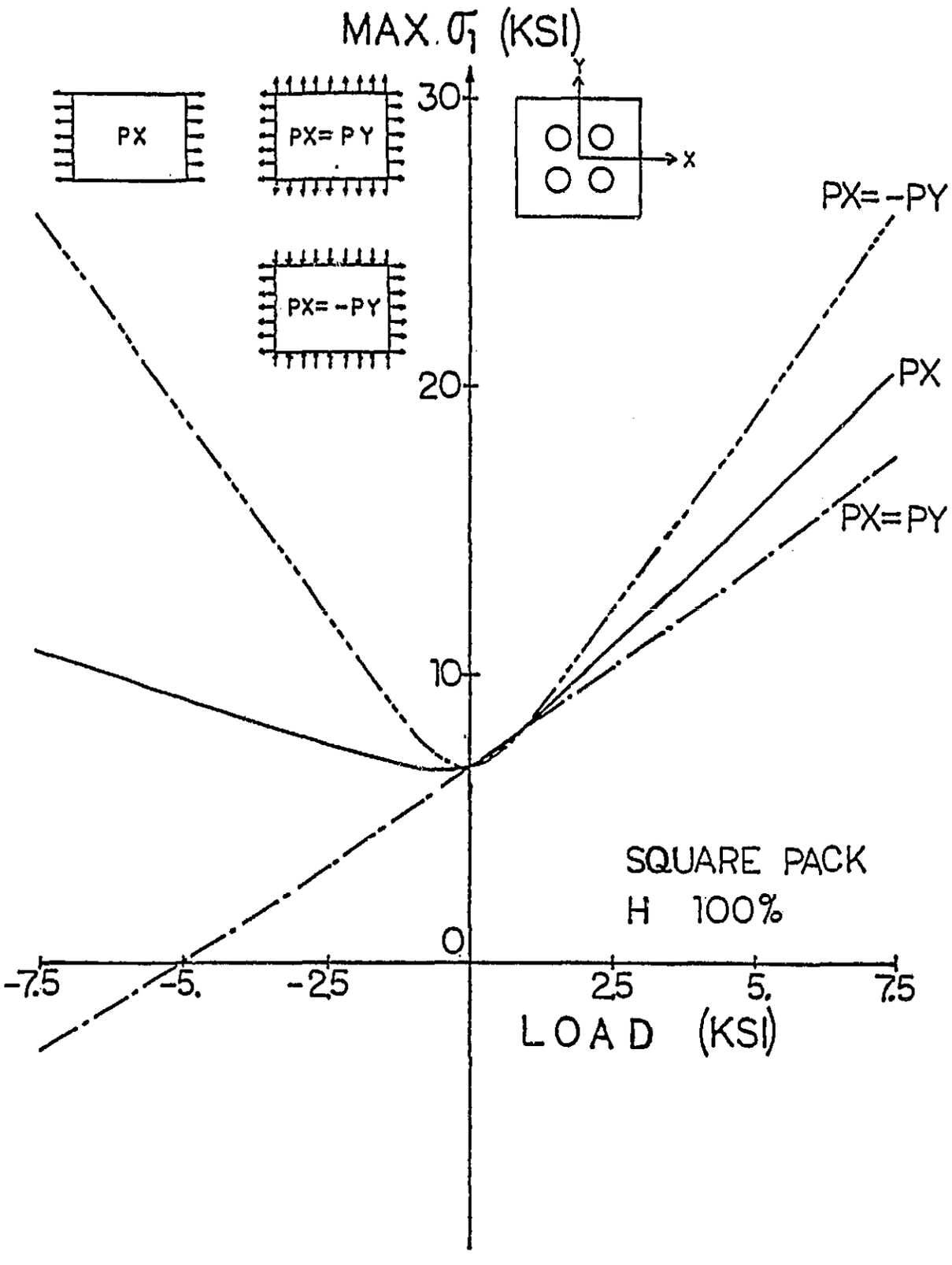

Figure III-D-4 Plot of Peak Value of First Principal Stress as Function of Applied Load For the Square Packed Case

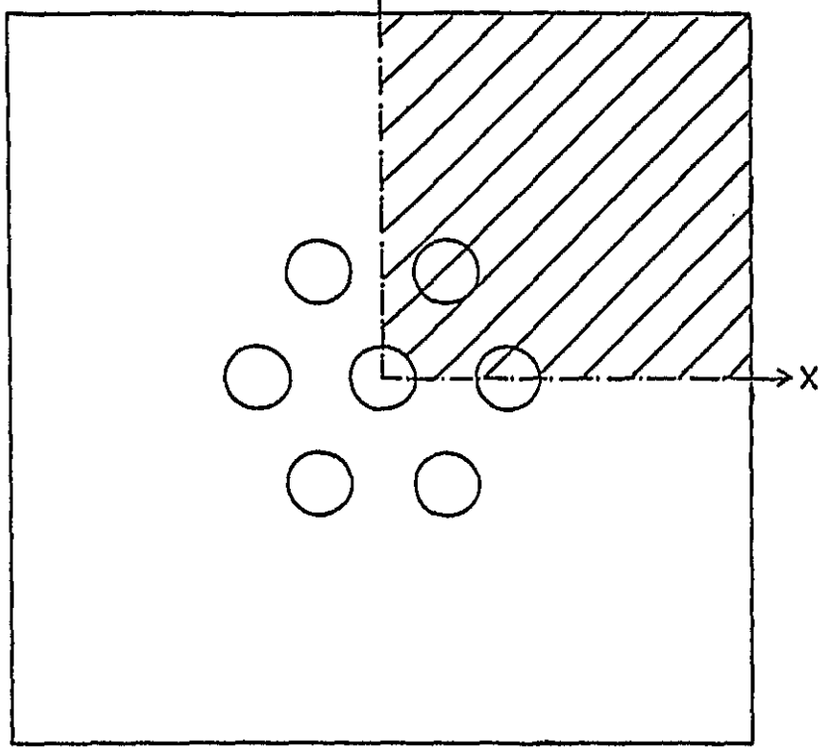

Figure III-D-5 Hexagonal Packed Geometry Configuration

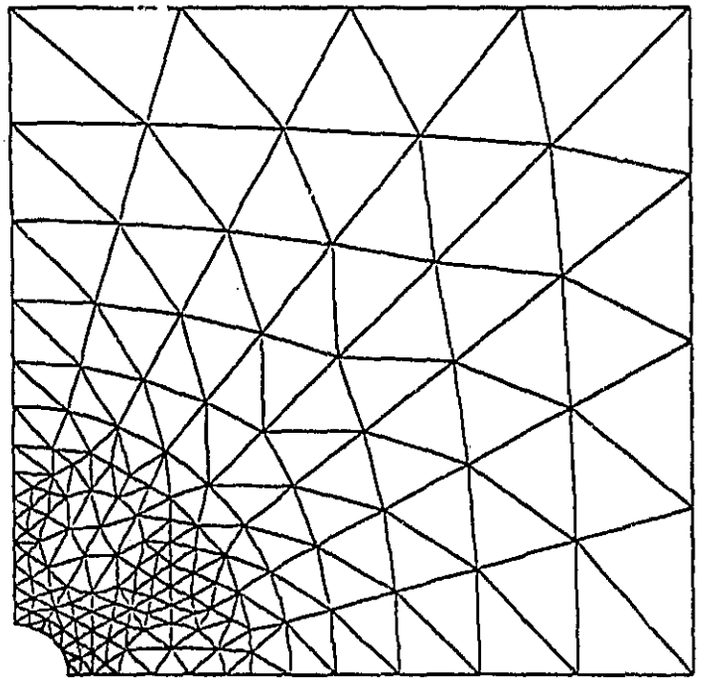

Figure III-D-6 Hexagonal Packed Finite Element Mesh

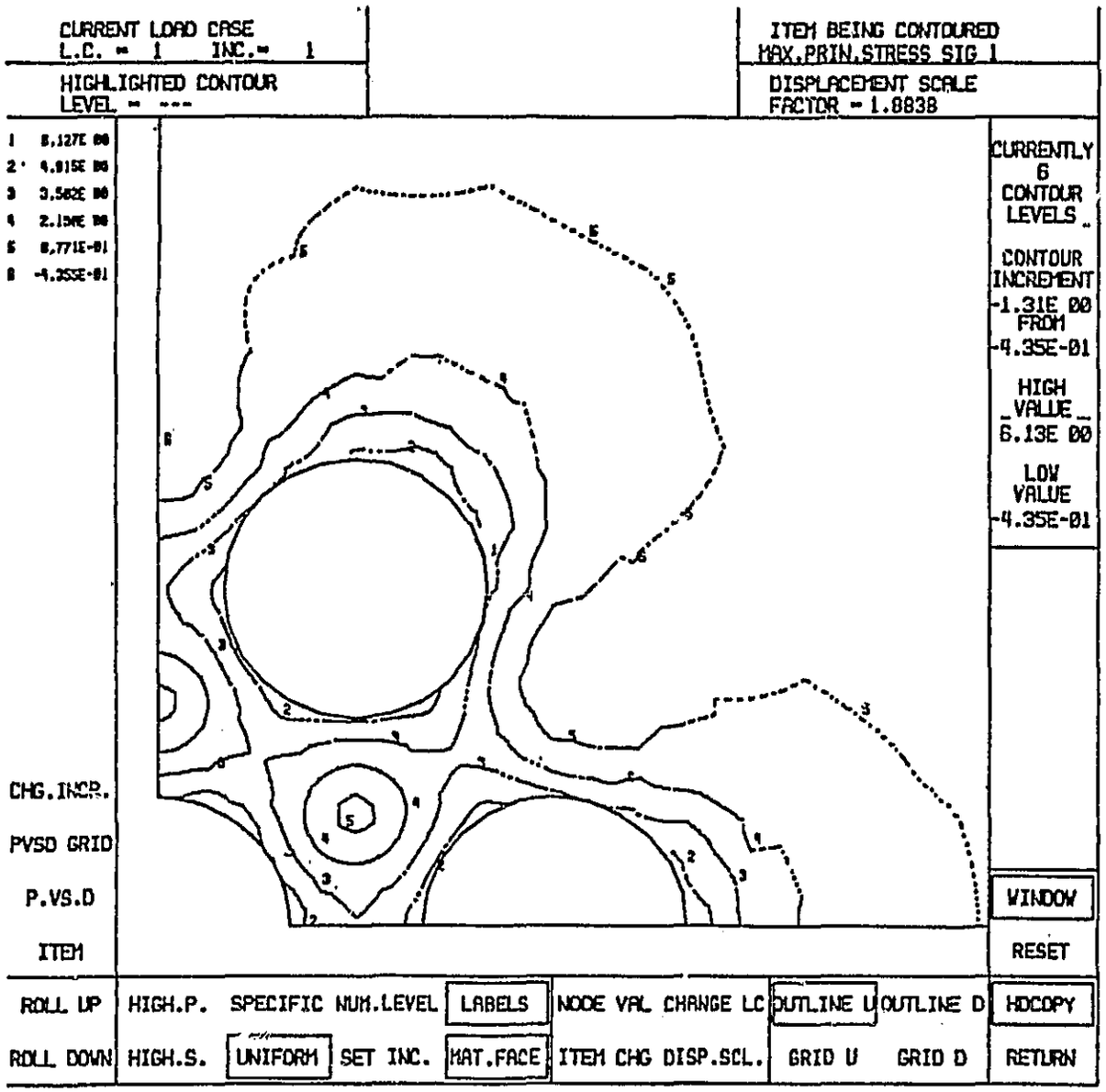

Figure III-D-7 Maximum Principal Stress Contours in Area of the Fiber for the Hexagonal Packed Case

Figure III-D-8 summarizes the results for these four load cases. This figure plots the maximum value of the first principal stress obtained at any point in the matrix as a function of load level. These trends are similar to those obtained for the two fiber and four fiber cases.

b. Comparison of Solution Techniques

The previous progress report discussed the various quasi-Newton update methods used in the program. During this reporting period, a study was done to determine the relative efficiency of the Davidon, Broyden and BFGS updates. Table III-D-1 gives a comparison of the number of operations required in the calculation of the increment step at the k^{th} iteration and the addition storage required past the initial triangulation for the three update methods and a standard Newton method. As can be seen from this table, the Newton method requires far more operations per step than any of the quasi-Newton updates.

Consideration of the convergence characteristics, Table III-D-2, indicates that the quasi-Newton methods require much less computer time than a standard Newton method, with the Davidon update requiring less than one-half the time. A comparison of the three updates indicates that the Davidon update required the least number of iterations, fewer line searches and the least computer time. Thus, it is concluded that the Davison update is the most efficient for this problem.

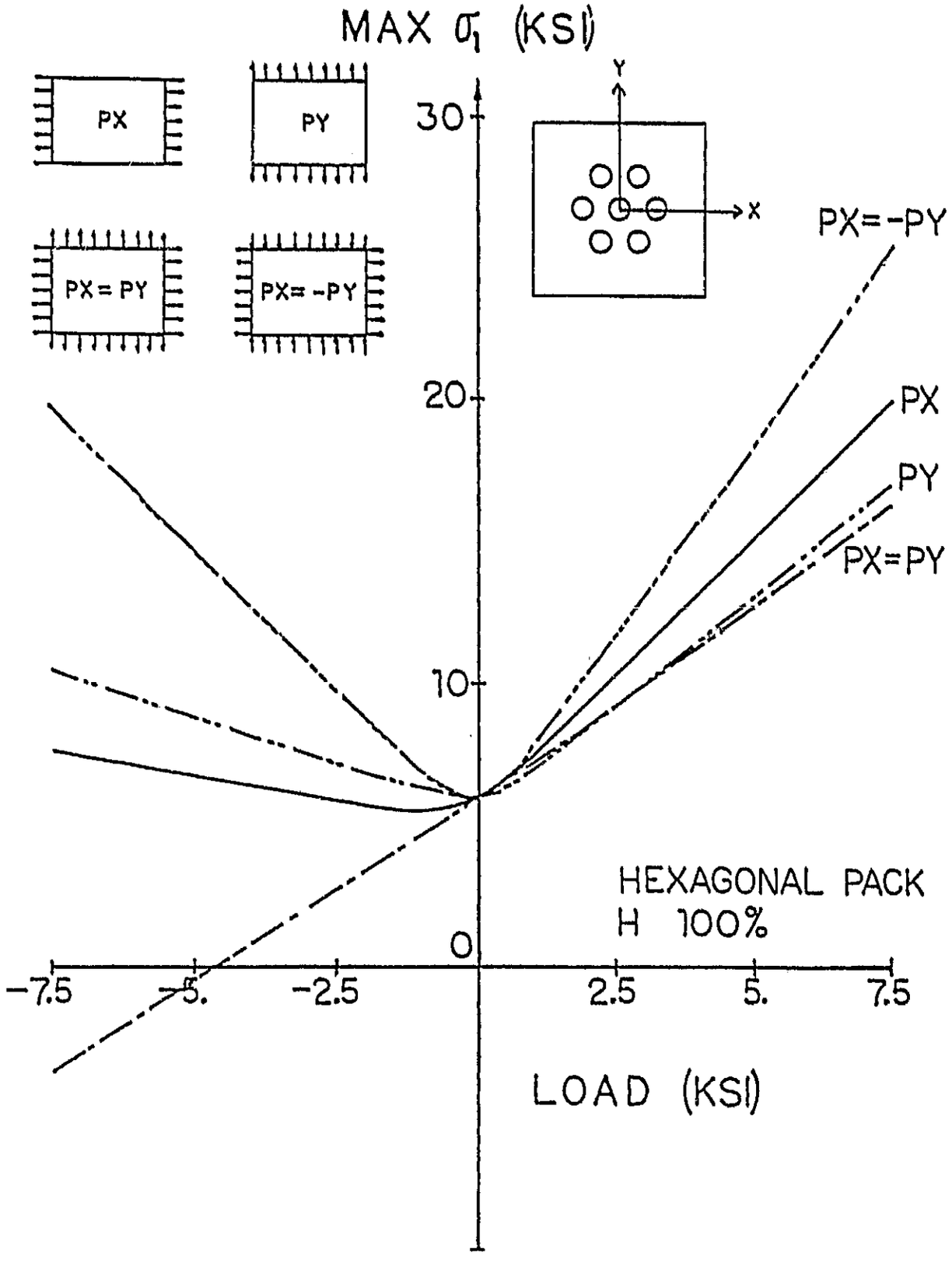

Figure III-D-8 Plot of Peak Value of First Principal Stress as a Function of Applied Load for the Hexagonal Packed Case

TABLE III-D-1

OPERATION COUNTS AND ADDITIONAL STORAGE

Method	No. of Multiplications	No. of Divisions	No. of Square Roots	Additional Storage
Newton	$mk\left[\frac{1}{2}n^2 - \frac{1}{3}\frac{n^3}{m} + \frac{2}{3}\frac{n^2}{m} - \frac{1}{2} - \frac{n}{6m}\right]$	$k(n-1)\left(m - \frac{n}{2}\right)$	------	------
Davidon	$mk(k+3)$	$k\left(\frac{1}{2}k + \frac{1}{2}\right)$	------	$k(m+1)$
Broyden	$mk(k+3)$	k	------	$k(2m)$
BFGS	$mk\left(2k + 4 + \frac{k}{m}\right)$	$k(2)$	k	$k(2m)$

Calculation of increment step at k^{th} iteration

m = Number of equations

n = Bandwidth

TABLE III-D-2

CONVERGENCE COMPARISON

Problem	Method	CPU*	No. of Iterations	No. of Searches
Hexagonal Pack	Davidon	17:21	9	1
P = 0	Broyden	20:26	9	5
H = 100%	BFGS	21:32	11	4
$(V_1)_{start} = 0.05$	Newton	38:40	8	6
Square Pack	Davidon	10:55	10	3
$P_x = 7.5$	Broyden	14:34	14	5
H = 100%	BFGS	14:48	16	3
$\underset{\sim}{\Delta}_o = (\underset{\sim}{\Delta})_{p=0}$				
Two Fibers	Davidon	6:51	10	6
(distance 10R apart)	Broyden	15:07	19	19
P = 0	BFGS	9:13	11	11
H = 50%				
$(V_1)_{start} = 0.024$				

*Times in minutes and seconds on a PRIME 500 computer

4. Plans for Upcoming Period

During the next reporting period, Frida Lumban-Tobing will be finishing the final analysis studies and concluding her doctoral research on this topic.

5. Current Publications or Presentations by Professor Shephard on this Subject

"Finite Element Analysis of Moisture Effects in Graphite-Epoxy Composites", with F. E. Lumban-Tobing and S. S. Sternstein.

To be published in Advances and Trends in Structural and Solid Mechanics, A. K. Noor and J. M. Housner, Eds., October 1982 and Computers and Structures, 1983.

To be presented at the Symposium on Advances and Trends in Structural and Solid Mechanics, Washington, D. C. by F. E. Lumban-Tobing, October 4, 1982.

III-E NUMERICAL INVESTIGATION OF THE MICROMECHANICS OF COMPOSITE FRACTURE

Senior Investigator: M. S. Shephard

1. Introduction

To understand the mechanisms of failure in composites it is necessary to develop insight into the micromechanical behavior, including interactions between matrix and fibers as the load is increased from zero to that corresponding to failure. Investigations of these phenomena, either experimental or numerical, are difficult. The purpose of this project, being carried out by graduate student Nabil Yehia, is to develop a nonlinear finite element analysis capability for performing numerical investigations of the micromechanical failure of composites.

2. Status

The overall structure of a general purpose finite element code for fracture problems has been designed and is currently being implemented and tested. The major design considerations for the program are that it can accomodate various types of fracture problems and house a variety of algorithmic approaches to fracture and debonding analysis. The linear portion of the program has been coded and tested. The initial fracture criteria have been selected and are currently being implemented.

3. Progress During Report Period

During the last reporting period, effort has been concentrated on implementing and testing the initial computational models for fracture mechanics computations. The areas under current consideration are the introduction of the singular elements, the determination of first cracking in an isotropic material, calculation of the crack tip stress intensity factors and the determination of the direction of crack propagation.

a. Singular Elements

This is the simplest of the fracture criteria to implement, since proper elastic crack tip singular elements can be obtained from the standard quadratic isoparametric elements by the proper positioning of the node points[1,2]*. Thus, a module has been placed in the program that will position the nodes of all elements at the crack tip in the proper position. Tests have been run on both the singular quadratic isoparametric triangle and collapsed quadratic isoparametric quadrilateral. The triangular element checked out very well, while the collapsed quadrilateral demonstrated some minor problems in satisfying equilibrium. This problem is currently being investigated.

*Numbers in brackets in this section refer to the references which are listed on page 65.

b. Determination of First Cracking

As mentioned in the previous progress report, the program is being designed to consider the possibility of a crack initiating under the action of the applied load. Thus far the maximum tangential stress criteron has been implemented and checked. This criterion predicts that a crack will start when the maximum tangential stress exceeds a specified value.

c. Calculation of Stress Intensity Values

The stress intensity factors K_I and K_{II} are being computed by the displacement method[3] which uses the local displacements along the crack surface and the two singular elements on that surface. The major advantage of this approach is that its local nature makes it straightforward to use in a variety of situations.

To test this module, the example problem suggested in Reference [4] was analyzed. The geometry and dimensions used in the analysis are shown in Figure III-E-1. This problem is a pure mode I situation with an accepted formula for the stress intensity factor[4]. Figure III-E-2 shows the geometry analyzed and conditions applied. The numerical results obtained indicate that good results can be obtained for a reasonable number of elements. However, seemingly minor changes to the mesh layout can play an important role in determining the accuracy of the result.

Figures III-E-3 and -4 show a typical element mesh used to analyze the problem. The error in K_I obtained using this

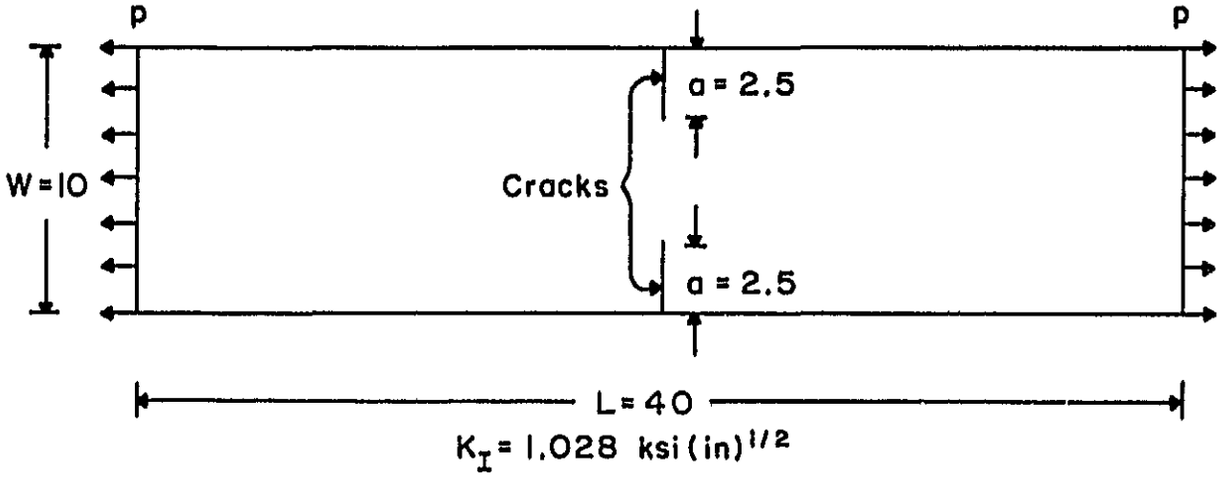

Figure III-E-1. Geometry of Double Cracked Plate

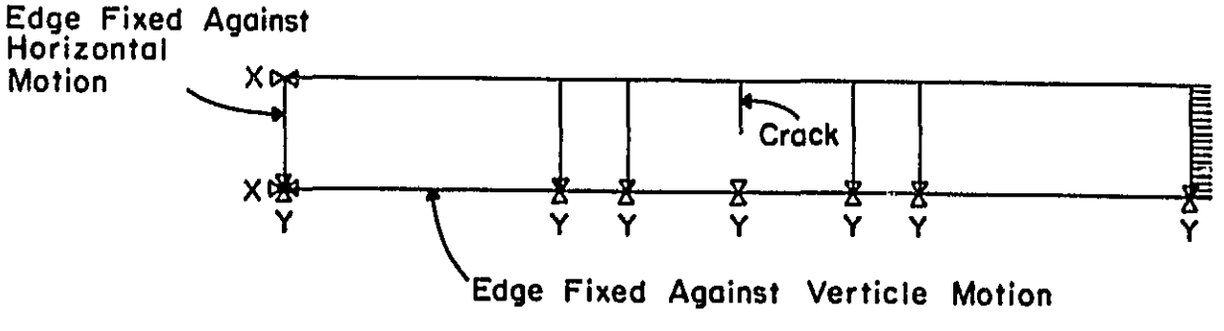

Figure III-E-2. Basic Idealization Used for the Finite Element Analysis of Double Cracked Plate

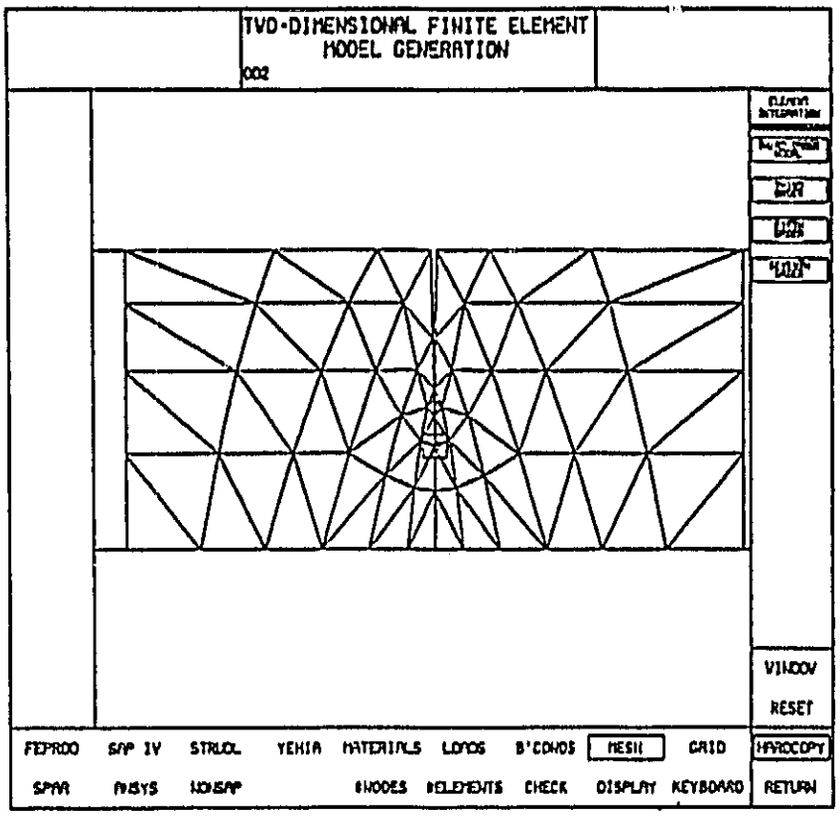

Figure III-E-3. Finite Element Mesh in Middle Section of Double Cracked Plate

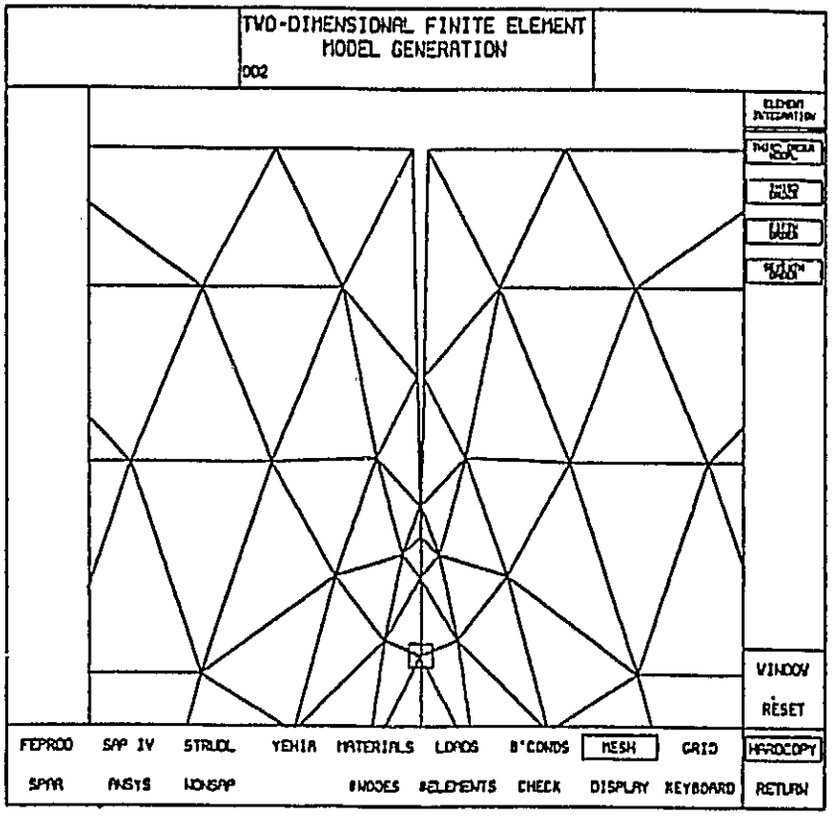

Figure III-E-4. Close-up of Finite Element Mesh in Area for Double Cracked Plate

basic mesh configuration, but changing the grading of the elements along the crack, ranged from 18.6% to 0.19%. The reason for this variation has yet to be confirmed, but two factors are considered important. One of the factors is the well-known influence of ratio of the length of singular element edge to the length of the crack. The other, which is currently being considered, is the shape of the singular elements. These aspects will be investigated further, and the results obtained will be considered in the development of future meshes to insure accurate results.

d. Determination of Direction of Crack Growth

The purpose of this module is to determine the direction of crack growth after it has been determined that the crack will propagate. The minimum strain energy factor criterion[5,6] is being applied in this prediction. This has been implemented and tested on the example problem discussed immediately above. The proper results were obtained, however, further testing is required.

4. Plans for Upcoming Period

During the next reporting period, effort will concentrate on continued implementing and testing of the various modules required for crack initiation and propagation problems. In addition, some specific micromechanical analyses will be carried out on composites that can be properly represented with those features available in the program.

5. References

1. Barsoum, R. S., "On the Use of Isoparametric Finite Elements in Linear Fracture Mechanics", Int. J. Num. Meth. Engng., Vol. 10, 1976, pp. 25-37.

2. Barsoum, R. S., "Triangular Quarter-Point Elements as Elastic and Perfectly-Plastic Crack Tip Elements", Int. J. Num. Meth. Engng., Vol. 11, 1977, pp. 87-98.

3. Ingraffia, R. A. and C. Manu, "Stress-Intensity Factor Computation in Three Dimensions with Quarter-Point Element". Int. J. Num. Meth. Engng., Vol. 15, 1980, pp. 1426-1445.

4. Brown, William T., Jr. and S. E. Srawley, "Plane Strain Crack Toughness Testing of High Strength Metallic Materials", ASTM, STP 410, 1966.

5. Sih, G. C., "Strain-Energy Density Factor Applied to Mixed Mode Crack Problems", Int. J. Fracture, Vol. 10, No. 3, September 1974, pp. 305-321.

6. Sih, G. C., "Mechanics of Ductile Fracture", Fracture Mechanics and Technology, G. C. Sih and C. L. Ches, Eds., Vol. II, 1977, pp. 767-784.

PART IV
GENERIC STRUCTURAL ELEMENTS

IV-A MECHANICAL JOINTS IN COMPOSITES

1. Analysis of Heavily Loaded Mechanical Joints
2. Pin-Loaded Holes in Uniform Composite Plates
3. Compact Lug Design
4. Failure Criteria for Stress Concentrations

IV-B SCALING EFFECTS IN TESTING COMPOSITE STRUCTURES

IV-C END EFFECT DECAY IN PRISMATIC MEMBERS

INTRODUCTION

The redesign of flight-critical structural components currently in service as metal parts on existing aircraft was included in earlier stages of RPI's composite materials and structures program to assure relevance and realism to the project's direction and to contribute to the nation's pool of innovative structural design concepts. Two such components were selected in cooperation with major commercial airframe manufacturers, Boeing Commercial Airplane Company and Lockheed California Company, and with advice from NASA. The first was the 727 airplane's elevator actuator attachment rib, and the second was the wing-mounted engine drag strut for the L-1011 airplane. In previous progress reports, several areas of research in which results were needed for such redesigns - but were not then available - were identified. From among those, several which continue to represent gaps in needed technology are under investigation. Results to date will be reported, and probable directions of future work will be described.

IV-A MECHANICAL JOINTS IN COMPOSITES

The 727 elevator actuator attachment rib redesign in composites at RPI, reported in earlier progress reports, led to separate research projects. One deals with heavily loaded holes in composites such as are encountered at the actuator attachment; the second deals with lightly loaded mechanical joints, such as occur, for example, in a row of small bolts or rivets, typified by the more or less continuous joint between rib flange and the elevator skin. Both of these problems have required the development of new analysis and/or test methods.

The conceptual redesign of the L-1011 drag strut has emphasized the importance and difficulty of designing compact lugs in composite materials. Two efforts pertinent to compact lug design have been pursued. First, unique structural configurations have been investigated that may increase the strength of such lugs. Second, failure criteria appropriate to the stress fields that exist in such lugs have been examined.

All four of these projects are described in the paragraphs to follow.

1. Analysis of Heavily Loaded Mechanical Joints

Senior Investigator: C. Muser

a. Introduction

Independent of the materials used, there often will be discontinuities in structural members, such as openings in panels and holes to accomodate mechanical joints. Although the fibers in advanced composites can be arranged in any imaginable manner (magnaweave, magnaswire, stylusweave, etc.), the materials currently used for plates including those containing discontinuities are mainly orthotropic with respect to cartesian coordinates. The present investigation deals with cylindrically orthotropic materials, since they promise to yield lower stresses around circular openings.

b. Status

A closed form solution for the stress distribution in a circular plate with a circular hole at its center, subjected to uniaxial traction, was found by N. J. Hoff for the case when its material is homogeneous and cylindrically orthotropic. The geometry of that plate can be seen in Figure IV-C-1-a of the 41st Semi-Annual Report. This analysis was extended to incorporate nonhomogeneous materials. The constitutive equations with compliances which are a function of the radius are:

$$\varepsilon_i = S^*_{ij}(1 + Q_{(i)(j)} r^h)\sigma_i$$

$$\gamma_{r\theta} = S^*_{66}(1 + Q_{66}r^h)\tau_{r\theta}$$

where i,j = r, and ( ) indicates no sum.
The exponent h describes the rate of change of material properties along the radius r. The constants S^*_{ij} and Q_{ij} are a function of the size of the plate and the parameter h. The compliances S_{ij} can be prescribed at both boundaries independently of the choice of the parameter h, so long as the convergence criteria are observed.

Such material property variations allow the choice of structural characteristics which yield low stresses in the vicinity of discontinuities, but leave the capabilities of the plate as a structural element unaffected. The results were encouraging, and it was decided that the same analysis be used to treat a bolt-loaded circular plate. The geometry of such a plate is shown in Figure IV-C-1-b of the 41st Semi-Annual Report. The goal, in this case, is to develop an algorithm capable of handling any boundary conditions which are expressible in a Fourier series. To find the exact bondary conditions was considered beyond the scope of this phase of the research.

c. Progress During Report Period

The form of the solution selected incorporates stress functions, $\underline{\phi}$, expressed as an infinite series. A typical stress function $\underline{\phi}$ is shown as follows:

$$\overline{\Phi} = \sum_{n=1}^{\infty}\left(\sum_{p=1}^{4} A_p^n \sum_{m=1}^{\infty} K_p^m(n)\, r^{t_p(n)} + hm\right)\cos n\theta$$

There are four boundary conditions expanded into a series of n terms ($n \to \infty$). The corresponding constants are A_p^n. For every n, the compatibility equation needs to be satisfied in its limit. The constants $K_p^m(n)$ emerge from this process. The homogeneous case yields the roots $t_p(n)$.

A computer program was written to calculate the resulting stresses. It needs as input the material properties at the boundary of the hole, at the outer boundary of the plate and the value of the parameter h. At this writing, the stress distribution in a plate subjected to uniaxial uniform traction (the empty hole case) can be calculated. The actual computation is very efficient, using about one dollar's worth of computer time.

The program has been extended to handle the case of the bolt-loaded plate. However, more analytical work is needed to determine the roots of the first term in the series ($n = 1$).

d. Plans for Upcoming Period

The analytical work needs to be completed, and the results incorporated in the otherwise finished computer program. Once that has been done, stress distributions in circular, bolt-loaded plates - the materials of which are cylindrically orthotropic and vary radially - will be calculated numerically.

e. Current Publications or Presentations by Dr. Muser on this Subject

"Stress Concentration Factors for Cylindrically Orthotropic Plates", with N. J. Hoff.

Published in the Journal of Composite Materials, Vol. 16, July 1982, pp. 313-317.

"Stress Concentrations in Cylindrically Orthotropic Plates with Radial Variation of the Compliances", with N. J. Hoff.

To be presented at the Fourth Conference on Composite Materials (ICCM-IV), Tokyo, Japan, October 25-28, 1982.

2. Pin-Loaded Holes in Uniform Composite Plates

Senior Investigator: R. G. Loewy

a. Introduction

In performing stress analysis of mechanical joints with clearances between fastener holes and loading pins (or bolts), one encounters uncertain boundary conditions at points along the fastener hole edges. There are similarities in this situation with the more usual elastic contact problems having uniform contact boundaries.

The single fastener joint, the simplest case, has been studied as the first step, in the hope that this may be extended to several other cases of interest. If the motions of hole edge points on the pin-hole contact boundary can be prescribed properly, then the only remaining task is to determine the amount of contact. It is clear that the amount of pin-hole contact is a function of applied load, joint geometry and the laminate properties of the plate. As discussed in a previous report, this relationship is non-linear, and as a result, the whole problem is non-linear. The results reported here are the work of doctoral candidate Wonsub Kim.

b. Status

A system of linear constraint equations has been introduced in a finite element method (FEM) analysis to describe the motions of hole edge points. The derivation of these

constraint equations is based on the fact that any hole edge point within the pin-hole contact region must move with the surface of the loading pin (assumed rigid and frictionless) and remain somewhere on the surface at equilibrium for a given applied load. The region of contact may be represented by $2\theta_c$ (Figure IV-A-2-a) and is initially undetermined.

Three ways to determine θ_c for any given load level were established and explained in detail in the last report. They were (a) the "semi-empirical method", in which isochromatic fringes obtained in a photoelastic experiment were correlated with the maximum shear strain distributions calculated by FEM with an assumed value of θ_c; (b) the "computer graphics terminal method", which seeks the θ_c value which produces the smoothest deformed shape of the hole edge and (c) the "minimum energy potential of applied load (or minimum strain energy) method", which searches for the value of θ_c that results in minimum energy potential for the given load application. All of these methods require iterative FEM analysis to find the correct θ_c.

Among these techniques, the "minimum energy potential of applied load method" is the most convenient, since its physical (or mathematical) interpretation is quite clear and it requires only minimum numbers of iterations, roughly four or five, as discussed in the previous report.

Using these methods, analyses of a single fastener mechanical joint with pin-hole clearance (Figure IV-A-2-a)

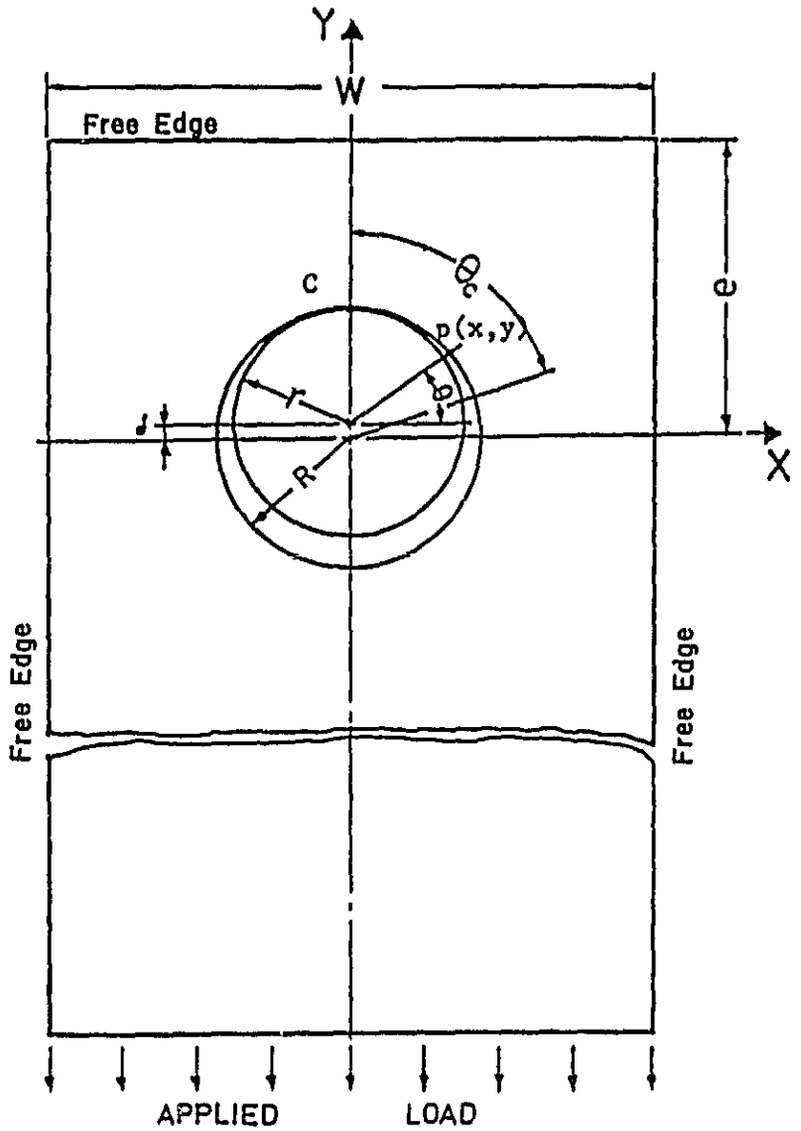

Figure IV-A-2-a. Idealized Model of Single Fastener Joint

were performed for two types of laminate, and the results were presented and discussed in the previous report. Among the results, it was pointed out that the non-linearity of the stress behavior was evident, even for a very small amount of pin-hole clearance (0.0015 inch). Further, a slight difference in laminate type, for example $[\pm 45°/0°]_{ns}$ versus $[\pm 30°/0°]_{ns}$, resulted in quite distinguishable differences in stress behavior. It was also observed that stress increases, in individual layers with differing fiber orientation, were different within the same laminate.

There were also, however, some common features among the stress distributions in different laminates. For example, the position of the maximum radial stress within any individual lamina was at the point where fibers are perpendicular to the hole edge, and the maximum tangential stress was always located at the point where fibers are parallel to the hole edge. Stress concentration factors are also changed by varying the level of applied load. This is indicative of the non-linearity of the problem, since stress concentration factors remain unchanged in linear cases. (See [1]* for details about these discussions.)

*Numbers in brackets in this section refer to the references which are listed on page 83.

c. Progress During Report Period

It would appear that the concept used for a single fastener is applicable to multi-fastener cases. An analysis model for a multi-fastener joint has been established as follows: The joint model is pictured as having a single row of equally spaced fastener holes infinite in number. This row of holes is parallel to the end of the joined plate (Figure IV-A-2-b). As shown in this figure, the mathematical model (see enlarged section) can be established by isolating a representative fastener hole. The plate width, W, of this model is taken as equal to the fastener spacing, s.

The boundary conditions for the model of Figure IV-A-2-b are the same as for the single fastener hole case (Figure IV-A-2-a), except for those along the boundaries where $x = \pm W/2$. On these particular boundaries it is clear in Figure IV-A-2-b that displacements in the x-direction must be equal to zero, whereas the normal stresses are undetermined. On these boundaries in the single-fastener joint model of Figure IV-C-2-a just the reverse was true. Note that, in both cases, however, shear forces along these boundaries must be zero.

In order to make comparisons between the stress behaviors of these two cases, we plan to set all the geometrical and laminate parameters of this model to be exactly the same as those of the previous single-fastener model. In addition, since there are no geometrical changes, we will use the identical FEM mesh which was used for the single-hole case. The

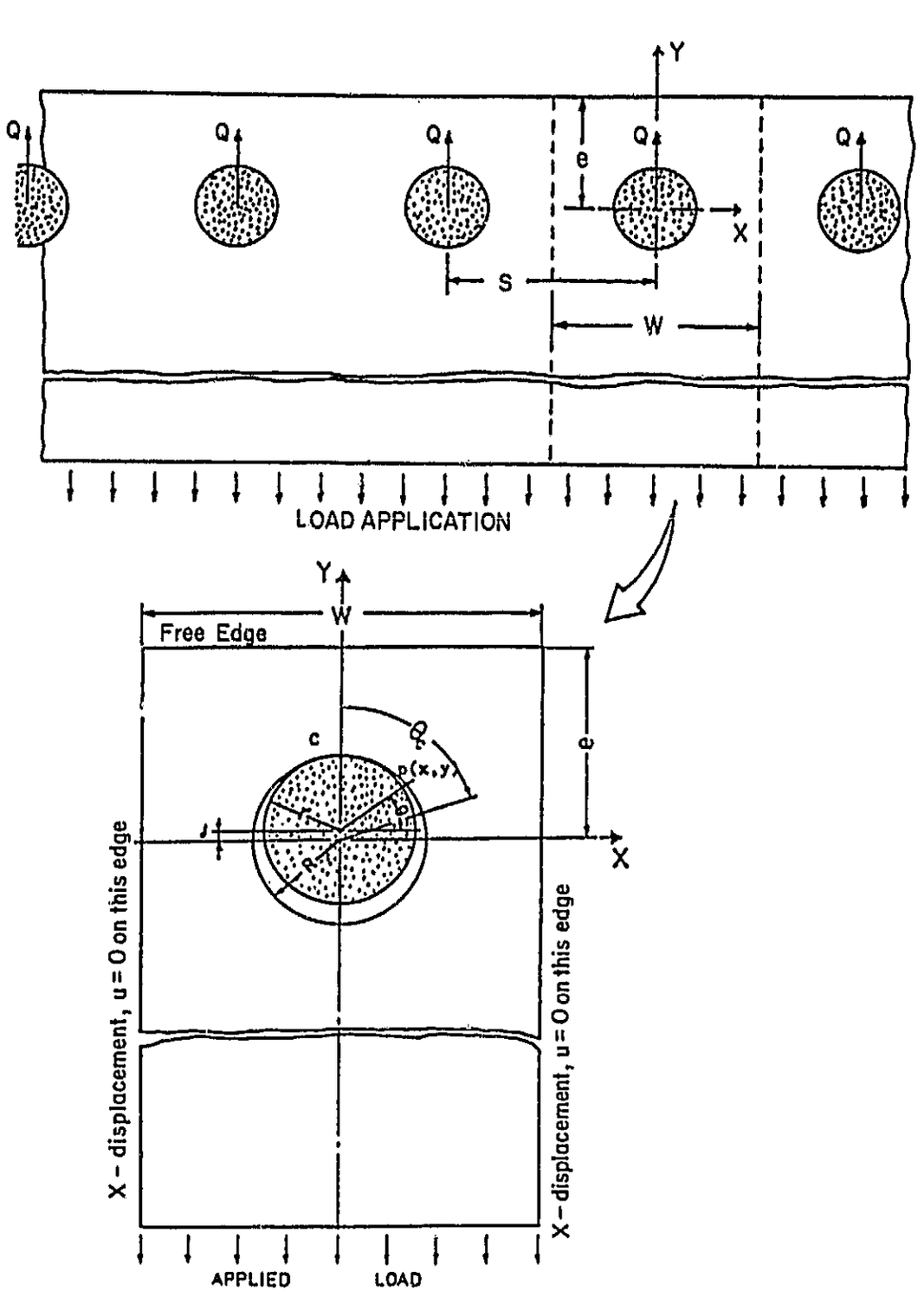

Figure IV-A-2-b.
Model Idealization of Multifastener Joint Problem

applied loads will be chosen such that the load transmitted per pin will be 4,000 pounds and 6,000 pounds for B-type ($[\pm 45°/0°]_{ns}$) and 4,000 pounds and 5,760 pounds for F-type ($[\pm 30°/0°]_{ns}$) laminates as before.

Rather than repeat all three analyses, however, we will use the minimum energy potential technique exclusively in the analysis of the multi-fastener joint.

d. Plans for Upcoming Period

We plan to complete the analyses which have been outlined in this report and to compare those results against those from the single-hole case.

We will also plan to explore the application of the technique developed in this research to interference-fit cases.

e. References

1. Kim, W., "Stress Analysis Methods for Clearance-Fit Mechanical Joints in Laminated Composites", Ph.D. Dissertation, Rensselaer Polytechnic Institute, Troy, New York, 1982.

3. Compact Lug Design

Senior Investigator: D. B. Goetschel

a. Introduction

A critical aspect of many aerospace structural elements is the load transfer that takes place between the connecting lugs at the ends of the structure and the portions of the structure wherein the loads are well-distributed if not uniform. An example is provided by the engine drag strut of the L-1011 aircraft (see Figure IV-A-3-a). Such lugs are highly loaded and have a very complex stress state (see Figure IV-A-3-b). Further, since they must mate with connecting parts, these lugs are usually designed within rather stringent dimensional envelope constraints. As compared to lugs which (as in the case of the L-1011 strut) are made from 200 ksi steel, meeting the geometric constraints, even with a composite structural design making maximum use of unidirectional graphite-epoxy, could prove to be a difficult task. This research is intended to solve the load-volume problem in favor of composites rather than either reverting to designs using 200 ksi steel lugs attached to a composite strut or forcing the dimensional constraints to be relaxed with a redesign of the mating parts.

b. Status

Several initial test lugs using various ply layups were manufactured and tested. The results from these tests

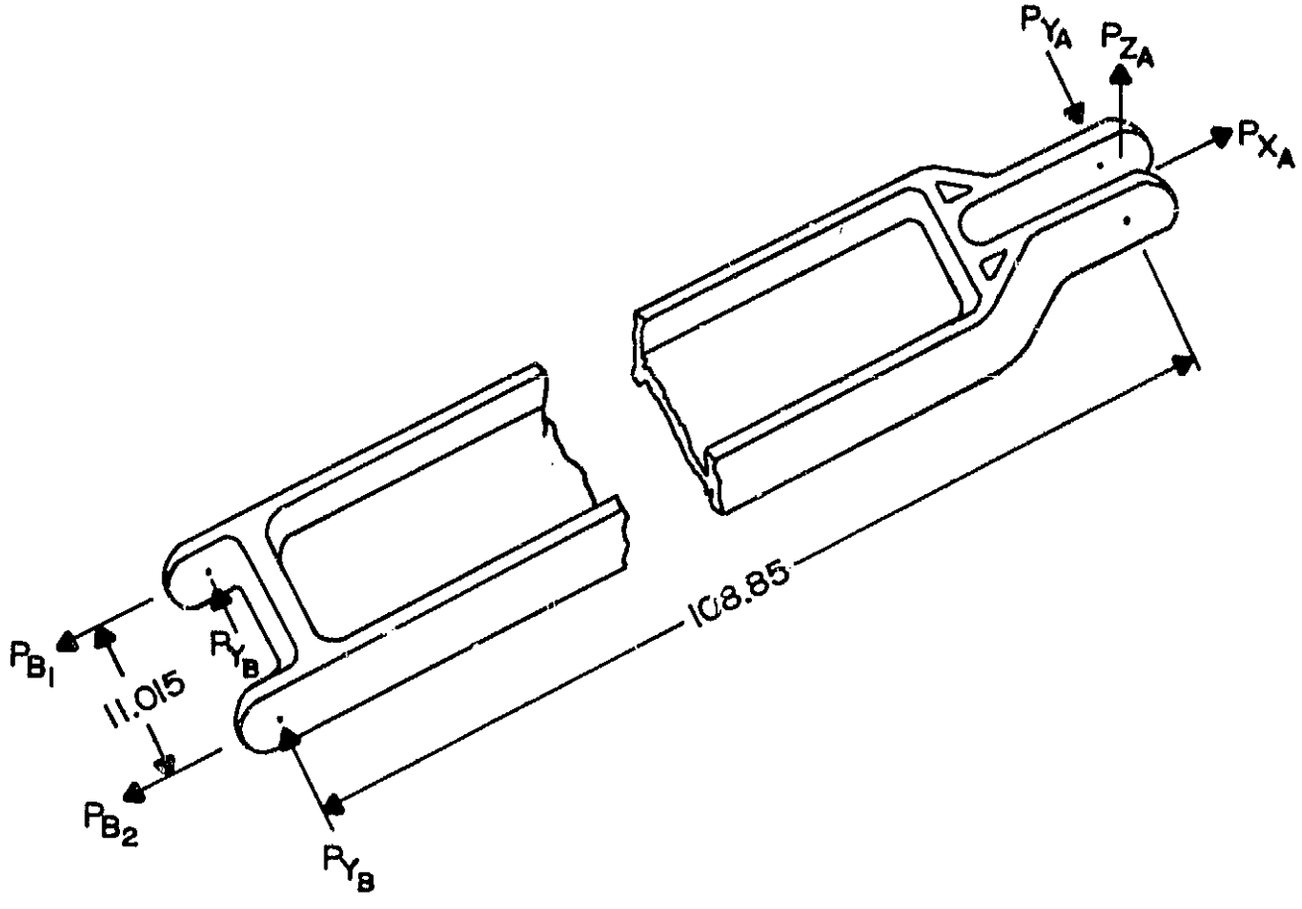

Figure IV-A-3-a.
Lockheed L-1011 Engine Drag Strut (Schematic)

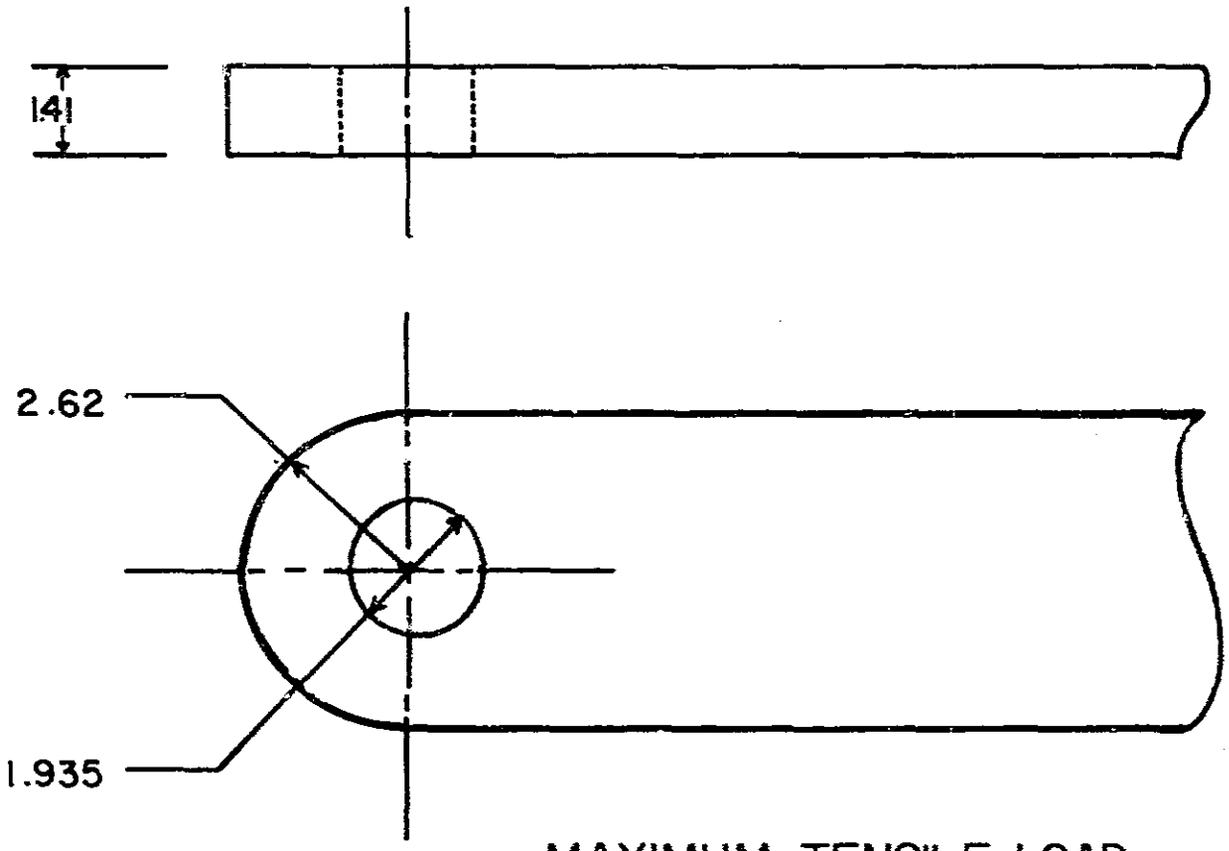

MAXIMUM TENSILE LOAD - 207.7 KIPS
MAXIMUM COMPRESSIVE LOAD - 236.8 KIPS
MAXIMUM LATERAL LOAD - 12.0 KIPS

DIMENSIONS IN INCHES

Figure IV-A-3-b. Lug Experiment: Full-Scale L-1011 Drag Strut

suggested some design modifications; namely, using bushings bonded inside the hole and slots at the sides of the hole. A second round of exploratory tests were performed to evaluate these design modifications. Some improvements could be seen, but the large scatter in the results made definite conclusions impossible.

c. Progress During Report Period

Graduate student Matt Cackett began work on the lugs in June. Initial testing was done using small quasi-isotropic, $[0/45/-45/90]_s$, strips loaded through a .5-inch diameter pin hole. These initial specimens were not scaled to the Lockheed dimensions; instead, available cured graphite plate material was used. Two slotted and one unslotted specimens were made (see Figure IV-A-3-c).

An attempt was made to determine the stress concentration at the side of the hole experimentally, using Stress-Kote strain lacquer. However, it was not possible to accurately observe lacquer cracks. The test results are listed in Table IV-A-3-a. Note that the slotted specimen failed at a 22% higher load. It also failed in the bearing mode instead of net tension.

Another attempt to determine the stress concentration at the edge of the hole was made using quarter-scale lugs with and without slots with a ply layup of $[0/45/-45]_s$ (see Figure IV-A-3-d). Photoelastic coatings were mounted on

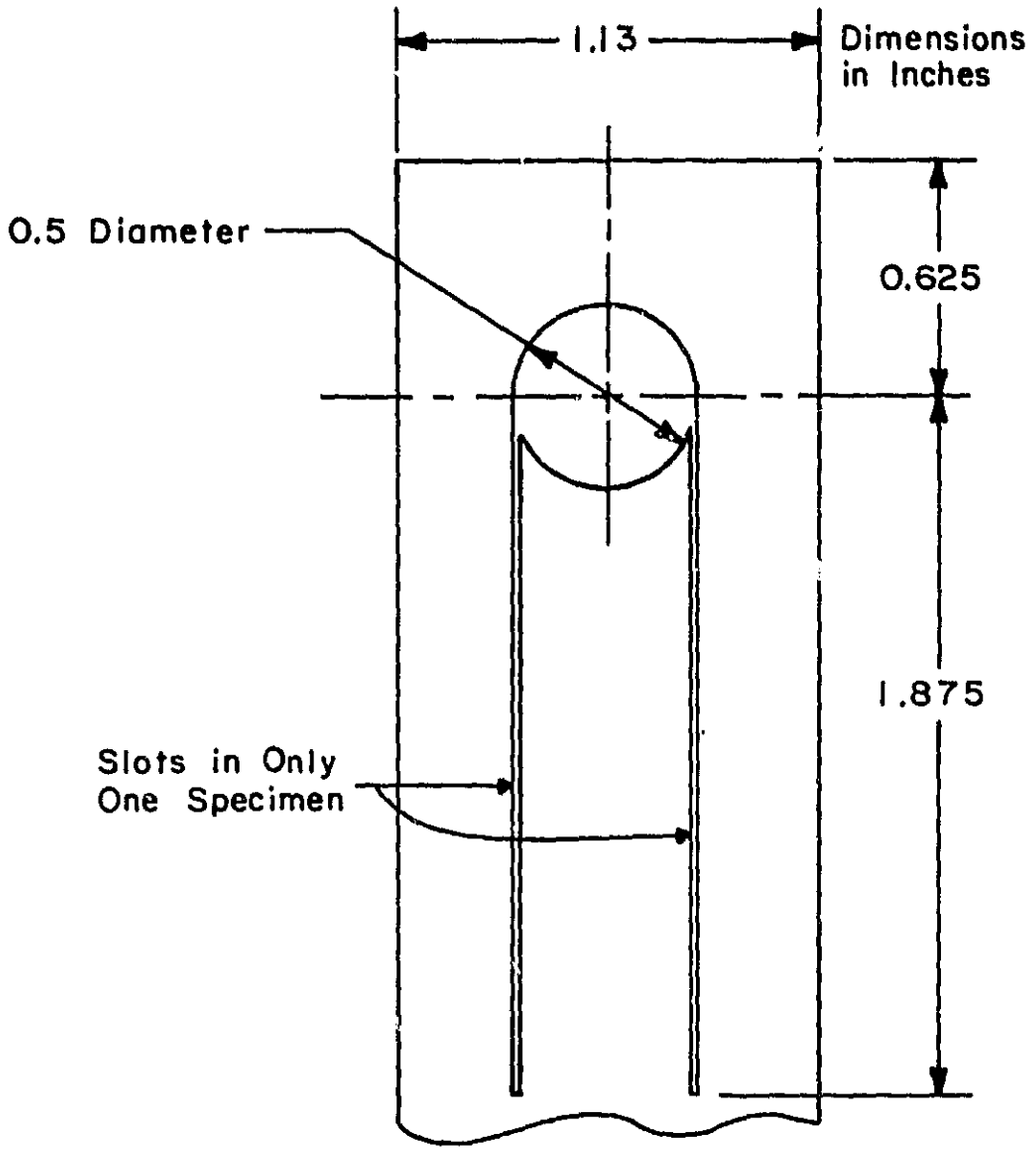

Figure IV-A-3-c. Lug Geometry for Stress-Kote Tests

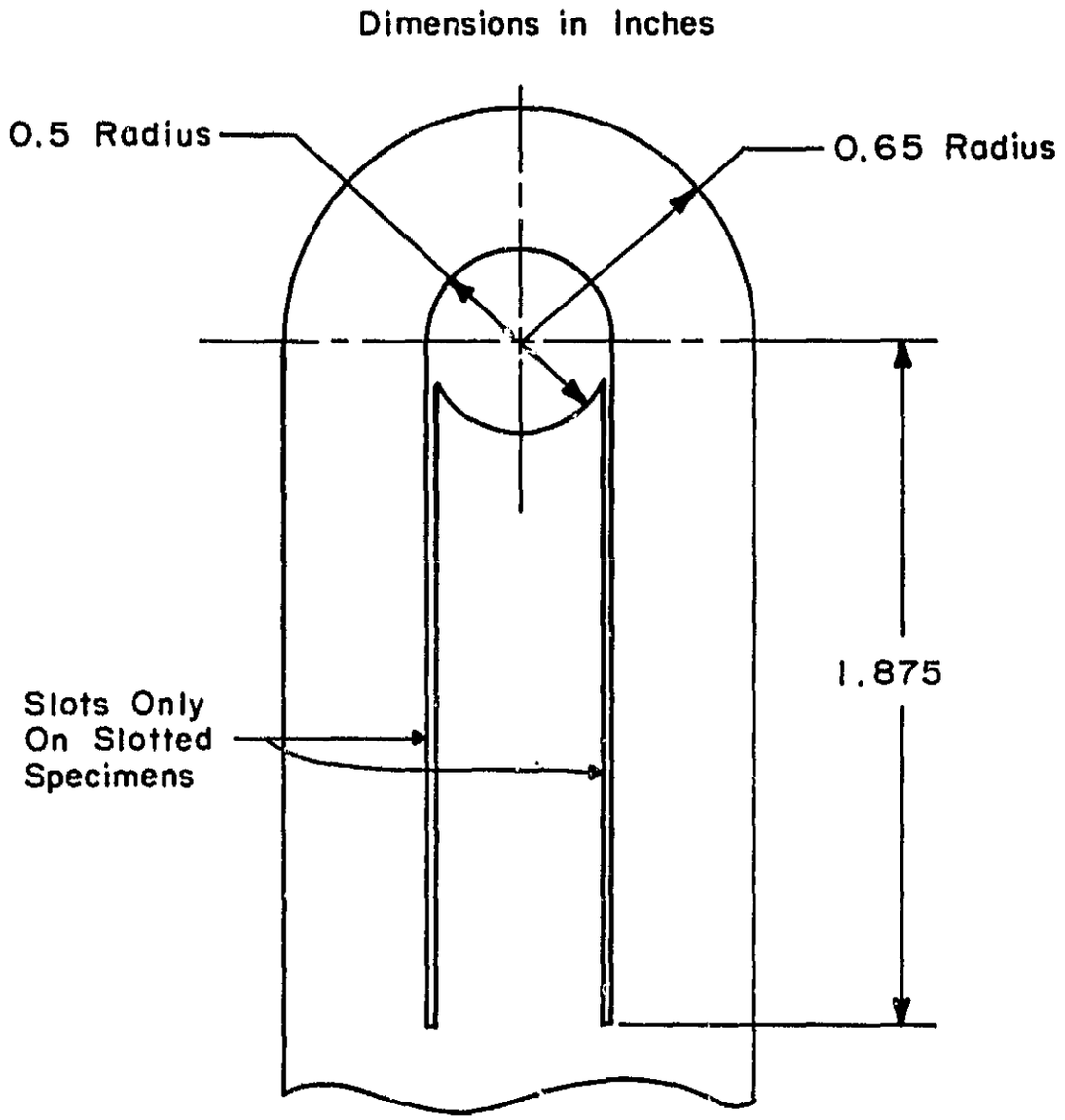

Figure IV-A-3-d. Lug Geometry for Photoelastic Tests

TABLE IV-A-3-a

STRENGTH COMPARISON OF VARIOUS LUG ARRANGEMENTS

Specimen Number	Type	Failure Load (lbs.)
1	unslotted	4370
2	unslotted	4265
3	slotted	5475

these specimens. This technique was used effectively by Wonsub Kim for determining stress distributions in bolt-loaded plates. Residual stresses from tight fitting bolt connections and the small coating area in the region of interest contributed to inconclusive results from this method.

It was decided to make a 12-specimen comparison between slotted and unslotted lugs. To simplify the interpretation of differences, both types should be made to fail in net tension. Thus, we desired a layup whose strength approached that of samples used during the previous reporting period, which did fail in net tension. A layup of $[0/45/-45]_s$ was chosen for this slotted versus unslotted comparison. Twelve specimens of 5208/1048 AIE graphite/epoxy were cut from the same plate. The cured plate thickness was found to vary from .454 inches near the center to .397 inches near the edges. This appeared to be due to using too thin (.125 inches thick) an aluminum plate on top of the laminate during autoclave cure. The aluminum deformed under the 100 psi

autoclave pressure resulting in uneven resin bleed-out. Following removal of the plate from the autoclave, it was noticed that the bleeder material near the center of the plate was not saturated with resin. To ensure uniform clamping in the testing machine, one face of the lug was ground parallel to the other face over 1.5 inches in the gripped region only.

Machining the specimens to size was done first using a carbide band saw to rough cut the lugs. Then the bolt hole was drilled using successively larger high speed steel bits and, finally, a .5-inch carbide tipped bit. Drilling was done at a feed rate of about .5 inches per hour. The slow feed rate was used to minimize hole surface flaws and break-out damage. No breakout was detected at this speed, and the hole surface appeared smooth. The outside surface was then ground to size using a heat treated steel template pinned to the lug as a guide. The slots were cut using a .03-inch thick diamond wheel mounted on a routing machine. Cuts were made from each side of the lug to maintain symmetry.

The twelve specimens were tested on an Instron by clamping one end and applying a load through the hole with a hardened pin. The test results were unexpected, in that the slotted lugs failed at an average load only three percent higher than the unslotted lugs. Finite element analysis results had predicted that the tensile strength should be about twenty percent higher, based on peak tensile stresses. Three

points are worth noting, however. First, the results were reasonably consistent, as shown by the standard deviations listed in Table IV-A-3-b. The higher deviations for the slotted slugs may be attributed to the extra manufacturing process of slotting which was difficult to duplicate from piece to piece. Second, although the failure loads were quite similar, the failure modes were not quite the same. Both types failed in a combined tensile and shear tear-out,

TABLE IV-A-3-b
TEST RESULTS OF UNSLOTTED AND SLOTTED LUGS

Unslotted Lugs		Slotted Lugs	
Specimen Number	Failure Load (lbs.)	Specimen Number	Failure Load (lbs.)
1	12,125	2	13,250
3	12,220	4	11,210
6	12,970	5	12,715
8	12,715	7	12,360
9	11,480	10	14,120
11	12,830	12	12,125
Average =	12,390	Average =	12,630
Standard Deviation =	559	Standard Deviation =	996

but the angles of the failure planes were different, as shown in Figure IV-A-3-e. This indicates that the unslotted specimens are tending more towards net tension failure than are the slotted ones. Thus, slots must reduce the tensile stresses by some palpable amount. Third, two lugs actually surpassed the Lockheed criteria (13,000 pounds-scaled). One slotted lug even reach 14,000 pounds. The average failure loads for both types were within five percent of the design load.

In order to isolate the effect of slots, twelve new specimens were made of a quasi-isotropic layup ($[0/45/-45/90]_{2s}$) with square extended heads (see Figure IV-A-3-f). This modification is a further attempt to reduce the possibility of shear failure by increasing the area of the shear plane. It was found, however, that these 16-ply specimens are susceptible to bearing failure at very low loads. They re currently being reduced in width to force net tension failure.

The use of peak stress in failure criteria for the bolt-loaded lug appears to be a conservative approach. An alternative failure criterion for bolt-loaded holes has been proposed by Agarwal[1]*. His criterion assumes failure will occur when the average stress over a certain distance is equal to the laminate strength. This approach also allows

*Numbers in brackets in this section refer to the references which are listed on page 100.

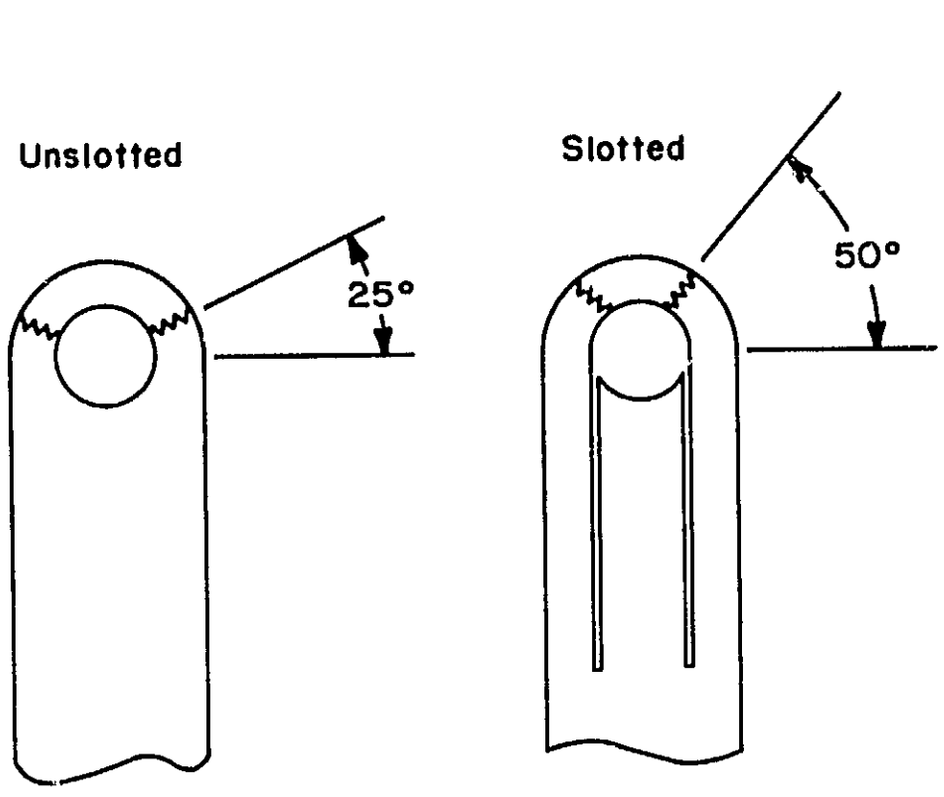

Figure IV-A-3-e. Comparison of Angle of Failure Planes for Unslotted and Slotted Lugs

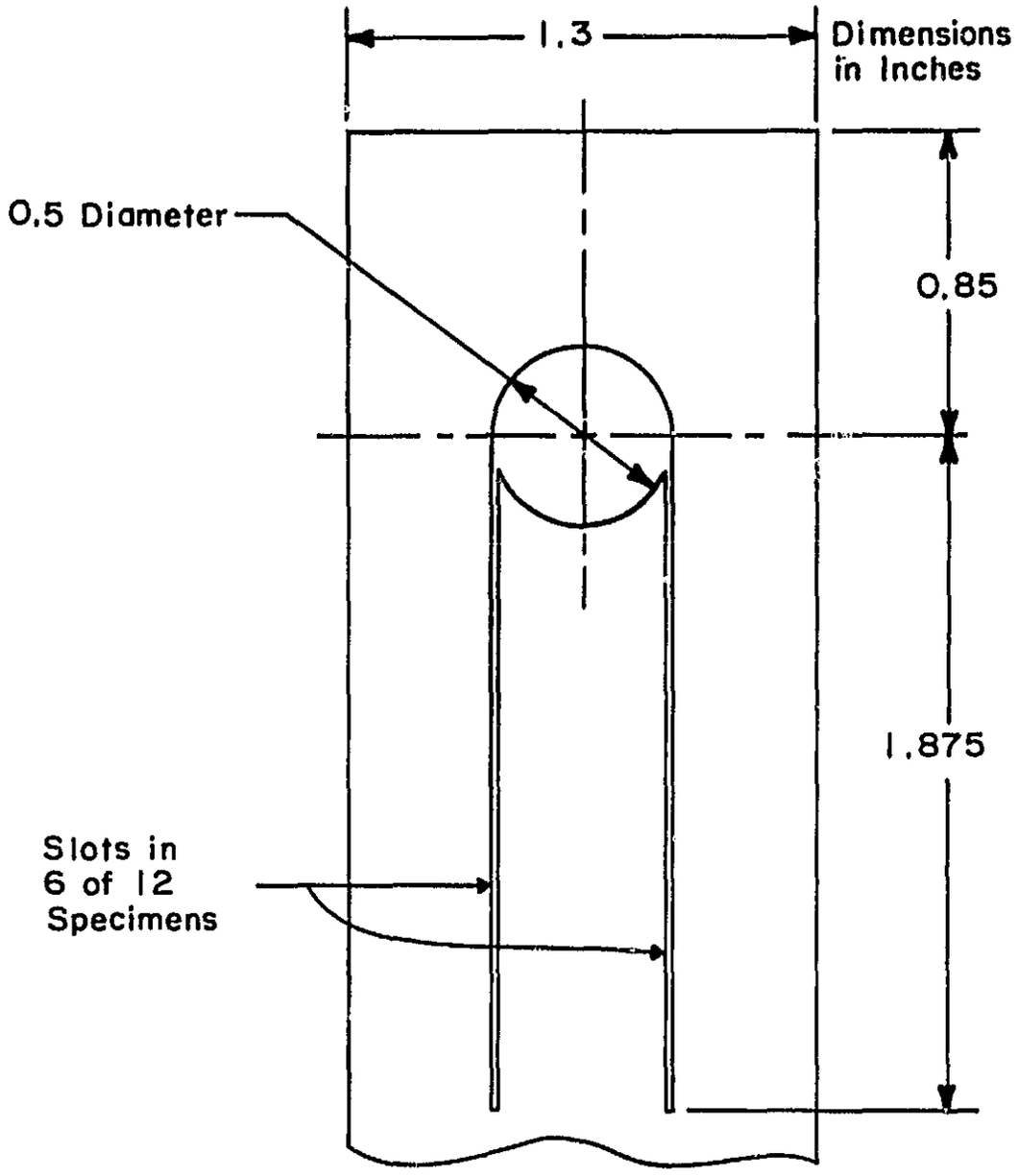

Figure IV-A-3-f.
Specimens Modified to Enforce Net-Tension Failure

for the three modes of failure; net tension, shear and bearing. This theory is now being applied to the aforementioned 16-ply lugs using a finite element analysis.

A capstrip (consisting of only 0°-plies wrapped around the outer edge of the lug) modification is now being investigated. Instead of using a capstrip across the entire net tensile area, it was suggested by undergraduate student Tom DeMint to bond a partial capstrip to the lug (see Figure IV-A-3-g). The advantage of this geometry is that the partial capstrip would increase the strength of the tensile cross section while retaining the bearing properties of the inner laminate. This design has the potential to be optimized by varying the partial capstrip width until the stress concentration at the interface causes the capstrip to fail at the same instant the inner laminate fails in tension (unless, of course, some other failure mode has become active). The increased stiffness of the capstrip should reduce the stress concentration at the edge of the hole, allowing the inner laminate to fail at a higher average load level. Initial testing is being done with a partial capstrip of .10 inch thickness.

A lug with a partial capstrip was tested earlier in this project by Christoph Muser[2]. A steel bushing was used to take the bearing load, and the capstrip extended from this bushing, as shown in Figure IV-A-3-gC. This lug failed in tension at a net tensile stress of 92,857 psi.

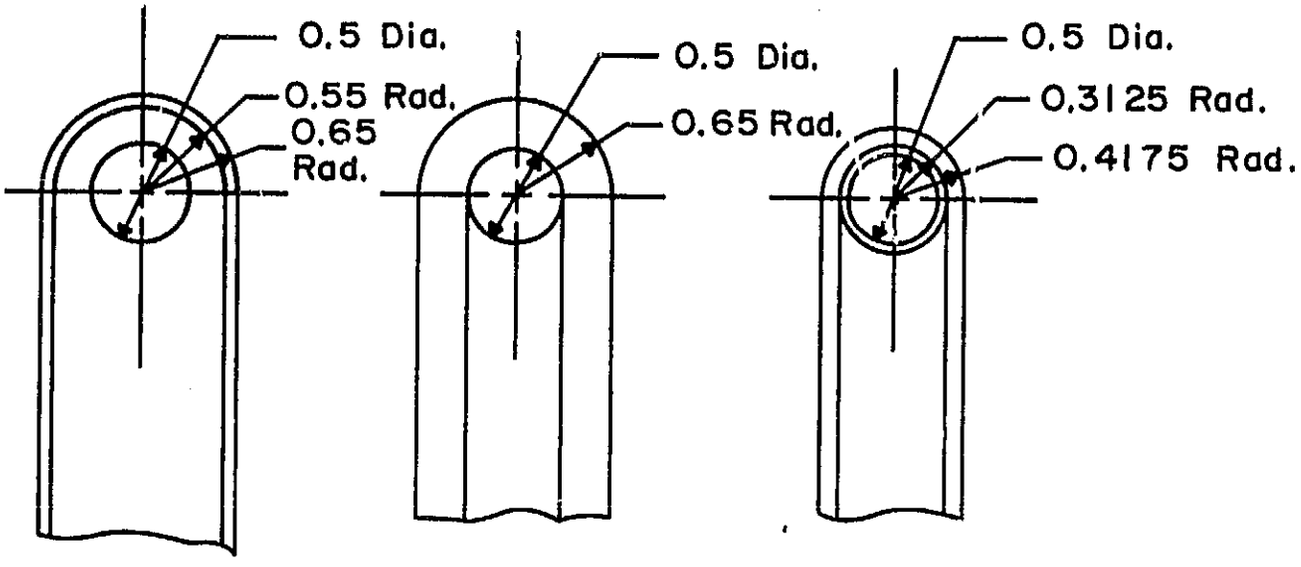

Dimensions in Inches

Partial Capstrip	Total Capstrip	Muser Design
A	B	C

Figure IV-A-3-g. Capstrip Design

C-2

Following up on these promising results, a partial capstrip of .10 inches was tested, failing at 12,750 pounds or 36,890 psi. The capstrip sheared from the inner laminate in the bond area along the sides of the lug away from the end. By improving the bond, the capstrip should produce good results.

d. Plans for Upcoming Period

Plans for the coming period include improving the capstrip design by strengthening the bond and optimizing the thickness. Also, a softening strip design will be investigated with use of Kevlar or glass inlays near the hole, in place of 0°-graphite-plies. Undergraduate student Bob Benson is pursuing a similar design using metal inlays.

An accurate finite element model will be completed, either by using a cosine normal load distribution or by modeling the pin itself. Results from this will be used in conjunction with Agarwal's failure criterion to determine the criterion's usefullness in predicting failure loads of compact lugs.

A paper by T. A. Collings[3] indicates that a layup of [0/45/0/-45] may be more effective in all modes of failure than the [0/45/-45] layup used in the slotted versus unslotted test. This new layup also has been shown to have a twelve percent higher peak stress concentration[4] than the [0/45/-45]. This would highlight the effect of slotting the

lugs and may be pursued for another quarter scale test. It appears that the effectiveness of slotting may be more of a function of layup than was originally expected. The focus of continued work will be to quantify the effect of slotting on a reasonable layup and to evolve a design that will satisfy a high load lug requirement (as typified by the Lockheed criteria).

e. References

1. Agarwal, B. L., "Static Strength Prediction of Bolted Joints in Composite Materials", AIAA Journal, Vol. 18, No. 11, November 1980, pp. 1371-1375.

2. "Composite Structural Materials", RPI Semi-Annual Progress Report under NGL 33-018-003, October '78 through April '79, pp. 36-41.

3. Collings, T. A., "Designing with Fiber Reinforced Materials", I. Mech. E Conference Publications, Mech. Eng. Publications, Ltd., London, 1977, pp. 29-32.

4. Walters, R. E., "A Finite Element Analysis of a Graphite/Epoxy Aircraft Engine Drag Strut Lug", May 7, 1982 (unpublished).

4. Failure Criteria for Stress Concentrations

Senior Investigator: D. B. Goetschel

a. Introduction

It has been observed that when holes are drilled in advanced composite plates whose dimensions are very large compared to the hole diameter, the failure load varies with hole size, even though the elastic solution for peak stress next to the hole is independent of hole size. This shows that there is some mechanism other than peak stress contributing to failure when stress concentrations exist in structures made from advanced composites. Some reduction of the peak stress due to non-linear material response would be expected, but large variations have been found in advanced composites which are too brittle for this to be a reasonable explanation. Since lugs contain large stress concentrations, this behavior must be taken into account when they are analyzed.

The work described here has been performed by Fola Ogunlari in research conducted in partial satisfaction for a Masters Thesis.

b. Status

The most attractive and general way of dealing with this phenomenon (i.e., where stress concentrations affect failure load) appears to be to use an average stress

criterion as described by Whitney and Nuismer[1]* and by Wu[2]. The essential feature of this criterion is use of an average stress calculated over a characteristic distance along a stress gradient. When the average stress, calculated in this way, exceeds the failure stress for the material in a uniform stress field, it is postulated that the specimen will fail. The rational for this is as follows: (a) brittle failure of a body under a given stress field is generally attributed to the existence of inherent flaws of various dimensions distributed throughout the body[3]; (b) Weibull statistics[4] estimate the effect that these flaw distributions in a given material have on the failure strength of particular specimens and (c) it follows that the sharper the stress concentration, the less likely it is that a critical flaw will be encountered by the peak stresses, and thus, the higher the peak stress can go before failure occurs. The use of the average stress defined above is simply an approximate method that appears to have some reliability in quantifying this behavior. Agarwal[5] applied this criterion to a particular bolted joint design and found that it accurately predicted static strength.

*Numbers in brackets in this section refer to the references which are listed on page 106.

c. Progress During Report Period

Before the Whitney/Nuismer - Wu average stress criterion can be applied to the structural design process, it should first be tested for greater generality than has been evident in the literature to date. Accordingly, exact elastic solutions were sought and found for various types of (empty) holes and notches in isotropic elastic plates under load. From among these, solutions were selected for hole geometries that could be conviently manufactured and which provide a full range of stress concentration intensity. Figure IV-A-4-a shows the configurations selected. As the diameters of the round holes increase relative to the width of the test strips, the stress fields approach uniformity. In the other extreme, the square ended notches provide a stress singularity.

The specimens were manufactured from 1048 AIE graphite/epoxy using a layup of $[0/90/45/-45]_s$. To determine the unnotched strength and the characteristic dimension for integration, a series of tests were conducted on unnotched and round-holed specimens. A minimum root-mean-square error analysis resulted in a characteristic dimension of .195 inches. Table IV-A-4-a shows the results of the final test sequence. As can be seen, the average stress criterion was found to be very reliable over a wide range of stress concentration levels.

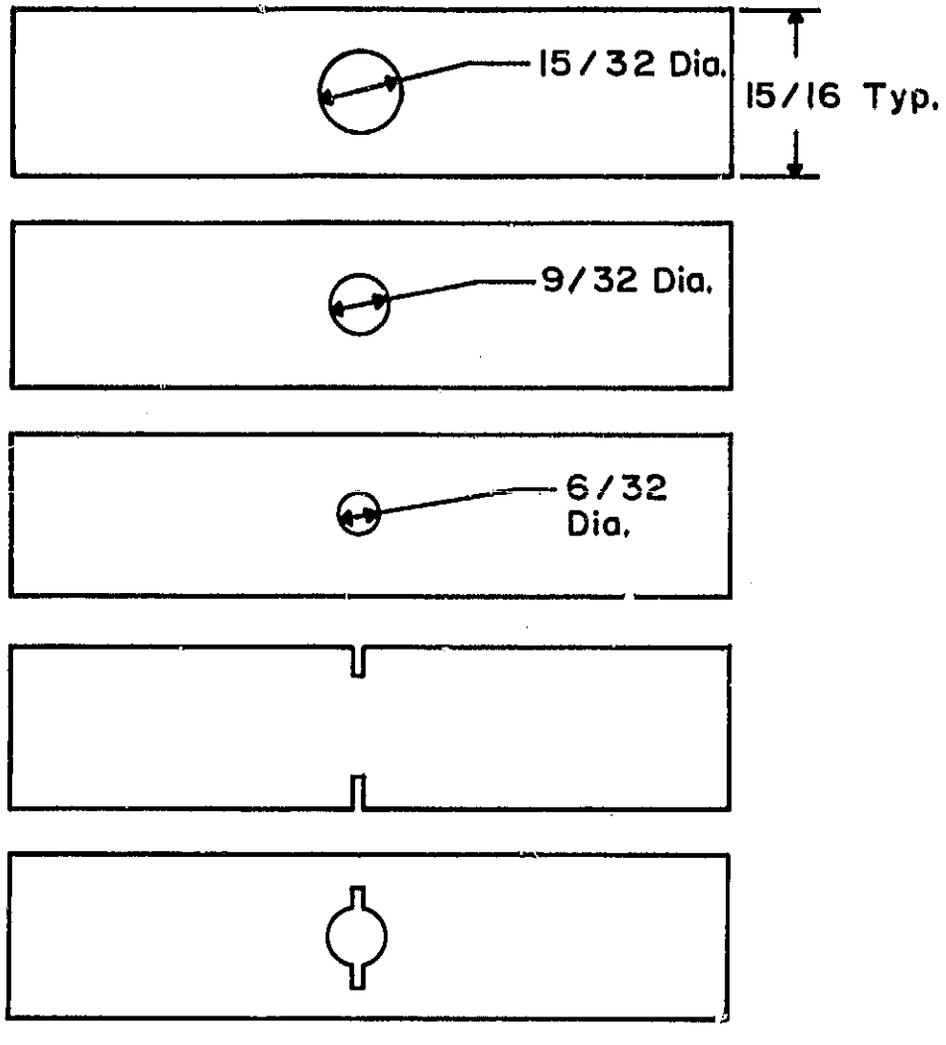

Figure IV-A-4-a. Specimen Configurations

TABLE IV-A-4-a

SUMMARY OF AVERAGE STRESS AND PEAK RESULTS

Hole and Crack Geometry	Test Failure Load (pounds)	Average Stress Prediction (load/ % error)	Peak Stress Prediction (load/ % error)
6/32 dia.	3450	3712 / 7.6	1908 / -44.7
9/32 dia.	3038	3183 / 4.8	1781 / -41.4
15/32 dia.	2042	2393 / 17.2	1392 / -31.8
Double edge	2760	2884 / 4.5	0 /-100.0
Center crack	2633	2619 / -.5	0 /-100.0

d. Plans for Upcoming Period

The dependence on plate thickness of the characteristic integration length will be the next subject for investigation. If the rational for using an average stress criterion is based on the probability of a critical sized flaw occurring in the area of the largest stresses, then thicker plates should increase that probability and shorter characteristic lengths should be used with thicker plates, in recognition of the fact that failures will occur sooner relative to an uniform stress material allowable.

If this is successful, the method will be exercized in analyzing lugs made using advanced composites.

e. References

1. Whitney, J. M. and R. J. Nuismer, "Stress Fracture Criteria for Laminated Composites Containing Stress Concentrations", J. Composite Materials, 8 (2), 1974, p. 253.

2. Wu, E. M., "Strength and Fracture of Composites", Fracture and Fatigue, J. L. Broutman, Ed., Academic Press, 1974.

3. Griffith, A. A., "The Phenomena of Rupture and Flow in Solids", Philosophical Transactions of Royal Society (London), Series A, Vol. 221, 1920, p. 163.

4. Weibull, W., "A Statistical Distribution Function of Wide Applicability", Journal of Applied Mechanics, 18, 1951.

5. Agarwal, B. L., "Static Strength Prediction of Bolted Joint in Composite Material", AIAA Journal, Vol. 18, November 1980, pp. 1371-1375.

IV-B SCALING EFFECTS IN TESTING COMPOSITE STRUCTURES

Senior Investigator: D. B. Goetschel

1. Introduction

It can be extremely valuable in terms of both time and money to be able to test small scale models when designing large structures. This is especially true for structures fabricated from composite materials such as graphite/epoxy, since the material itself is relatively expensive. On the other hand, the knowledge required to interpret results from small scale models, accurately and with confidence, is essentially nonexistent, mostly because the effects of the unique characteristics of composite materials are only partially understood.

2. Status

Undergraduate student Scott Baxter conducted a preliminary set of tests for a series of samples with different scales, loaded in simple static tension. Good correlation was found for strength variation with scale between experiment and the theory that was developed for the limited number of tests that were run. The predictions were based on free edge and Weibull statistical effects.

3. Progress During Report Period

Wherever statistics are involved, there will be a question as to the adequacy of the number of samples tested.

The preliminary tests, reported earlier, were considered too few. Work has been carried out to conduct a final set of verification tests for simple static tension, which will broaden our statistical base.

4. Plans for Upcomming Period

A final set of tests on simple static tension will be completed and compared with the developed theory. Work will be started on the scaling of bearing failures at pin-loaded holes. Exploratory tests are also being planned to investigate in a broader sense the scaling of experiments on joints in composite materials.

IV-C END EFFECT DECAY IN PRISMATIC MEMBERS

Senior Investigator: D. B. Goetschel

1. Introduction

Saint Venant's Principle states that all statically equivalent systems of loads on a body will produce nearly identical stress fields in regions that are remote from the loaded area. The usual engineering approximation of neglecting Saint Venant's end effects at distances of about one width from the ends is justified for isotropic members of compact cross section. For composites like graphite/epoxy, however, or for open thin-walled cross sections, these approximations can be substantially in error. It is often important to be able to analytically quantify these effects, in general, for any material system and cross sectional geometry. It is particularly useful to be able to provide this type of analysis for long, uniform struts such as are found in structures like the L-1011 aircraft, wing-mounted engine drag strut. Much shorter specimens could be used for testing, if such analyses could define minimum lengths above which stress distributions are not altered. Work by graduate student Tsay-hsin Hu to accomplish this analysis is described here, but first some background information will be given.

2. Status

Toupin[1]* and Knowles[2] independently presented theorems for upper bound estimates of the strain energy

$$V(x) = V(0)*\exp(-2\lambda x)$$

where: λ = characteristic decay rate of end effects,

$V(0)$ = total strain energy and

$V(x)$ = strain energy in body beyond x.

Then, because of the quadratic nature of strain energy in terms of the mechanical variables, the displacements, strains and stresses relationships are, respectively,

$$u_i(x) \leq u_i(0)*\exp(-\lambda x)$$
$$\varepsilon_{ij}(x) \leq \varepsilon_{ij}(0)*\exp(-\lambda x)$$
$$T_{ij}(x) \leq T_{ij}(0)*\exp(-\lambda x)$$

Choi and Horgan[3,4,5,6] evaluated λ for some specific cases by employing the Airy stress function ϕ

$$\phi(x,y) = F(y)*\exp(-\lambda x)$$

This solution form enables the mathematics to be reduced to an eigenvalue problem involving a fourth order ordinary differential equation in $F(y)$. Since all the exponents are negative, the eigenvalue with the smallest real part characterizes the dominant exponential decay rate.

Dong and Goetschel[7] developed a method for finding

*Numbers in brackets in this section refer to the references which are listed on page 117.

the decay rate of edge effects in a plate composed of an arbitrary number of anisotropic layers. Instead of the Airy stress function, the in-plane displacements were adopted as the primary independent variables. One-dimensional finite element polynomial interpolation functions were used to model the behavior through the thickness of the plate. The computer program "Plate" was the result of this approach to quantifying edge effects in semi-infinite plates. "Plate" has a serious limitation, however, in that it can only deal with plates with orthotropic layers. This is because it lacks displacement degrees of freedom in the direction parallel to the free edge of the plate.

A program called "Prism" was partially developed subsequent to "Plate's" being established; its purpose was to quantify end effects in prismatic members, as shown in Figure IV-C-1. By restricting the degrees of freedom it can handle, "Prism" is also to model general anisotropic layered plates. Development of this program reached the point of assemblying the governing system matrices, but it was not completed to the point of solving the resultant eigenvalue problem.

"Prism" uses a semi-analytic finite element method to quantify the end effects. Two-dimensional finite element polynomial interpolation is used to model displacement variations across the member cross section. Then an exponential decay of displacement is assumed along the length of the

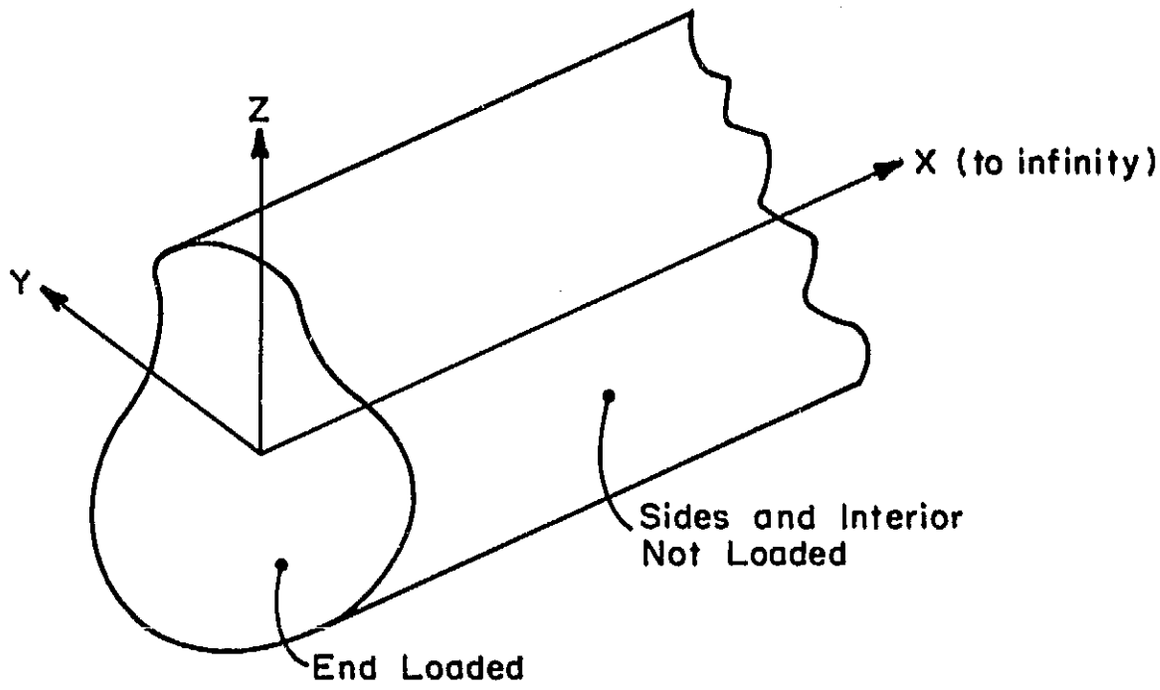

Figure IV-C-1. Geometry of a General Prismatic Member

member. The resulting equations form a second order eigenproblem, whose roots are the characteristic decay rates and whose corresponding eigenvectors are the displacement distributions across the cross section. The complete displacement field is then obtained by multiplying the cross sectional variation by the axial exponential decay. The stress field is easily obtained from the displacement field as a final step.

The semi-analytic finite element formulation assumes a displacement field of the form

$$u(x,y,z) = p(y,z)*\exp(-\lambda x)$$

where: $p(y,z)$ = polynomial interpolation across the cross section and

$\exp(-\lambda x)$ = exponential decay interpolation along the length.

A typical four-noded finite element is shown in Figure IV-C-2.

The usual finite element force-displacement matrix equation is

$$[k]\ \{u\} = \{f\}$$

where: $[k]$ = stiffness matrix,

$\{u\}$ = vector of displacement degrees of freedom and

$\{f\}$ = vector of force degrees of freedom.

The stiffness matrix is composed of three parts:

$$[k] = [k_o] + [k_s] + [k_v]$$

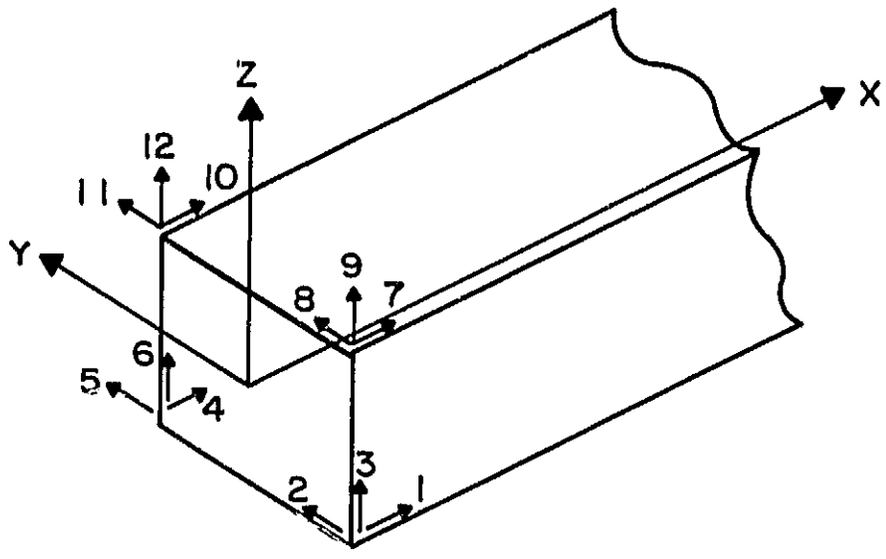

the small arrows marked from 1 to 12 are
the finite element degrees of freedom

Figure IV-C-2.
Configuration of a Typical Four-Noded Finite Element

Here $[k_e]$ is calculated by integrating tractions over the end of the element, $[k_s]$ is calculated by integrating tractions over the sides (including top and bottom) of the element and $[k_v]$ is calculated by integrating body forces over the volume of the element. The activation of any one of the displacement degrees of freedom defines a displacement field throughout the element. This displacement field can be used to find the corresponding stress field. The stress field, in turn, defines the tractions that are integrated over the surface of the element. The derivatives of the stress field, when inserted into the differential equilibrium equation, define unbalanced body forces that are integrated over the volume of the element. The displacement interpolation functions are used as weighting functions when performing the various integrations.

The problem under consideration requires that there not be any tractions on the sides or body forces within the interior of the element, therefore,

$$([k_s] + [k_v])\{u\} = \{0\}$$

The differentiations and integrations cause $[k_s]$ and $[k_v]$ to be made up of three different matrices with different powers of λ

$$[k_s] + [k_v] = \lambda[k_2] + [k_1] + \frac{1}{\lambda}[k_0]$$

Thus, the eigenproblem to be solved can be written as

$$(\lambda^2[k_2] + \lambda[k_1] + [k_0])\{u\} = \{0\}$$

The solution for eigenvalues is complicated by the fact that, although $[k_2]$ and $[k_0]$ are symmetric, $[k_1]$ is anti-symmetric.

3. Progress During Report Period

As a first step, "Plate" was transferred successfully into the RPI computer system. This was to provide a basis of comparison for the newly developed program "Prism". "Prism" can be used to model plate problems, so intermediate results from the two programs during various steps of the solution process can be compared as an aid in debugging "Prism". "Prism" is now generating the same system matrices as "Plate".

Despite the fact that the system matrices are the same, the new program was not getting answers in agreement with the old one. It was discovered that some of the system matrices are singular and the frequency shift technique is needed to overcome this problem. "Plate" uses a solution algorithm that performs frequency shifts automatically, however, this solution algorithm is very unreliable and frequently produces spurious results. It is not being used in "Prism".

Although the singularity problem would seem to have been solved, consistent results are still not being produced by "Prism". It appears that the problem is ill-conditioned for the solution methods that have been tried to date, because

some correct results have been produced, and the accuracy of the results decays as the number of degrees of freedom is increased.

4. Plans for Upcoming Period

Work will be continued on the solution algorithm for "Prism" until consistent results can be obtained. Once this is accomplished, the program will be verified for prismatic members by comparing it to available results from exact analytic solutions[8,9,10,11,12,13,14]. The program will then be used to investigate several problems of interest. In layered composite plates, the variation of edge effects as ply orientation and stacking sequence are varied will be examined. For prismatic members, the end effects of cross-sectional geometry (i.e., I-beams versus round tubes versus rectangular beams, etc.) will be investigated.

5. References

1. Toupin, R. A., "Saint-Venant's Principle", Archive for Rational Mechanics and Analysis, Vol. 18, 1965, pp. 83-96.

2. Knowles, J. K., "On Saint-Venant's Principle in the Two-Dimensional Linear Theory of Elasticity", Archive for Rational Mechanics and Analysis, Vol. 21, 1966, pp. 1-22.

3. Horgan, C. O., "On Saint-Venant's Principle in Plane Anistropic Elasticity", Journal of Elasticity, Vol. 2, 1972, pp. 169-180.

4. Horgan, C. O., "Some Remarks on Saint'Venant's Principle for Transversely Isotropic Composites", Journal of Elasticity, Vol. 2, 1972, pp. 335-339.

5. Choi, I. and C. O. Horgan, "Saint-Venant's Principle and End Effects in Anisotropic Elasticity", Journal of Applied Mechanics, Vol. 44, No. 3, 1977, pp. 424-430.

6. Choi, I. and C. O. Horgan, "Saint-Venant End Effects for Plane Deformation of Sandwich Strips", International Journal of Solids and Structures, Vol. 14, No. 3, 1978, pp. 187-195.

7. Dong, S. B. and D. B. Goetschel, "Edge Effects in Laminated Composite Plates", submitted to the Journal of Applied Mechanics.

8. Knowles, J. K and C. O. Horgan, "On the Exponential Decay of Stresses in Circular Elastic Cylinders Subjected to Axisymmetric Self-Equilibrated End Loads", International Journal of Solids and Structures, Vol. 5, 1969, p. 33.

9. Klemm, J. L. and R. W Little, "The Semi-Infinite Elastic Cylinder Under Self-Equilibrated End Loading", SIAM Journal of Applied Mathematics, Vol. 19, 1970, pp. 712-729.

10. Power, L. D. and S. B. Childs, "Axisymmetric Stresses and Displacements in a Finite Circular Base", International Journal of Engineering Science, Vol. 9, 1971, pp. 241-255.

11. Duncan Fama, M. E., "Radial Eigenfunctions for the Elastic Circular Cylinder", Quarterly Journal of Mechanics and Applied Mathematics, Vol. 25, 1972, pp. 479-495.

12. Mitra, D. N., "On Axisymmetric Deformations of a Transversely Isotropic Elastic Cylinder of Finite Length", Archiwum Mechaniki Stosowanej, Vol. 17, 1965, pp. 739-747.

13. Warren, W. E., A. L. Roark and W. B. Bickford, "End Effect in Semi-Infinite Transversely Isotropic Cylinders", AIAA Journal, Vol. 5, 1967, pp. 1448-1455.

14. Horgan, C. O., "The Axisymmetric End Problem for Transversely Isotropic Circular Cylinders", International Journal of Solids and Structures, Vol. 10, 1974, pp. 837-852.

PART V
PROCESSING SCIENCE AND TECHNOLOGY

V-A INITIAL SAILPLANE PROJECT: RP-1

V-B SECOND SAILPLANE PROJECT: RP-2

V-A INITIAL SAILPLANE PROJECT: THE RP-1

Senior Investigators: F. F. Bundy
R. J. Diefendorf
H. Hagerup
H. Scarton

1. Status

Recognizing that the resins in composite materials can change properties somewhat with aging and exposure to temperature/moisture cycles, the wing/fuselage ensemble structure of the RP-1 glider has been static tested about once a year since its initial fabrication in '79-'80. The last such test was done at RPI on August 5, 1981, preparatory to winch launch flight tests at Schenectady County Airport. That test consisted of simple bending using a distributed load up to a maximum of 590 pounds per wing, which corresponds to a little over 4 g's for average pilot weight.

2. Progress During Report Period

After the failure of the wing beam "carry-through" structure of the RP-2 glider in November 1981, the corresponding parts of the RP-1 glider were studied with an eye to making it stronger and more fail-proof. Two changes were made in the carry-through structure: (i) the female open box member was wrapped with an additional layer of 45°/45° Kevlar fiber and bonded with resin and (ii) the aluminum pin which goes through both wing stubs at the midpoint of the carry-through region was replaced with a stronger steel pin,

and the lands on the beam webs on which the pin bears were made thicker. The latter change was made to insure that the pin assembly could absorb any tension generated from tendencies to pull the wing beams apart, such as occur with wing fore-aft bending.

In the present tests, the wing-fuselage assembly was subjected to simple bending, as in previous years but, in addition, to a bending-torsion test, which would simulate the stresses in a high speed pull-out. It was in this mode that the RP-2 wing beam carry-through failed (see Section V-B).

As a safety measure to prevent catastrophic failure of the whole structure in case of a failure of one part during the test, the wings each had two "safety stops" under them - one at about half span and the other a little inboard of the wing tip. As the wing loading and corresponding deflections increased, the "stop-supports" were adjusted so that the wing and load could fall no more than ¼" to ½" before being adequately stopped and supported.

In addition to monitoring bending and twisting deflections, the wing root regions were monitored by attached microphones for any "acoustic events" associated with the stressing of the structure. The microphones were in contact with the wing skin on the top and bottom sides of each wing near the root ribs and as close as possible to the carbon fiber capstrips of the wing beams. This AE monitoring was done by

Professor H. Scarton and graduate student G. Bobal, using a four-channel physical acoustics model 3400 AE analyzer system.

The other changes on the glider made since the previous strength tests (i.e., closing in the bottom of the cockpit area with foam ribs and belly skin, and streamlining the skid and wheel) had no effect on the main structural elements being test and, although they were in place at the time, were irrelevant to these tests.

The RP-1 was assembled for testing and placed in an inverted position, with the fuselage booms resting on a support about 36 inches above the floor. Deflection measuring stations were established at inboard, mid and outboard points on the leading and trailing edges of each wing, making a total of twelve stations (as shown in Figure V-A-1). At each station a vertical steel rod, supported by a cast iron base on the floor, held a vertical steel metric scale at roughly the level of the wing's leading and trailing edges. Crossed with the vertical scale was a horizontal scale attached to the wing (i.e., at that same spanwise station). This arrangement made it possible to read both vertical and horizontal displacements as the wing was loaded.

In the simple bending tests, the fuselage was held in a horizontal position and the ten-pound sand bag weights were laid on, one per foot of span, directly over the wing beam. In the bending/torsion tests, the fuselage was positioned on

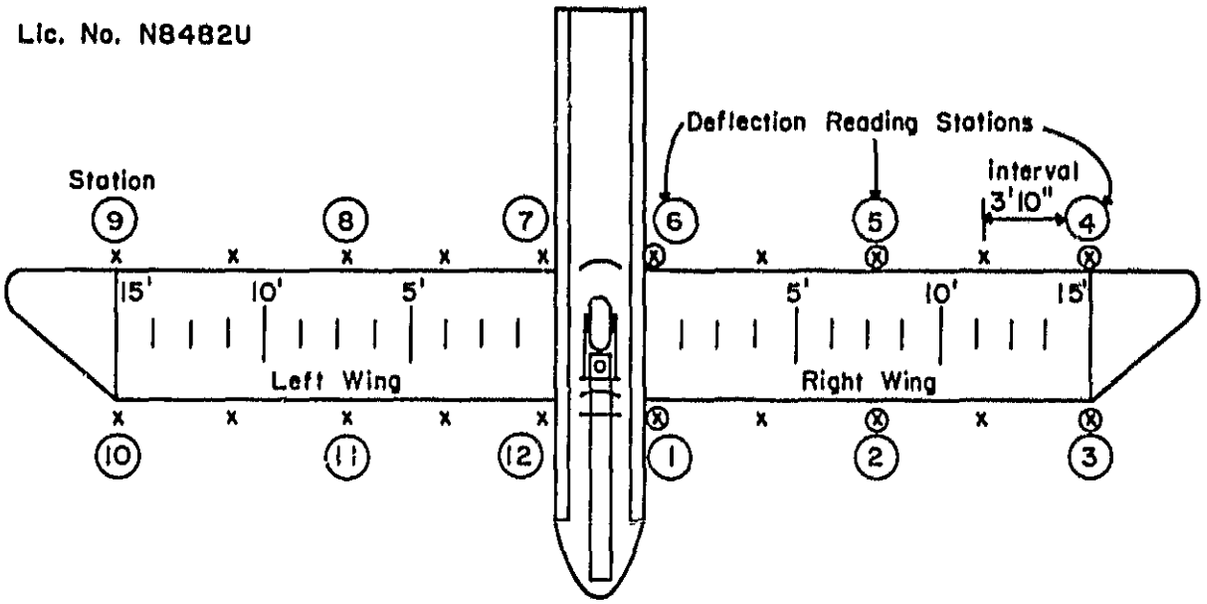

NOTE: Sand bags were loaded symmetrically and simultaneously left and right, starting at inboard end.

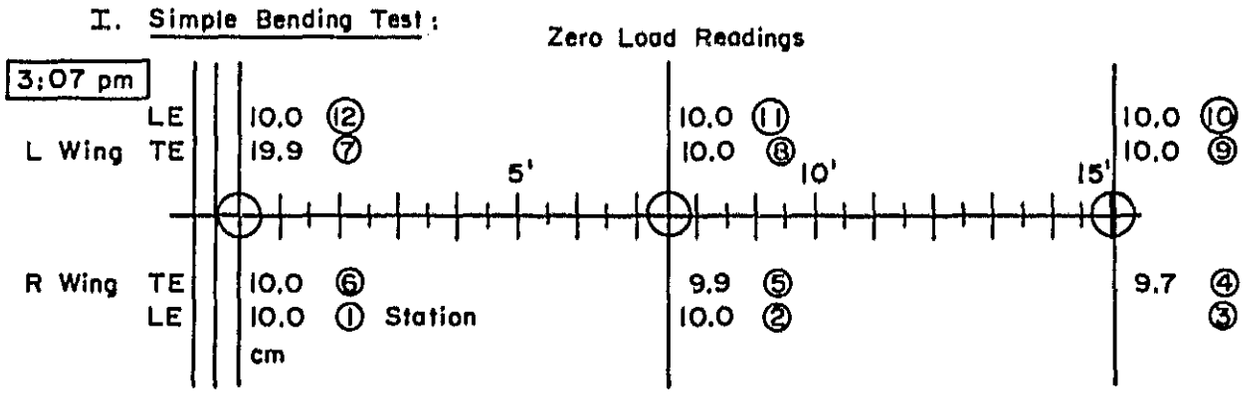

Figure V-A-1.

Static Loading Tests of RP-1 Glider Wing for Bending, Torsion and Fore-Aft Deflections

a ten degree slant (nose low, tail high, inverted) and the sandbag weights placed on a line 14 cm aft of the wing beam. Thus, both torsion and fore-aft bending were induced, in addition to vertical bending. These two static tests were survived very successfully. The deflections at the different simple bending loadings are plotted in Figure V-A-2. These deflections compare closely with those obtained in the test of August 5, 1981. Upon unloading, the deflection readings came back to within 0.1 to 0.3 cm of the initial values, indicating that the structure had suffered no permanent deformation.

The results of the bending/torsion test at the 4 g loading are presented graphically in Figure IV-V-3. Differences in trailing edge deflections relative to the leading edge divided by the chord distance gave the angles of twist shown in this figure. By usual standards, this is a very stiff wing.

A major concern, because of the RP-2 failure, was how much the wings deflect <u>forward</u> during the bending/torsion test mode. The horizontal scale readings of deflections at the six stations at the leading edge had to be combined with vertical scale readings, since the bending axis of the wing was tilted ten degrees to the horizontal. Thus, if there were no deformation of the wing in its own plane, the transverse deflections would cause the leading edge to move aft as measured by the horizontal scales. This proper combination

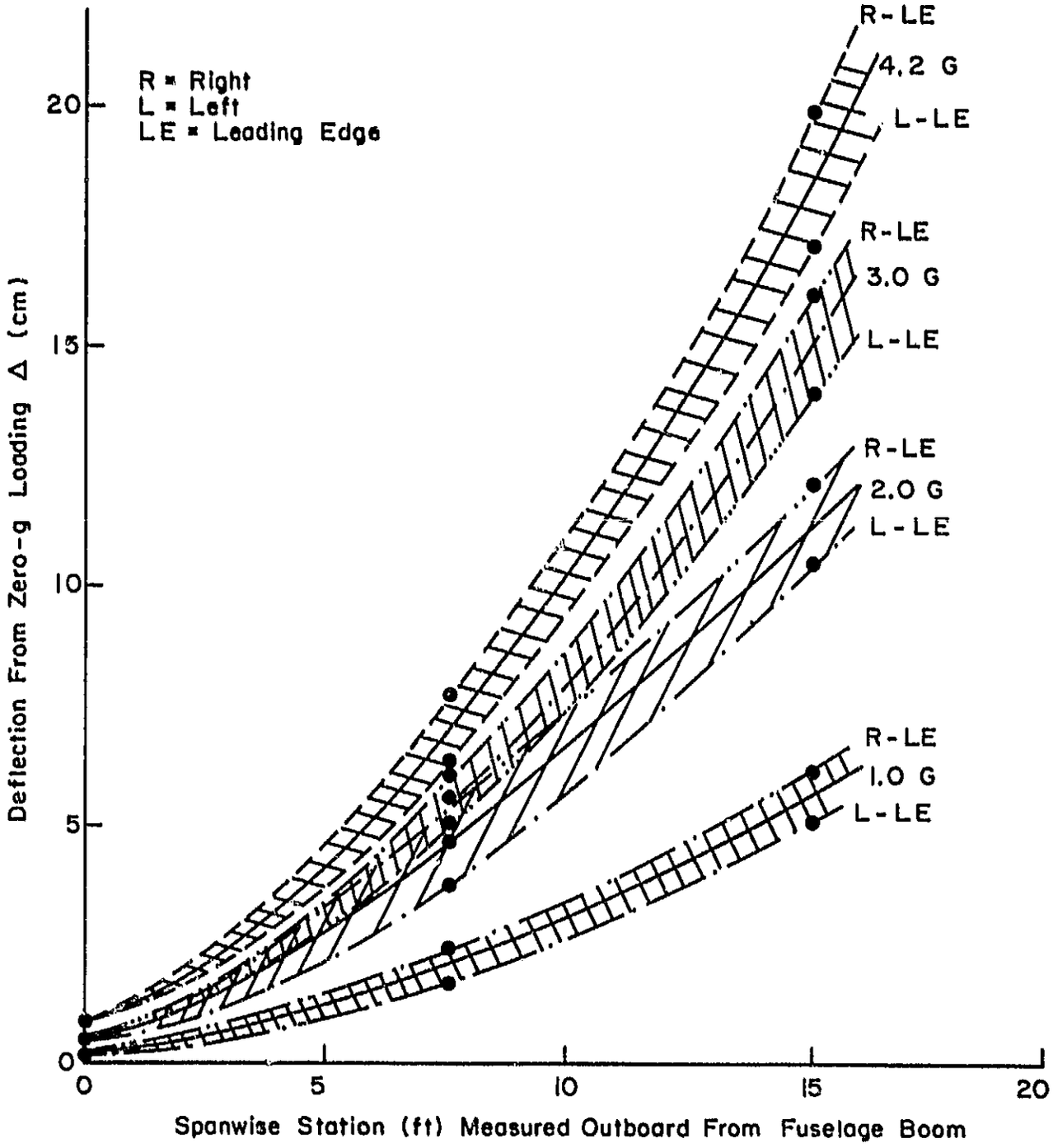

Figure V-A-2. RP-1 Glider: Static Bending Test
(1 July '82)

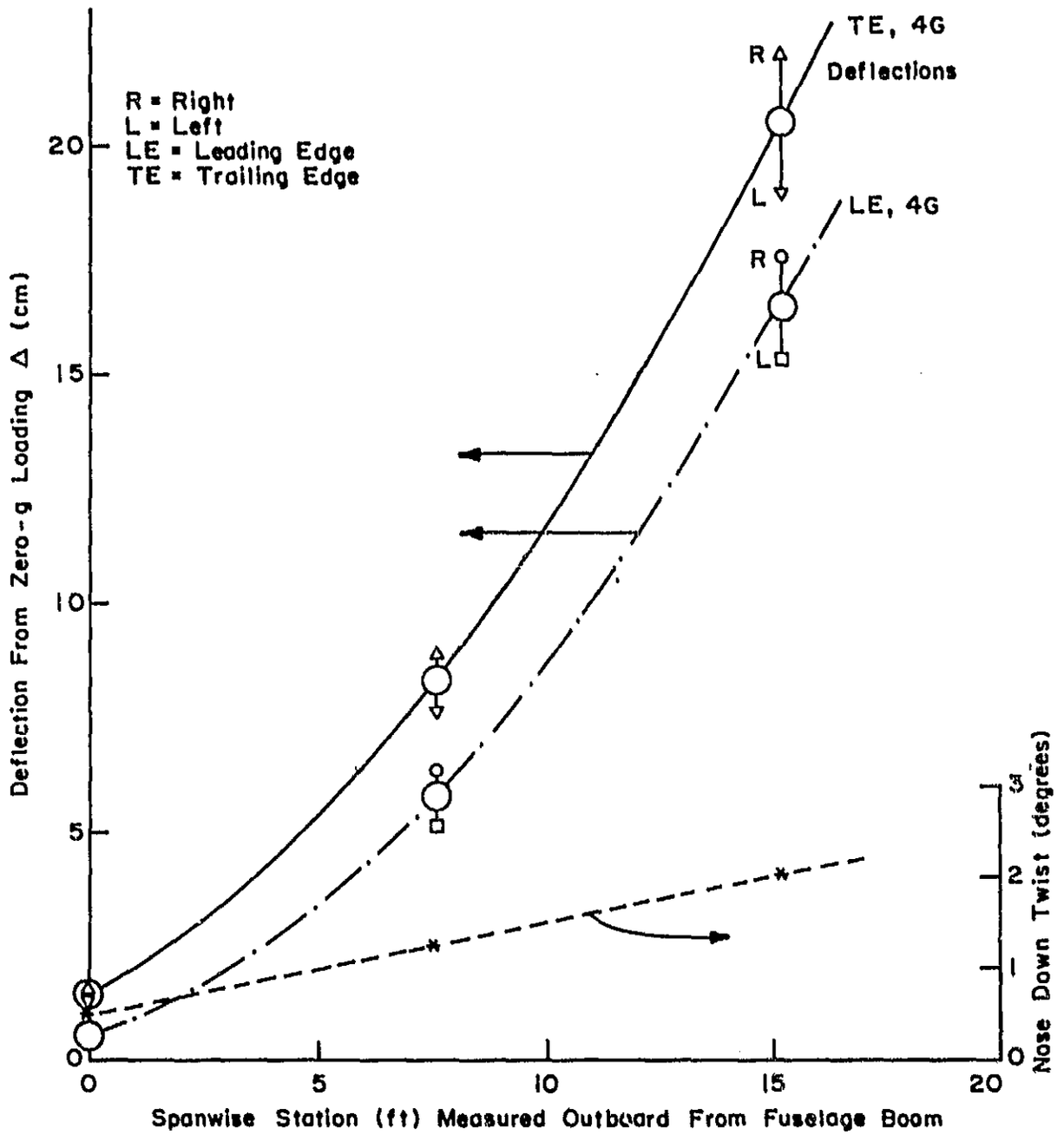

Figure V-A-3. RP-1 Glider: Bending Torsion Test
(1 July '82)

of these measurements led to an estimate of total forward deformation of the wing at the outboard end of 36 mm. To ascertain the degree to which carry-through structure might be carrying fore-aft bending moments, the aft wing pin was watched during the loading and unloading. If there was any pull-out of the pin from its socket, it appeared to be less than a fraction of a millimeter.

A substantial amount of acoustic emission data was taken during the test. The most salient of the output occurred during the bending/torsion portion. The four sensors located near the points of maximum stress (wing spar center section carry-through) recorded AE events of significant amplitude only at loadings between three and four g's. The counts versus time plot presented in Figure V-A-4 showed some indications of being critically active, according to the ASTM E569 criterion. Figure V-A-5 reveals seven large amplitude events above 76 dB; none occurred before the three g load point. A Hsu-Neilson lead-break calibration directly opposite the sensor on the root rib (0.5 mm lead) produced an amplitude of 86 dB. This same lead break calibration was not resolvable at a distance of two feet from the sensor. We thus conclude that all data in Figures V-A-4 and -5 is produced by local activity. In the absence of definitive indications, the elastic behavior of the structure had led us to believe that these relatively strong AE events were more

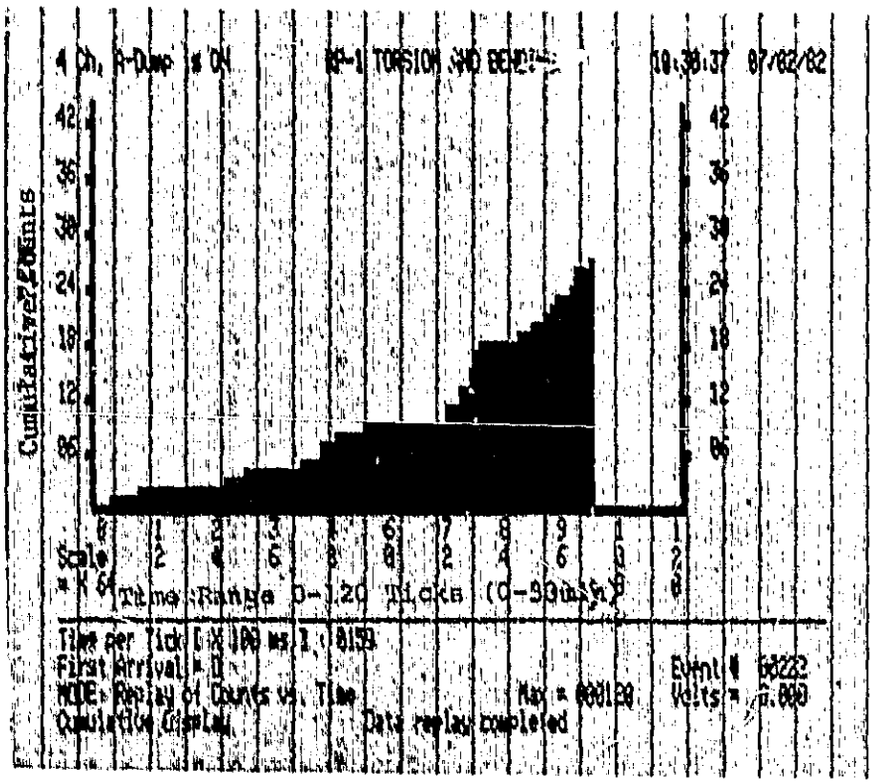

Figure V-A-4. AE Counts versus Time Plot
RP-1 Bending Torsion Test to 4.5 g's
(inverted, 10° nose down)

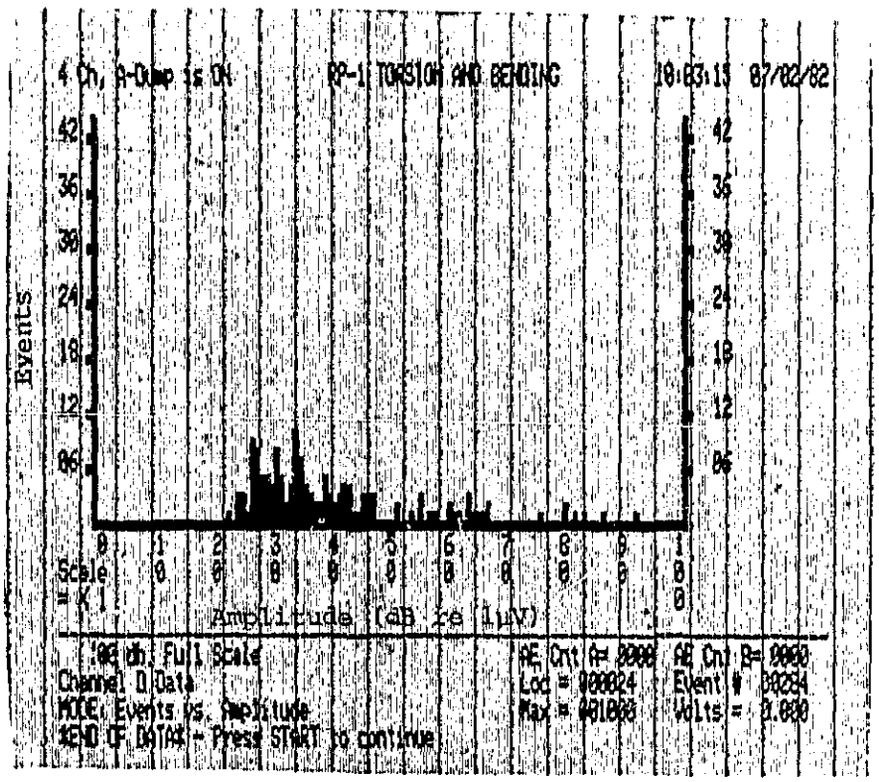

Figure V-A-5. AE Amplitude Distribution
(Events Count vs. Amplitude)
RP-1 Bending-Torsion Test tc 4.5 g's
(inverted, 10° nose down)

likely due to relative stick-slip motion of mating (but not bonded) surfaces rather than breakage of stressed fibers.

Following the static tests, winch-launched flight tests were carried out on July 23 and 30, 1982 at the Saratoga County Airport for measurements of sink rate versus flight speed at a gross weight of 340 pounds (F. Bundy, pilot). In some of these flights, the air was stable enough to yield sink rate data of reasonable reliability over the speed range from 25 to 45 mph. The effect of aerodynamic fairings was to lower the minimum sink rate to about 200 FPM (from 250 FPM in the unfaired configuration) and to increase the optimum glide slope from about 10 or 11:1 to 14:1. Flight tests were also made at a gross weight of 380 pounds (M. McCarron, pilot) on September 17 and 24, 1982, but, except for a 30 mph run and a 40 mph run, the air was convecting too much to yield meaningful sink rate data. Two rather creditable soaring flights were accomplished; the first, on July 23rd, was a 2600-foot, 20 minute thermal soaring flight, and the second, on September 24th, reached 1500 feet, with an endurance of 19 minutes under overcast conditions.

Tests were conducted on five identical elements of two different kinds, typical of structural elements used on the RP-1 and hidden from view, in the Fall of '81 and five more in September '82. The two joint types are shown in Figure V-A-6. These tests are intended to provide the first indication of possible strength degradation that, with time,

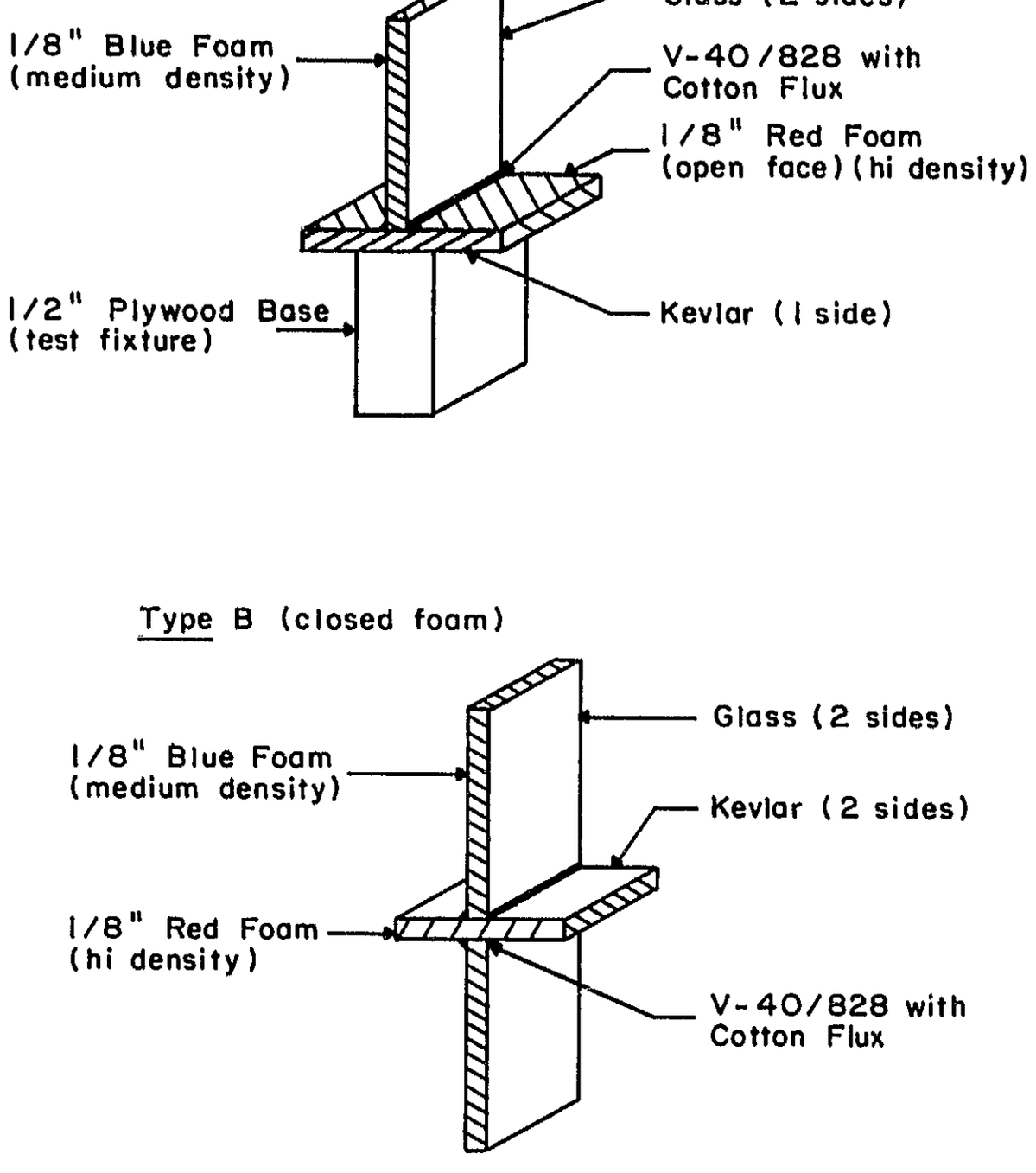

Figure V-A-6. Two Types of Structural Joints Used in the RP-1 (lightly-loaded, low-cost composite structures)

might be encountered with the RP-1. All elements are stored under the same conditions as the aircraft. Comparative results of the tests in '81 and '82 are shown in Figures V-A-7 through 9. It appears that degradation with time is well within the spread in strength due to fabrication or materials quality. No further conclusions can be drawn with confidence at this time.

One unexpected result from these tests is that the joint to a single sandwich skin is stronger than that to a double sandwich skin. It appears that in the former case, the resin penetrates the foam and bonds to the single outer skin. This results in tensile strength greater than the "peel strength" between inner skin and foam core which is called into play in the latter case.

3. Plans for Upcoming Period

The RP-1 has now logged 51 flights and about four hours of flight time.

In its present form, the machine is a reasonable glider, but it can be improved further by streamlining the upper pilot area (smooth bubble canopy) and by making the ailerons more control effective. Steps to accomplish these changes will be considered during the next period.

Testing of typical structural elements will continue in the year ahead to see if any supportable trends can be established as to how such elements degrade with time.

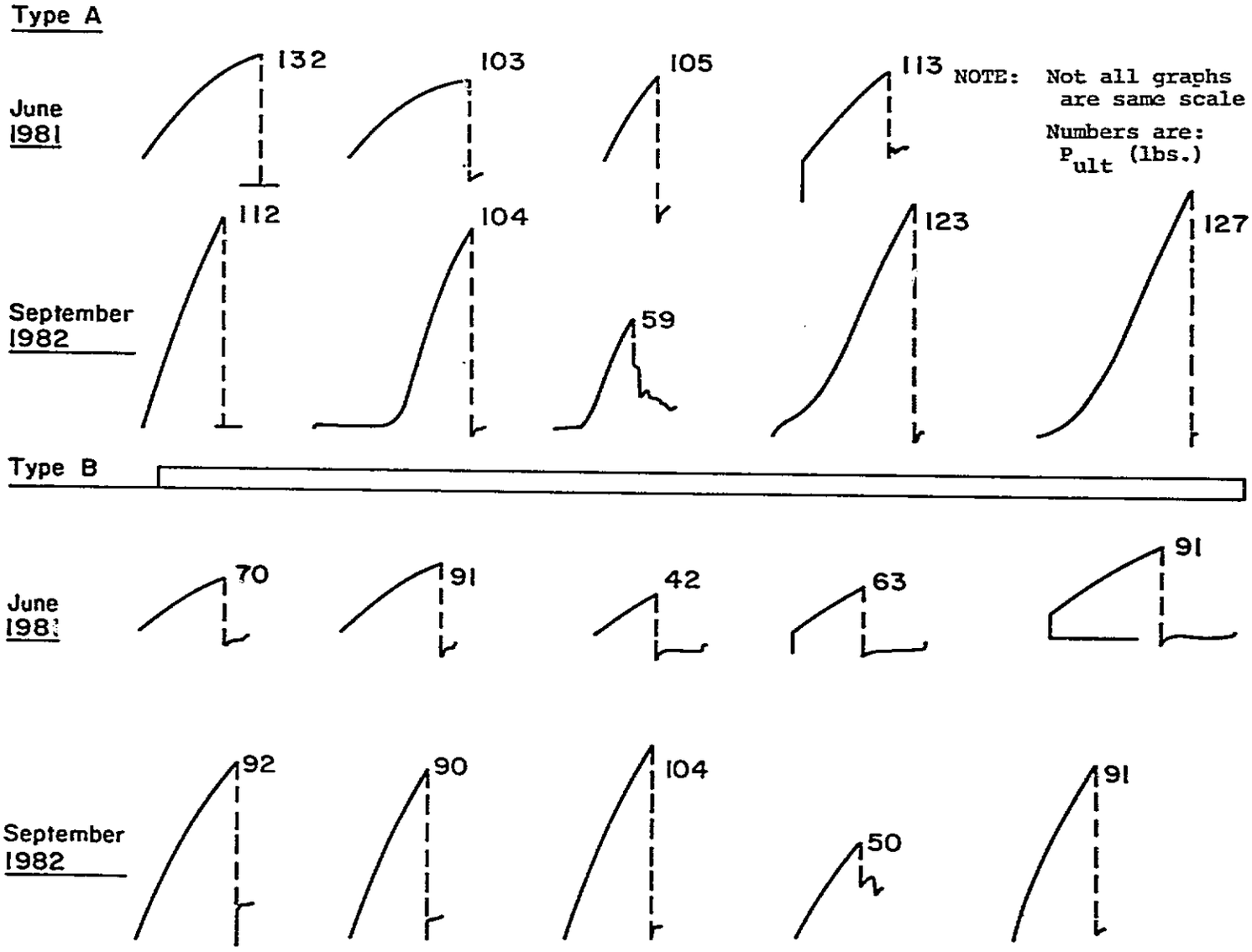

Figure V-A-7. Results of Tensile Tests to Failure of the Structural Joints Shown in Figure V-A-6

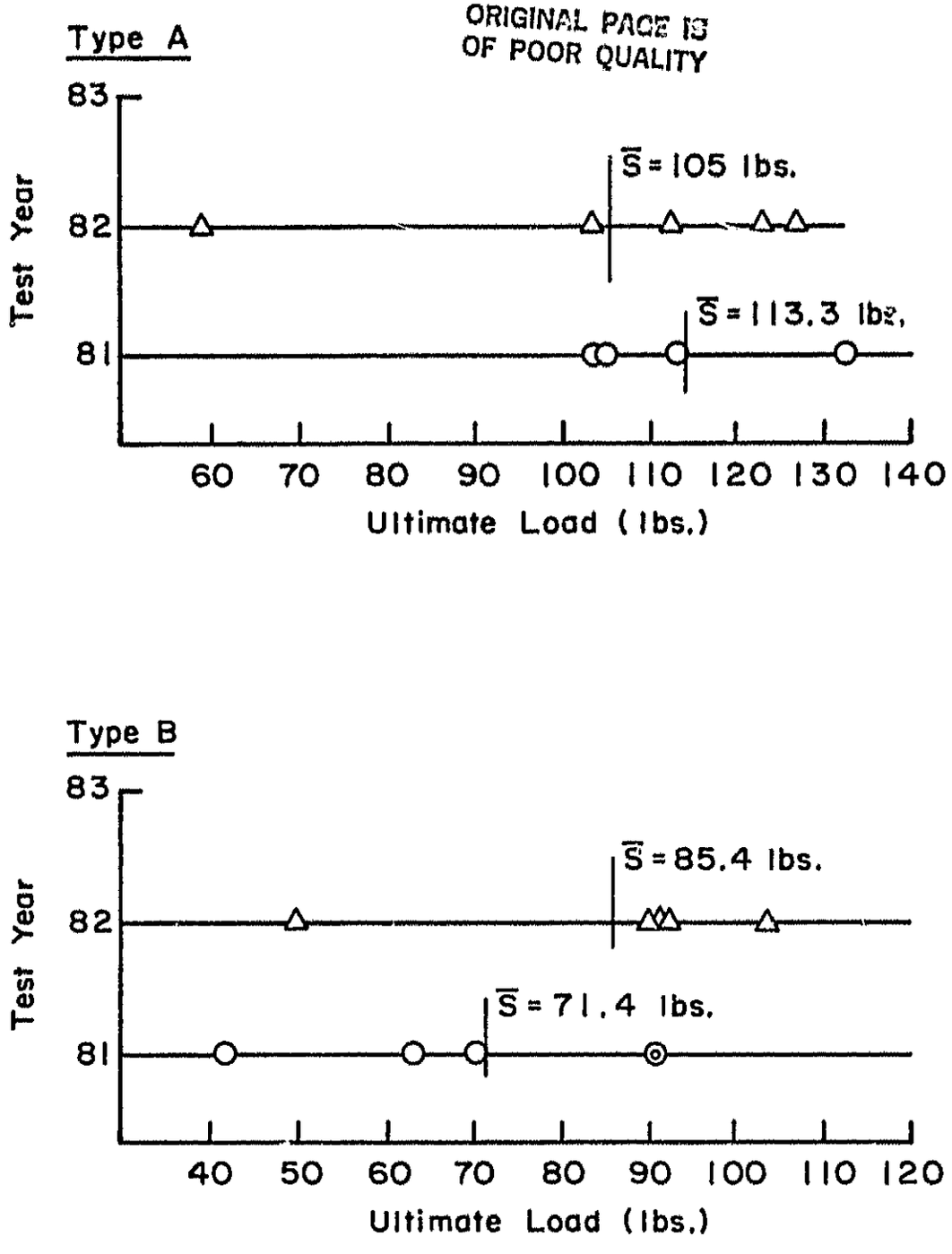

Figure V-A-8. Comparison of 1981 and 1982 Data Showing Spread and Mean

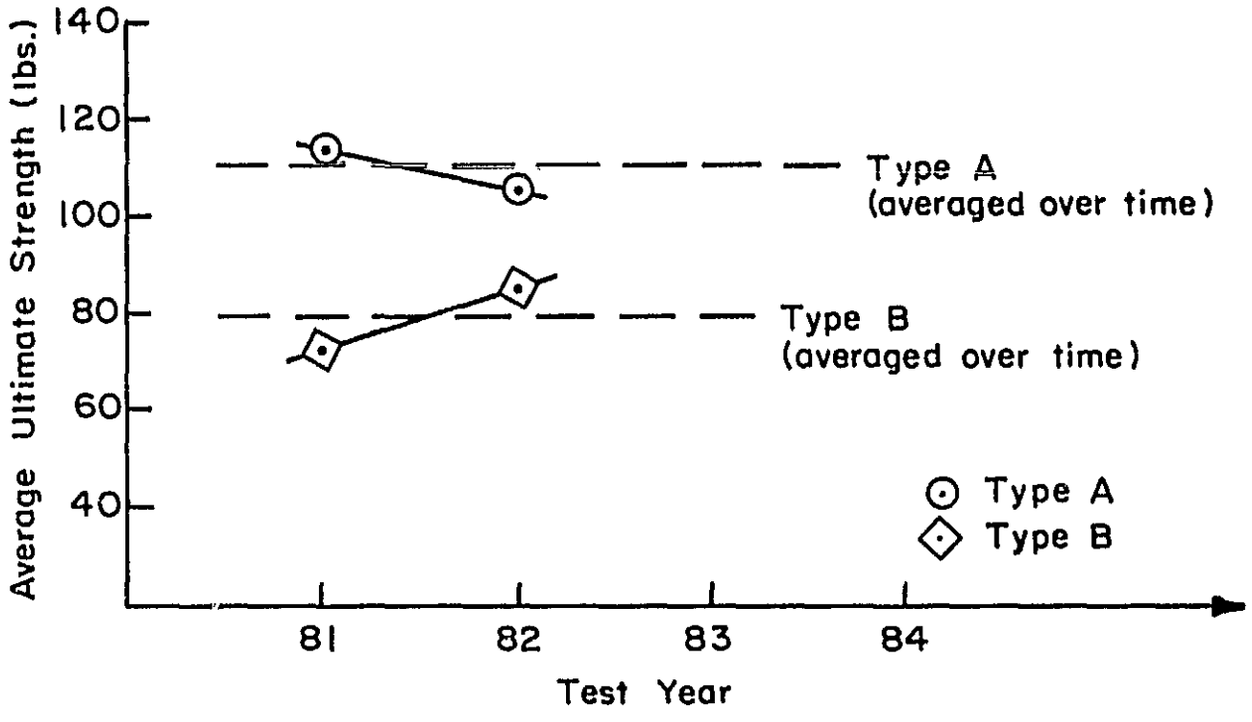

Figure V-A-9. Change in Average Ultimate Strength Over Time

4. Current Publications or Presentations by Professor Bundy on this Subject

"Rensselaer RP-1 Progress Report"
Published in Soaring, July 1982, pp. 7-8.

V-B SECOND SAILPLANE PROJECT: THE RP-2

Senior Investigators: F. Bundy
R. J. Diefendorf
H. Hagerup
C. Muser

1. Status

As reported earlier, the RP-2 sailplane was statically tested in October 1981. It successfully survived the 5.9 g bending test, but during the combined bending-torsion tests, the wing carry-through structure failed. This failure caused secondary damage to the outer wings, since they were only supported at the fuselage, and the wing tips fell to the floor. The damage was analyzed and several stress and deflection calculations performed, as a result of which it was concluded that the failure initiated as a result of the carry-through structure being loaded in fore-aft bending and torsion, which it was not intended to carry. Repair techniques were developed for the outer wings. The splices to be used to restore the structural integrity of the broken capstrips of the wing I-beam were successfully tested on a separate test beam. The wing carry-through structure was redesigned to provide for a better vertical shear transfer mechanism and to prevent inadvertently becoming a load-path for torsion and fore-aft bending, per se.

2. Progress During Report Period

In the current reporting period, reconstruction proceeded to the following point. The broken capstrips (at about one-half span) of both wings have now been repaired, by employing the splice technique developed during the previous reporting period. One wing has been rebuilt, except for the carry-through portion of its spar, and a portion of its top wing skin remains to be installed. An existing test beam was taken apart in the carry-through region and flaws were introduced to simulate the damage in that area as it existed on the actual wing. The testbeam carry-through structure was tested up to the 5.9 g limit of the test fixtures. The load was kept at its highest level for three minutes, and there was no evidence of damage of any kind. The new carry-through connection has been designed to withstand three times that load. Following this test the decision was made to install the new design of the actual wing of the RP-2. This wing connection was partially rebuilt at the end of the reporting period.

The fuselage was also modified to accommodate the larger parts in the new wing-connection. Testing of the compression strut that is to be mounted in the fuselage between the two shear-torsion pins, which carry the load from wing root rib into the fuselage, has begun. This strut is the member which stiffens deflections associated with fore-aft wing bending and, thereby, helps to prevent the wing-carry through from carrying such loads.

3. Plans for Upcoming Period

The reconstruction of the wings will continue until the end of the year. This includes rebuilding the wing connection to ailerons, mounting the flaps, replacing the actuator mechanisms and splicing the wingskins. The steering mechanism in the cockpit also needs to be partially rebuilt. The compression strut will be finalized, following testing, and will be fabricated and installed. Finally, a test fixture will be designed and built to allow static testing of the completed airframe.

PART VI
COMPUTER SOFTWARE DEVELOPMENTS

VI COMPUTER SOFTWARE DEVELOPMENTS

Senior Investigator: M. S. Shephard

1. Introduction

The objective of this portion of the project is to provide advanced and specialized computer "tools" for the analysis and design of composite structural elements and the study of structures-related phenomena in composite materials. The major thrust to date has been and will continue to be in the finite element area, with effort directed at implementing finite element analysis capabilities and developing interactive graphic preprocessing and postprocessing capabilities.

2. Status

The results achieved in this area of research during recent reporting periods have been used for the numerical analysis of moisture effects and the numerical investigation of the micromechanics of composite fracture discussed in Parts III-D and III-E of this report. In addition, the POFES* system, which is available to the composites program, continues to be developed through student class projects and projects supported by the Graphics Center's Industrial Associates Group.

*POFES (People Oriented Finite Element Software) is RPI's finite element software system.

3. Progress During Report Period

Projects of interest to the composites program supported out of the Center for Interactive Computer Graphics and the Department of Civil Engineering are discussed in the following two subsections.

a. Three-Dimensional Preprocessor, Based on Extrusion Capabilities

The extrusion preprocessor allows for the definition and meshing of three-dimensional objects by first defining components with planar faces and then extruding them in the third dimension and patching them to similarly-defined components[1]*. During the last reporting period, the capabilities of this program have been expanded to include more extensive patching modes. In addition, the mesh generating capabilities are being improved.

In addition to the simple face to face component patching available previously, it is now possible to patch new components to planar sides. Also, the ability to do linear extrusion in which a face is extruded in a linear manner to a new face that is a scaled version of the original has been added. Figure VI-1 displays an example of the type of geometric object that can be generated with these capabilities.

The mesh generating capabilities have been extended to allow for the meshing of component faces in terms of any

*Numbers in brackets in this section refer to the references which are listed on page 151.

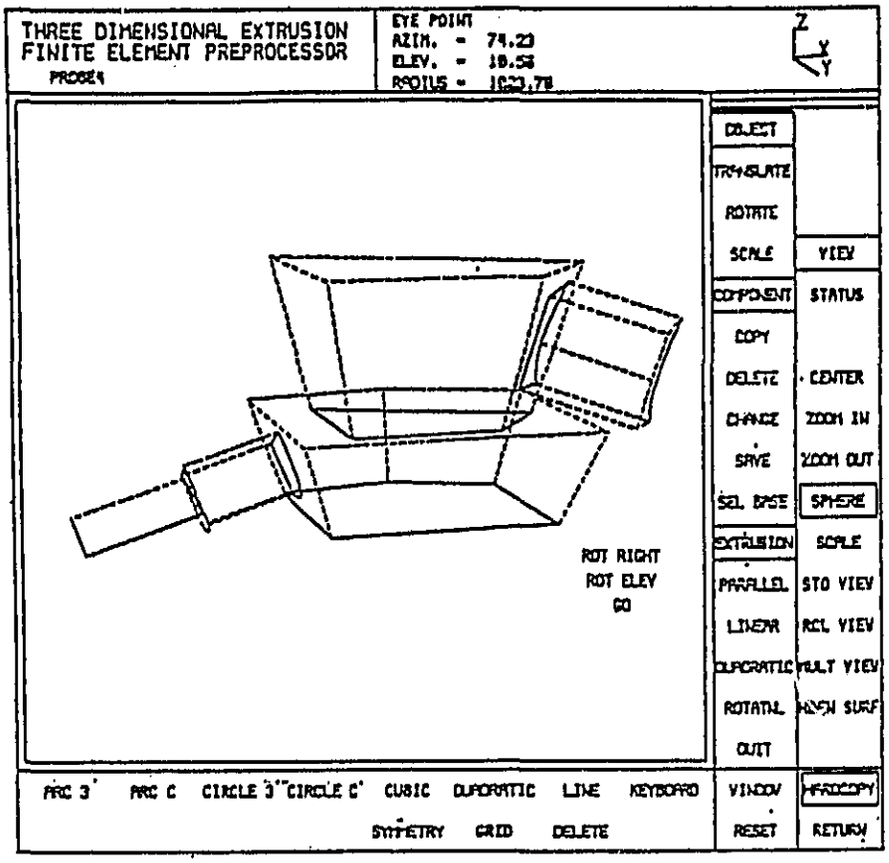

Figure VI-1 Example of Patched Components

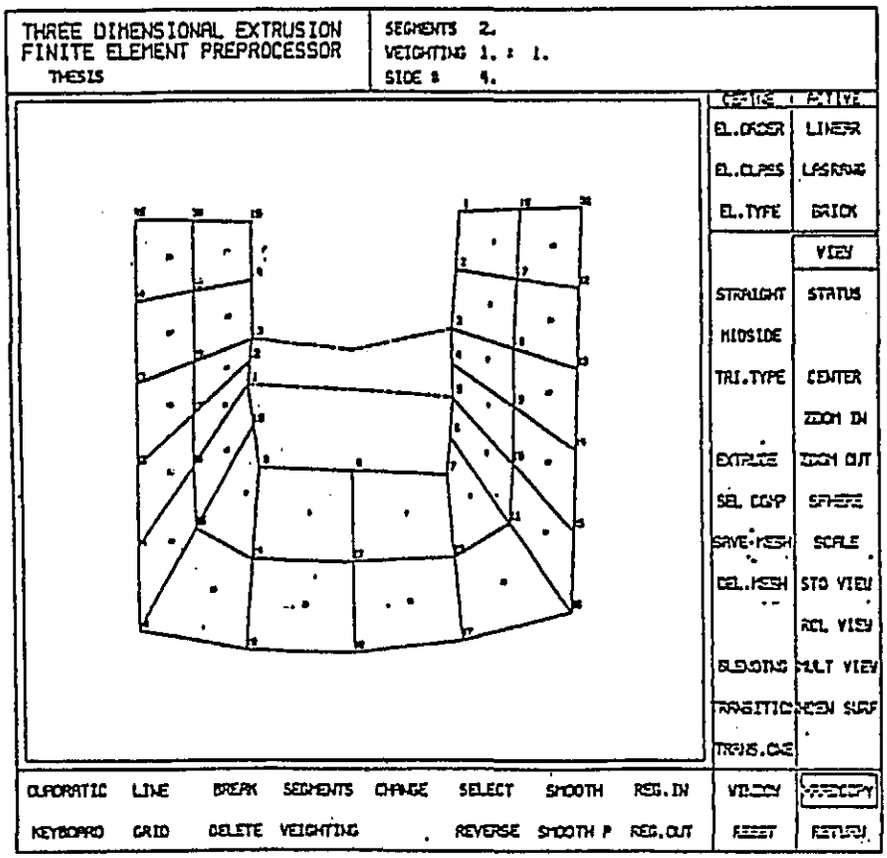

Figure VI-2 Subregion Mesh Patch

number of subregions (Figure VI-2) which can then be extruded to form a solid mesh within that region (Figure VI-3). The meshes for various compatible subregions can then be patched together. Figure VI-4 shows a two-component object fully meshed.

b. Composite Plate and Shell Element

As discussed in the previous progress report, an element was being established in our in-house finite element analysis program for the analysis of composite plates and shells. The element selected is a flat triangular element which results from the superposition of the DKT plate bending element [2] and a constant strain triangle for membrane behavior.

The DKT plate bending element was first incorporated and tested. The results obtained for this case were very good. The next steps were to add the constant strain triangle and the laminated plate capabilities [3]. Both of these capabilities have been tested and good results obtained [4]. The final steps in the element derivation include providing the bility to place this element in a general three-dimensional domain and add a corrective stiffness term to account for the rotational degree of freedom normal to the element [5].

To facilitate the testing of the shell element, a link is currently being created between the shell preprocessor and the analysis program. This link also allows for the

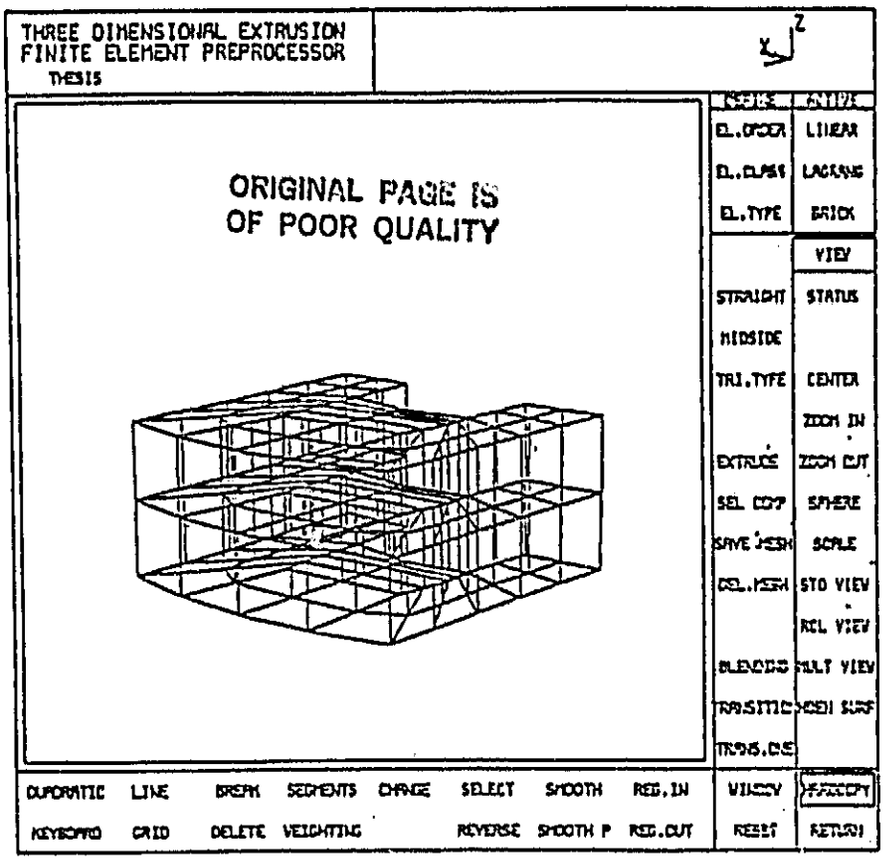

Figure VI-3 Three-Dimensional Mesh in Extruded Component

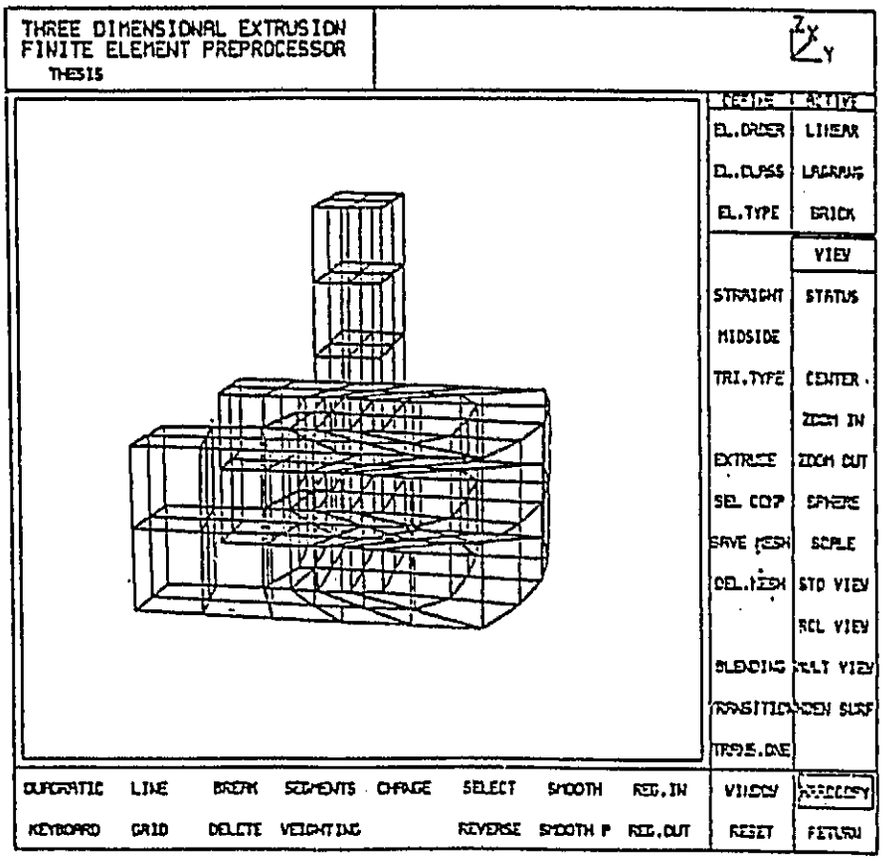

Figure VI-4 Completed Three-Dimensional Mesh

interactive alpha-numeric specification of problem loads, material properties and boundary conditions. The analysis results are also being linked to the three-dimensional displacement postprocessor. Initial shell analysis runs indicate satisfactory results, although they are somewhat less accurate than the bending results. This was expected, since the constant strain triangular representation of membrane behavior is only an approximation. It is very difficult, however, to develop combined elements for shells with better than linear membrane models.

4. Plans for Upcoming Period

During the next reporting period additional features will be added to the extrusion program and shell preprocessor (discussed in previous progress reports). In addition, a final set of test problems will be run on the composite flat shell element added to the in-house finite element program.

An investigation is also being initiated to investigate the use of modified-quadtree mesh generation capability[6] developed at RPI in a finite element analysis program to automatically track down propagation. If such a procedure is successful, it could have a large impact on the efforts in the numerical investigation of micromechanical composite fracture discussed in Part III-E.

5. References

1. Kanellopoulou, M., "Generation and Finite Element Modeling of Sweep-Based Solids", TR-82010, Masters Thesis, Center for Interactive Computer Graphics and Civil Engineering, Rensselaer Polytechnic Institute, Troy, NY, 1982.

2. Batoz, J. L., K. J. Bathe and L. W. Ho, "A Study of Three-Noded Triangular Plate Bending Elements", Int. J. Num. Meth. Engrg., Vol. 15, 1980, pp. 1771-1812.

3. Jones, R. M., "Mechanics of Composites Materials", McGraw Hill, 1975.

4. Agarwal, N., Masters Thesis in preparation, Rensselaer Polytechnic Institute, Troy, NY.

5. Zienkiewicz, O. C., "The Finite Element Method", 3rd ed., McGraw-Hill, Chapter 10, 1977.

6. Yerry, M. A. and M. S. Shephard, "Finite Element Mesh Generation Based on a Modified-Quadtree Approach", Accepted for Publication, IEEE Computer Graphics and Applications, 1983.

6. Current Publications or Presentations by Professor Shephard on this Subject

"Interactive Finite Element Programs"

Published in Proc. NCGA '82, Vol. 1, Anaheim, CA, June 1982, pp. 49-58.

Presented at NCGA '82 Conference, Anaheim, CA, June 16, 1982.

"Finite Element Models from Geometric Models"

Published in Proc. NCGA '82, Vol. 2, Anaheim, CA, June 1982.

Presented at NCGA '82 Conference, Anaheim, CA, June 17, 1982.

"An Approach to Automatic Finite Element Mesh Generation", with M. A. Yerry.

Published in Computers in Engineering, Vol. 3, ASME, August 1982, pp. 21-28.

Presented at the 2nd Int. Computer Engineering Conference, San Diego, CA, August 17, 1982.

"Finite Element Mesh Generation Based on a Modified-Quadtree Approach", with M. A. Yerry.

Accepted for publication, IEEE Computer Graphics and Applications, 1983.

"CAD/CAM Education in an Engineering Curriculum"

Presented at SIGGRAPH '82, Boston, MA, July 29, 1982.

"Preparing Mechanical Engineering Students for the CAD Environment"

Presented at the 2nd Int. Computer Engineering Conference, San Diego, CA, August 18, 1982.

"An Approach to Automatic Finite Element Mesh Generation"

Presented at the 2nd International Computer Engineering Conference, San Diego, CA, August 18, 1982.

PART VII
TECHNICAL INTERCHANGE

INTRODUCTION

Technical meetings, on- and off-campus, provide important opportunities for interchange of technical information. Because of the large number of composites meetings, a central catalog with all upcoming meetings is being maintained and distributed periodically. In this way we help to assure that a Rensselaer faculty/staff member can participate in important meetings. The calendar for this reporting period is shown in Table VII-1. Meetings attended by RPI composites program faculty/staff/students during the reporting period are shown in Table VII-2. Some meetings particularly relevant to composites, held on-campus with special speakers, are listed in Table VII-3. A list of composite-related visits to relevant organizations by RPI faculty/staff/students, with the purpose of each visit outlined, is presented in Table VII-4.

Two continuing education special courses, outgrowths of the composite materials and structures program, were presented for graduate engineers in industry and government, for the third time: "Advanced Composite Materials and Structures" during the week of July 12-16 and "The Finite Element Method" during August 2-6. Each course lasted a week, and the level of the material was again planned to be particularly useful to managers of engineering structures activities who are involved in technical work but who may not have taken

TABLE VII-1

CALENDAR OF COMPOSITES-RELATED MEETINGS

(April 30, 1982 through September 30, 1982)

1982

5/4-7	38th Annual Forum and Technical Display, Anaheim, CA. "Sponsored by AHS."
5/10-12	Structures, Structural Dynamics and Materials Conference, New Orleans, LA. "Sponsored by AIAA/AHS/SDM/ASME."
5/13-14	Workshop on Modeling, Analysis and Optimization Issues for Large Space Structures, Williamsburg, VA. "Sponsored by Air Force/NASA."
5/17-19	2nd International Very Large Vehicle Conference, Washington, DC. "Sponsored by AIAA."
5/17-21	Composite Metals Workshop, Berkeley, CA. "Sponsored by the University of California."
5/19	Polymer Symposium, Urbana, IL. "Sponsored by the University of Illinois."
5/20-21	13th Akron Polymer Conference on Fracture of Polymers and Composites Program, Akron, OH. "Sponsored by ACS."
5/25-27	Annual Meeting and Technical Display, Baltimore, MD. "Sponsored by AIAA."
6/14-18	Gordon Conference on Chemical Characterization of Structural Polymers, Plymouth, NH
6/16-17	Annual NCGA Conference, Anaheim, CA.
6/21-25	9th U. S. Congress of Applied Mechanics, Ithaca, NY. "Sponsored by AIAA."
7/12-16	IUPAC, Amherst, MA.
7/13-14	Symposium on Jointing in Fibre Reinforced Plastics, London, UK. "Sponsored by the Aeronautical Department, Imperial College and the Royal Aircraft Establishment."
7/15-19	2nd Annual Computer Engineering Conference, San Diego, CA. "Sponsored by ASME."
7/16-19	Symposium on Mechanics of Composite Materials, Blacksburg, VA. "Sponsored by IUTAM."
7/22-27	13th Congress, Seattle, WA. "Sponsored by ICAS/AIAA."

8/23-27	Gordon Conference on Interfaces, New Hampton, NH.
8/30-9/2	IUPAC Polymer Processing Symposium, Athens, Greece.
9/16-17	CFRC, Bonbanne, France. "Sponsored by the French Carbon Group."
9/20-24	Carbon '82, London, UK. "Sponsored by the Society of the Chemical Industry."
9/21-23	Symposium on Solid Mechanics, S. Yarmouth, MA. "Sponsored by the U. S. Army."
9/24-30	Aerospace II Symposium, Williamsburg, VA. "Sponsored by NAA."
9/27-10/2	33rd International Astro. Congress, Paris, France. "Sponsored by the French Aero. and Astro. Association."

TABLE VII-2

COMPOSITES-RELATED TECHNICAL MEETINGS ATTENDED OFF-CAMPUS

(April 30, 1982 through September 30, 1982)

1982

5/13-14 Air Force/NASA Workshop on Modeling, Analysis and Optimization Issues for Large Space Structures (Prof. Loewy), Williamsburg, VA.

5/19 University of Illinois Polymer Symposium (Prof. Sternstein), Urbana, IL.

Professor Sternstein gave invited lecture; "Deformation and Failure in High Performance Composites".

5/20-21 13th Akron Polymer Summit Conference on Fracture of Polymers and Composites Program (Prof. Sternstein), Akron, OH.

Professor Sternstein gave invited lecture; "Fracture in High Performance Laminates".

5/25-27 AIAA Annual Meeting and Technical Display (Prof. Loewy), Baltimore, MD.

Professor Loewy chaired a session on cruise missles.

6/14-18 Gordon Conference on Chemical Characterization of Structural Polymers (Prof. Sternstein), Plymouth, NH.

Professor Sternstein gave invited lecture; "The Influence of Resin Chemistry on Mechanical Properties" on June, 15 and was the morning discussion leader on June, 16.

6/16-17 Annual NCGA Conference (Prof. Shephard), Anaheim, CA.

Professor Shephard presented; "Interactive Finite Element Programs" and "Finite Element Models from Geometric Models".

6/21-25 9th U. S. National Congress of Applied Mechanics (Prof. Brunelle and Dr. Muser), Ithaca, NY.

Professor Brunelle presented paper; "Eigenvalue Similarity Roles for a Class of Rectangular Specially Orthotropic Laminated Plates".

7/12-16 IUPAC (Profs. Diefendorf and Sternstein), Amherest, MA.

Professor Diefendorf co-chaired a session on composites.

Professor Sternstein gave lecture; "Visco Elastic Characterization of Neat Resins and Composites".

8/16-19 IUTAM Symposium on Mechanics of Composite Materials (Dr. Muser), Blacksburg, VA.

8/17-18 2nd International Computer Engineering Conference (Prof. Shephard), San Diego, CA.

Professor Shephard presented paper; "An Approach to Automatic Finite Element Mesh Generation" and, in the Product Design with CAD Systems Panel, presented; "Preparing Mechanical Engineering Students for the CAD Environment".

8/23-27 Gordon Conference on Interfaces (Prof. Diefendorf), New Hampton, NH.

Professor Diefendorf chaired a session on composite interfaces.

8/30-9/2 IUPAC Polymer Processing Symposium (Prof. Sternstein), Athens, Greece.

Professor Sternstein gave lecture; "Deformation and Failure of Composites".

9/16-17 CFRC of the French Carbon Group (Prof. Diefendorf), Bonbanne, France.

Professor Diefendorf gave invited lecture; "Discotic Liquid Crystals".

9/20-24 Carbon '82, Conference of the Society of the Chemical Industry (Prof. Diefendorf), London, UK.

9/24-30 NAA Symposium, Aerospace II (Prof. Loewy), Williamsburg, VA.

Professor Loewy chaired a session on aeronautical research and development.

TABLE VII-3

COMPOSITES-RELATED MEETINGS/TALKS HELD AT RPI

(April 30, 1982 through September 30, 1982)

Topic	Date	Speaker(s)
A Survey of Advanced Composite Applications to Military Aircraft	5/4	Leslie M. Lackman Director, Structures Rockwell International North American Aircraft Op.
A University Program of Composite Sailplane Development	5/17	Robert G. Loewy Institute Professor Rensselaer Polytechnic Inst.
An Incremental Life Prediction Law for Creep-Fatigue Interaction	6/16	Makoto Satoh Doctoral thesis dissertation Department of Mechanical Engineering, Aeronautical Engineering and Mechanics
Damage Mechanics Applied to Crack Initiation and Growth in Structures	7/22	Jean LeMaitre Professor, University of Paris 6, Laboratoire de Mécanique et Technologie Cachan, France
Large Space Structures: The Big Picture. Presentation at 1st Workshop of the Megamechanics Research Consortium	8/27	Robert G. Loewy Institute Professor Rensselaer Polytechnic Inst.
Static and Buckling Analysis of Composites	9/10	N. G. R. Iyengar Department of Aeronautical Engineering I.I.T. Kanpur, India
Microstructure and Fracture Properties of Short Fiber Reinforced Thermoplastics	9/17	Dr. K. Friedrich Ruhr University Institute for Materials Bochum, West Germany

TABLE VII-4

COMPOSITES-RELATED VISITS TO RELEVANT ORGANIZATIONS

by RPI Faculty/Staff/Students

(April 30, 1982 through September 30, 1982)

Visited	Date	By	Purpose
National Materials Advisory Board of the NAS, Washington, DC	5/26	Prof. S. S. Sternstein	Participated in a special meeting on "Room Temperature Curing of Epoxy Resins"
Lewis Research Center, NASA (Workshop on Structural Dynamics)	6/15	Prof. R. G. Loewy	Presented talk: "Structural Dynamics Studies for Fan Turbine Designs"
SIGGRAPH '82 Boston, MA (Panel on CAD/CAM Education)	7/29	Prof. M. S. Shephard	Presented talk: "CAD/CAM Education in the Engineering Curriculum"
Vought Corporation, Dallas/ Fort Worth, TX	8/11, 12,13; and 9/2,3	Prof. R. J. Diefendorf	Discussed carbon/ carbon and ceramic matrix composites with B. Forscht
Acoustic Emission Working Group, Knoxville, TN	9/5-8	Prof. H. A. Scarton	Presented talk: "Acoustic Emission of Local Buckling in Thin-Walled Graphite Tubes"

courses for several years. Because of the wide variety of special courses available throughout the United States dealing with this subject matter, only rather unique aspects justify additional offerings in these areas. Our programs were planned from the outset to be unusual in the respect that "hands-on" experiences were inherent and required for completion of each course. These aspects were enhanced for this third offering. Use of hand-held programmable calculators, application of optimization programs using computer graphics, lay-up and cure of a simple part in graphite epoxy and testing tensile, shear and compression coupons to failure were all part of the composite materials and structures course. As part of the second course, workshop sessions were held in RPI's Computer Graphics Center. In these sessions the enrolled engineers and managers defined, "constructed" and analyzed their own finite element models on refresh graphics terminals.

It was gratifying to note that NASA Army, Navy and Air Force, both large and small industrial firms and other universities were represented among those who took the courses and that their post-course questionnaires were overwhelmingly favorable.

Faculty-staff and attendees for the courses were as follows:

Composite Materials and Structures

July 12-16, 1982

Program Director:

R. G. Loewy
Institute Professor
Rensselaer Polytechnic Inst.

Faculty:

R. Judd Diefendorf
Professor, Materials Eng.
Rensselaer Polytechnic Inst.

H. Gunther Helwig
Design Specialist
Composites Group
Dornier System Gmb H

S. Leigh Phoenix
Associate Professor
Mechanical and Aeronautical Engineering
Cornell University

Stephen W. Tsai
Chief, Mechanics and Surface Interactions Branch
Air Force Materials Lab.
Wright-Patterson AFB

Dick J. Wilkins
Sr. Engineering Specialist
General Dynamics
Fort Worth

Students:

Raymond Cannon
Structural Integrity Engr.
AFWAL/FIBE
Wright Patterson AFB
OH 45433

Joseph A. Corrado
Structural Engr.
DTNSRDC
Washington, DC 20590

George Delli Santi
Research Engr.
Zimmer
P. O. Box 708
Warsaw, IN 46580

Allan Ehlers
Senior Staff Engr.
The Bendix Corporation
Guidance Systems Division
Teterboro, NJ 07608

Craig Golisano
Mechanical Engr.
Eastman Kodak
901 Elmgrove Road
Rochester, NY 14650

Carl Holdren
Design Engr.
General Electric Company
Interstate 75 and Neumann Way
Cincinnati, OH 45215

Karen Jackson
Engineer
U. S. Army Structures Lab.
Langley Research Center MS 495
Hampton, VA 23665

A. Hugo Kruesi
President
Elfin Corporation
550 Chippenhook Road
Wallingford, VT 05773

Eugenio Rieghi
Engineer
Siai-Marchetti
21018 Sesto Calende
Via Indipendenda, 2 Italy

Giantaolo Rusconi
Engineer
Siai-Marchetti
21018 Sesto Calende
Via Indipendenda, 2 Italy

Dennis R. Schneider
Aeronautical Engr.
SA-ALC/MMSRE
Kelly AFB
TX 78241

Thomas F. Smith
Mechanical Engr.
SA-ALC/MMETM
Kelly AFB
TX 78241

Ray F. Wojcieszak
Manager of Special Projects
General Electric Company
MD - J134
Evandale, OH 45215

The Finite Element Method

August 2-6, 1982

Program Director:

M. S. Shephard
Associate Director, Center
for Interactive Computer
Graphics and Assistant
Professor of Civil Eng.
Rensselaer Polytechnic Inst.

Faculty:

Richard H. Gallagher
Dean, College of Engineering
University of Arizona

Charles Ritter
Vice President
Jordan, Apostal, Ritter
Associates Inc.
Davisville, RI

John Gray
Manager of Technical Services
General Electric CAE, Intl.

Harry Schaeffer
Founder & President
Shaeffer Analysis, Inc.

Students:

Alfredo Cires
Aerospace Technologist
NASA Langley Research Cntr.
MS 440
Hampton, VA 23665

Clifford Claypool
Structural Analysis Technician
Alcoa Technology Center
Alcoa Center, PA 15069

John Datko
Aerospace Eng.
AFWAL/POTX
Wright-Patterson AFB
OH 45433

Wendall Maciejewski
Mechanical Eng.
Naval Underwater Systems Cntr.
Fort Trumbull 3233
New London, CT 06320

Teresa May
Engineer
Gibbs and Cox
40 Rector Street
New York, NY 10006

Robert Niemeyer
Mechanical Eng.
Naval Surface Weapons Cntr.
Silver Springs, MD 20910

Michael Pappas
Professor
Mechanical Eng.
New Jersey Inst. of Tech.
323 High Street
Newark, NJ 07102

Guy S. Puccio
Vice President Eng.
ACME Highway Products Corp.
Creekside Drive
Amherst, NY 14150

Fred Romano
Physicist
North Carolina State U.
3211 Broughton Hall
Raleigh, NC 27650

Robert J. Sebests
Construction Eng.
Chevron USA
935 Gravier
New Orleans, LA 70112

B. Vincent Viscomi
Professor and Head
Department of Civil Eng.
Lafayette College
Easton, PA 18042

Victor Wahlberg
Regional Engineering Consultant
McDonald Douglas Automation
P. O. Box 344
24 Hanover Road
Florham Park, NJ 07932

PART VIII

PERSONNEL

AUTHOR INDEX

PERSONNEL

Co-Principal Investigators

Ansell, George S., Ph.D.	Dean, School of Engineering
Loewy, Robert G., Ph.D.	Institute Professor
Wiberley, Stephen E., Ph.D.	Professor of Chemistry

Senior Investigators

Brunelle, E. J., Jr., SC.D. (Aeroelastic and structural design and analysis, applied mechanics of composite structures)*	Associate Professor of Aeronautical Engineering
Bundy, F., Ph.D. (Physical chemistry and structures testing)*	Research Professor of Materials Engineering
Diefendorf[i], R. J., Ph.D. (Fabrication, resin matrix, fiber behavior, interfaces)*	Professor of Materials Engineering
Feeser[i], L. J., Ph.D. (Computer applications and graphics, computer aided design, optimization)*	Professor of Civil Engineering
Goetschel, D. B., Ph.D. (Structural analysis design and testing)*	Assistant Professor of Mechanical Engineering
Hagerup, H. J., Ph.D. (Aerodynamics, configuration, pilot accomodation, flight testing)*	Associate Professor of Aeronautical Engineering
Krempl, E., Dr.Ing. (Fatigue studies, failure criteria)*	Professor of Mechanics and Director of Cyclic Strain Laboratory
Scarton, H., Ph.D. (Acoustic emission NDE)*	Associate Professor of Mechanical Engineering and Mechanics

*Fields of Speciality

[i]Member of Budget Committee together with Co-Principal Investigators

Senior Investigators

Shephard, M. S., Ph.D. (Computer graphics, finite element methods)*	Associate Director, Center for Interactive Computer Graphics and Assistant Professor of Civil Engineering
Sternstein[i], S. S., Ph.D. (Failure analysis, matrix behavior, moisture effects)*	William Weightman Walker Professor of Polymer Engineering

Research Staff

Manager & Master Technician, Composites Laboratory

Paedelt, Volker

Research Associates

Kim, Wonsub, Ph.D.

Muser, Christoph, Dr.Eng.

Graduate Assistants

Baxter, Scott, B.S.
Bertolazzi, Andrew, B.S.
Bobal, Gail, M.E.
Cackett, Matthew, B.S.
Chen, Shu-ping, M.S.
DeMint, Thomas, B.S.
Father, Philip, B.S.
Helmer, James, B.S.
Hu, Tsay-hsin, M.S.
Lumban Tobing, Frida, M.S.
Niederer, Melvin, B.S.
Niu, Tyan-min, M.S.
Ogunlari, Fola, B.S.
Sing, Sachchida, B.Tech.
Uzoh, Cyprian, B.S.
Yehia, Nabil, M.S.
Yang, Philip, M.S.

Undergraduate Assistants - Seniors

Benson, Robert
Cerro, Eric
Chin, Hong
Cioffoletti, Anthony
Delzer, Francis
Ficarra, Fobert
Kloiber, James
Lafreniere, Suzanne
Malusa, Stephen
Nier, Laura
Olsen, Kenneth

---

*Fields of Speciality

[i]Member of Budget Committee together with Co-Principal Investigators

Undergraduate Assistants - Juniors

Dyer, Richard
Kolotylo, Michael
Lopez, Matthew
Martin, Randall
Michael, Thomas
Robertson, Scott
Tomlin, Rogers
White, Eric

Undergraduate Assistants - Sophomores

Dunlap, Robert
Hart, Laurence
Schiller, Paul

AUTHOR INDEX